POLITECNICO DI TORINO

UNIVERSITÀ DEGLI STUDI DI TORINO

New technologies and materials to improve diagnosis, therapy and surgery

Dott.ssa Alessandra Piccitto

Supervisors:
Prof. Mario Morino – Università degli Studi di Torino
Prof. Emilio Paolucci – Politecnico di Torino

A thesis submitted for the Degree of Doctor of Philosophy
in Bioengineering and Medical-Surgical Sciences
with the kind cooperation of

UCL · Royal Pharmaceutical Society · The University of Waikato · University of Oxford · University of New Haven

Abstract

The aim of this research project has been focused on improving diagnosis, therapy, and surgery by using new patented technologies and materials.

The first technology that has been examined in it has been SynDiag – a new software patented at Polytechnic School – University of Turin that represent the first step of a new concept of accurate diagnosis without using the X-ray technology but only ultrasounds. The output will be no more qualitative but quantitative and can be obtained from an existing full console machine connected to a 3D transducer with the result of keeping the costs to the minimum.

The second technology is a patent coming from the Russian Federation and called Proton Therapy. This new technology is based on the acceleration of both protons and neutrons and can be tailored on every human (child, adults, young, elderly, slim etc.…) and been effective on the detection and dissolution of brain cancer on which it is not possible to perform a surgery.

Another problem that has been explored is the big problem of the antibiotic resistance and the most dangerous superbugs (ranked by the WHO in February 2017) and their biofilms currently giving infections and post-surgery complication ending into an unlucky and poor prognosis. A solution has been found with evidences of efficacy cooperating with the USA, Germany, Australia, and New Zealand.

Concerning the materials, the research has been focused on medical application of polyurethane – a type of PU has been synthesized at Polytechnic School – University of Turin to study the complexity of the human ageing and trying to make a cardiac tissue model young and aged avoiding the use of the animal model.

Finally, a medical polyurethane (PU) has been treated to become an antimicrobial or self-sterilizing surface where superbugs cannot colonize, survive or spread to control nosocomial infections and prevent the misuse of antibiotics, and consequently try to overcome the big problem of the

antibiotic resistance. This research project origins from a bigger research area of the University College London that involves different knowledge and experience coming from the Medical School and the Dental Hospital, the School of Engineering, the Chemistry Dept. and the School of Pharmacy. The first prototype was a catheter containing a crystal violet and golden nanoparticles (NPs) solution that effectively kills *E. Coli*, MRSA and *Candida albicans*. The antimicrobial material of this dissertation is intended as an improvement of the existing one – most of the procedure has been changed and the solution was obtained using crystal violet and silver NPs but also silver NPs only. Silver nanoparticles showed the evidence to kill *P. aeruginosa* while staying inside the bulk of the material avoiding superficial oxidation processes. The coating material obtained can reduce bacteria biofilm caused diseases in humans and is on its way to be patented.

Acknowledgements

Thanks must firstly go to my father Bruno Piccitto to whom this dissertation is fully dedicated, because of his never endless support and for being the most wonderful father every daughter all over the world could desire to have. Subsequently many thanks should go to my whole family.

I am indebted to Professor Mario Morino – my PhD Coordinator and supervisor and to Professor Emilio Paolucci – my SynDiag project supervisor, under whose supervision this work has been carried out, for their continued encouragement and advices.

It is a pleasure to acknowledge the assistance of Dr Catherine Duggan and all the other members of the Royal Pharmaceutical Society of Great Britain for their professional support. It is also a pleasure to acknowledge Mrs Helen Gordon – CEO of the Royal Pharmaceutical Society until February 2017 and now CEO of the Royal Society of Medicine for her kindness.

My grateful thanks are expressed to Father Giuseppe Caviglia and all the Friars of the Ordo Carmelitarum Discalceatorum (Order of Discalced Carmelites) of Arenzano (Genoa – Italy) for their unconditioned support and prayers from Italy, Czech Republic and Central Africa.

I am also grateful to Professor Manfred Bochmann – Professor of Inorganic Chemistry at the UEA School of Chemistry (UK) and his colleagues for awarding me the prestigious NCS (UK National Crystallography Service) and RSC (Royal Society of Chemistry) Best Speaker Award 2017 prize at Burlington House London on the 28th June 2017.

I acknowledge all the other professionals who cooperated with me and made their best to support me to realize all the projects listed in this dissertation in their respectively dedicated chapter.

Table of Contents

List of Figures

page

List of Tables

page

Chapter 1

New Technologies to improve diagnosis, therapy and surgery

1.1. SynDiag

1.1.1. INTRODUCTION

The name of this new Italian patent is SynDiag that means "*syndrome diagnosis*" and it is focused on the detection of foetus facial dysmorphisms by using the ultrasound imaging technology.

Ultrasound is worldwide the most adopted and the safest screening method for prenatal imaging and diagnosis of possible fetal pathologies. It allows physicians to visualize in a non-harmful way the fetus development, despite the sensitiveness of ultrasound to scattering noise. Indeed, this represents the main drawback of the technology, impeding easy development of fully automatic images post-processing, which usually requires some level of human intervention[1]. This is true also for newest 3D ultrasound machines[2], whose output is a qualitative render obtained from registered bi-dimensional ultrasound scans.

In this manuscript, it is presented a recently developed algorithm for automatic extraction of a three-dimensional surface of fetus face from a registered stack of bi-dimensional ultrasound scans[3]. It operates without human intervention, elaborating input data in the standard DICOM format with a two-steps statistical analysis based on volumetric histogram processing and 2D segmentation. It outputs a quantitative triangular mesh in PLY format, ready for further mathematical analysis.

By way of method validation and as an example of the application, it is developed a diagnosis tool, based on the former elaboration, which succeeded in discriminating labio-schisis manifesting

individuals from healthy individuals[4]. Being a stochastic algorithm based on unsupervised clustering, its feasibility is tested upon a small set of available real fetus data and then extensively studied with adult individuals' dataset, known as Bosphorus[5]. The algorithm maps the individual's surface with geometrical descriptors useful to identify the face's landmarks, i.e. pronasion and labrum superior, and compute a distance measure between each faces couple. The algorithm correctly identifies left- and right-sided cleft lips, providing the physicians with a probability of pathology affection and supporting decision making.

Since the method is fully automatic and pathology independent, it allows to easily populate large database of quantitative fetus' faces individuals, enabling objective pathologies to be characterized and normotypes defined.

Consequently, for all the characteristics listed above, SynDiag can be considered as "*the new concept of prenatal diagnosis*".

1.1.2. EXPERIMENTAL

The SynDiag project started in 2012 as a cooperation between the Polytechnic School – University of Turin and the Polytechnic School – University of Milan with the purpose to help 10 million of newborns. In fact, it is nowadays statistically clear that only in Europe, more than 2% (10M) of the population suffers of congenital malformations. Unfortunately, a percentage like the 80% of congenital anomalies are not associated to a specific manifestation risk (e.g. it cannot be detected examining the parents) and only 52% of cases can be diagnosticated by prenatal diagnosis[6].

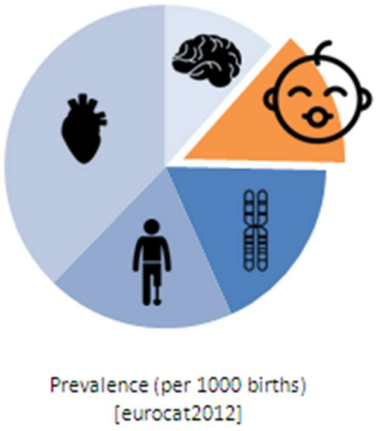

Figure 1. Congenital anomalies: foetus facial dysmorphisms are represented in orange colour. Courtesy of Arch. Stefano Fantucci – Polytechnic School – University of Turin.

It is clear that prenatal diagnosis is essential to rule out diseases that endangers the child's life at birth and to prevent the pregnant woman from giving birth in facilities that do not have a pediatric surgery department. It is also clear that ultrasound is a non-invasive test that is usually performed from the 5th month when the foetus dimensions allow an acceptable diagnostic definition[7].

The existing problem is represented by two conditions: the first one known as labio-schisis or cleft lip and the second one known as Foetal Alcohol Syndrome (FAS) that is a condition which is linked to drinking alcohol in pregnancy which affects the way a baby's brain develops. This condition was first identified in the United States of America in 1973 and its severity is thought be related to how much alcohol a mother drank during pregnancy[8-9]. Children with FAS have problems with their neurological development, abnormal growth, and have characteristic facial features that result from their foetal exposure to alcohol. Neurological problems are caused by damage to the central nervous system (brain and spinal cord). The problems experienced are likely to change as an infant grows up and different problems may be seen at different stages of development, from childhood, adolescence, and into adulthood[10-13]. The labio-schisis is explained in the following images.

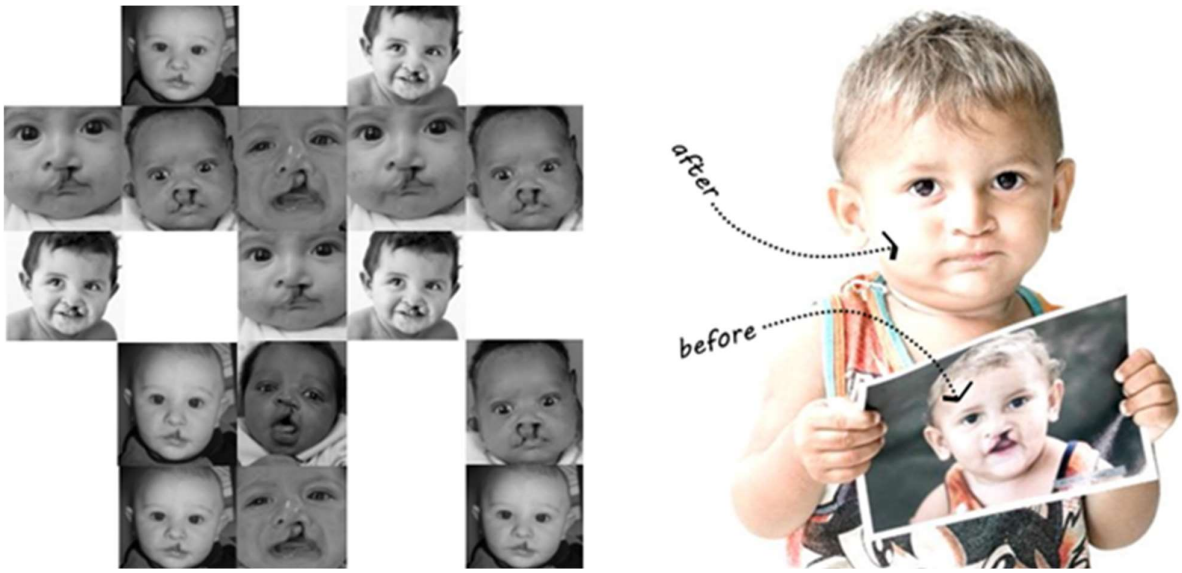

Figure 2. Clefts lips in children before and after the surgery. Courtesy of Arch. Stefano Fantucci – Polytechnic School – University of Turin.

Figure 3. An example of cleft lip surgery: it is clearly visible the little scar on the child's face. Courtesy of Arch. Stefano Fantucci – Polytechnic School – University of Turin.

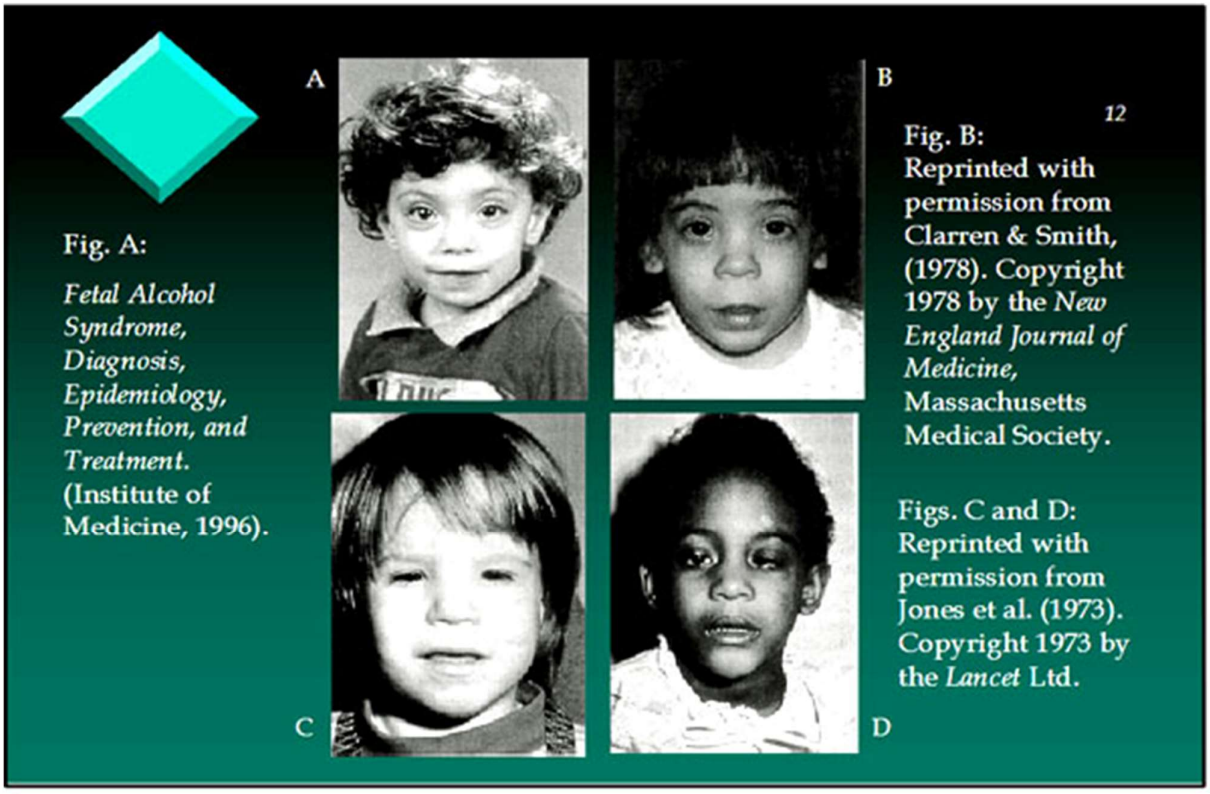

Figure 4. The Foetal Alcohol Syndrome (FAS) in children in the past. Source: PubMed – NCBI.

Figure 5. The Foetal Alcohol Syndrome (FAS) in children at present. Source: Google Library.

The SynDiag project: from September 2012 to January 2013, 30 three-dimensional volumes of 30 fetuses at 22 – 32 weeks' gestation were acquired. Written consent was obtained from the parents for publication of clinical details, clinical images, and videos. Principles outlined in the Declaration of Helsinki have been followed. Among these acquisitions, five were selected and processed for the purposes of the study. The remaining ones were excluded due to high noise or practical "inconveniences" such as baby's hands on face, or simply too much inaccuracy in the scanning process. The ultrasound equipment was a Voluson system (GE Healthcare, Wauwatosa, WI, USA), with a RAB 4–8 (real time 4D convex transducer probe). The GE RAB 4–8 has a frequency range of 4 MHz to 8 MHz and is used for OB applications (Footprint 63.6×37.8 mm, FOV 70°, V 85°×70°). The procedure is completely automatic, enabling fully unattended segmentation. This leads to the possibility of creating a large database of 3D facial point clouds, like the ones required for morphological studies through statistical analyses, without the necessity of human intervention. The algorithm works with standard protocols and file format (DICOM as input and any mesh file format as output), so it is completely platform-independent. The same idea of algorithm may also be extended to internal tissues segmentation to reach a complete 3D model of the fetuses' face and of other organs (e.g. the heart). Furthermore, it can be extended to other applications of ultra sound imaging and for working with different 3D imaging techniques (CT or MRI), taking advantage, in this case, of the absence of the speckle noise effect[14].

The SynDiag patent is a procedure for medical images processing, aimed to the detection of oro-facial dysmorphisms (e.g. Labio/Palato-schisis). The value of this new procedure is that it can easily overcome the limits of the current ultrasound imaging technology that are based on a qualitative rendering without a quantitative elaboration with the consequence that only expert physicians can recognize an abnormal fetus development. The result unfortunately is that many of them are not currently diagnosticated with the consequences illustrated in the above pictures[14-15]. The SynDiag procedure allows a quantitative analysis and a pre-birth accurate and fast diagnosis becoming a really good support for physicians' decisions. It is a unique procedure because is based on an ultrasound imaging technology that is a fast and non-invasive method and allows diagnosis as early as possible, and in addiction to this it can outputs 3D quantitative images from registered 2D ultrasound scans, consequently it is affordable if compared with existing 3D ultrasound imaging devices because it is a plug-in software adaptable to any full console machine on the market[15-16].

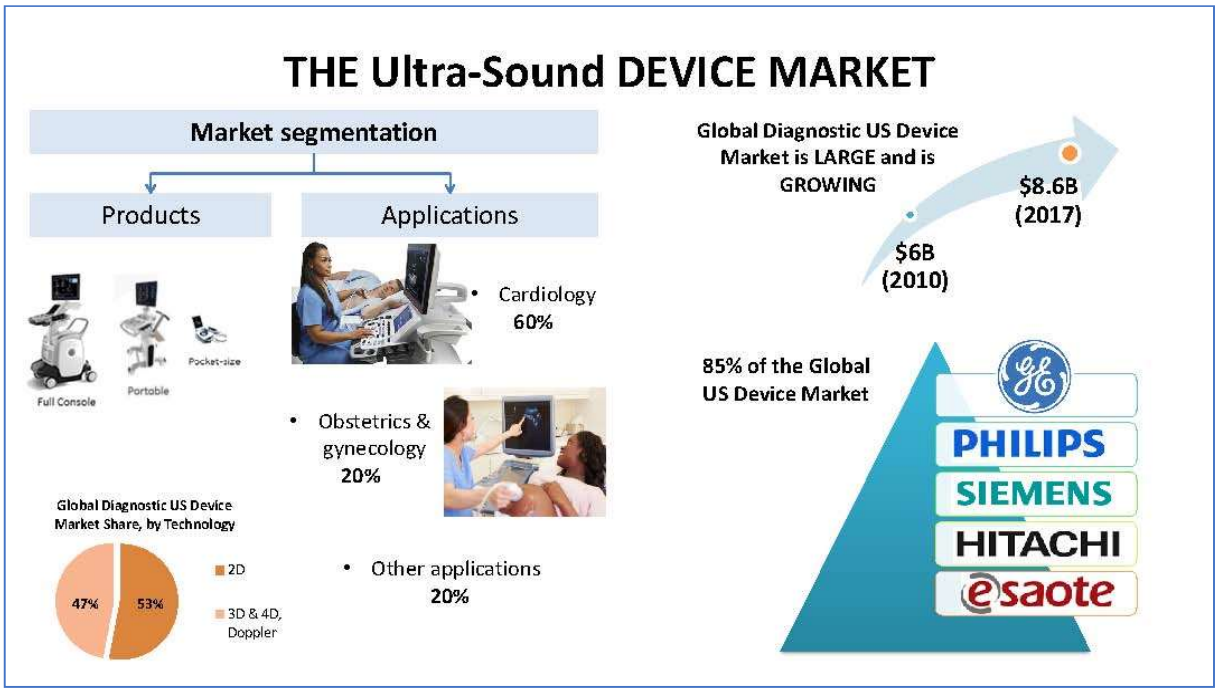

Figure 6. The Ultrasound device market – the importance and impact of the growing global ultrasound imaging technology market. Courtesy of Arch. Stefano Fantucci – Polytechnic School – University of Turin.

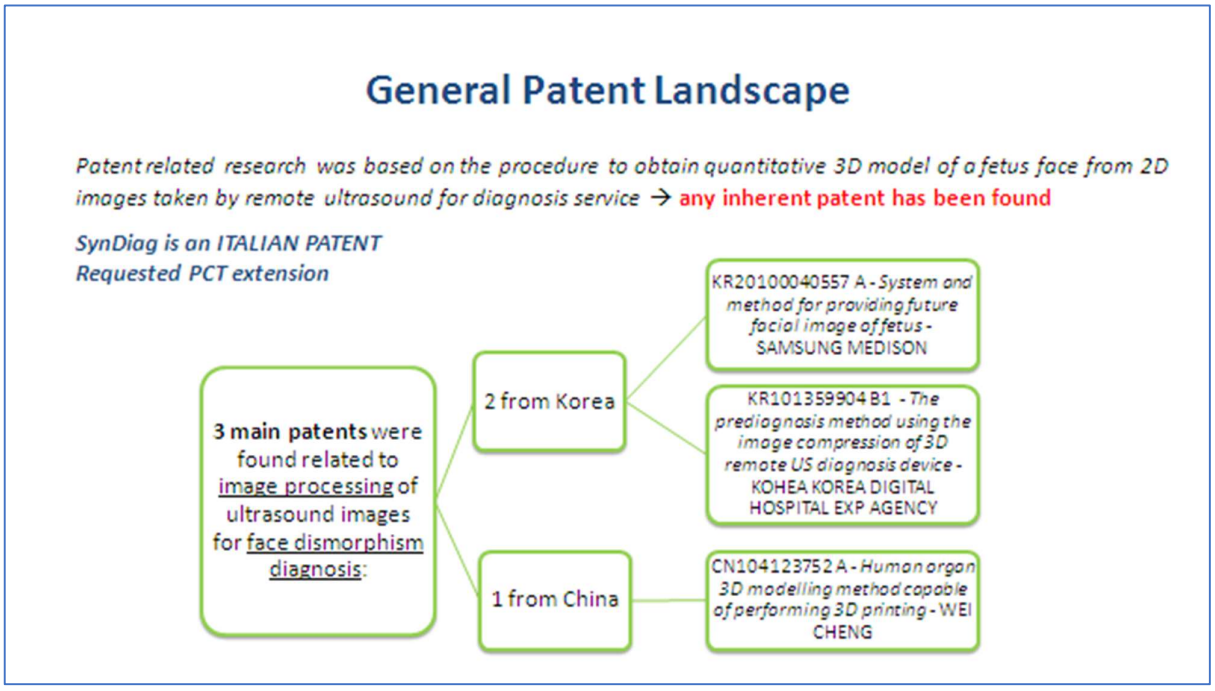

Figure 7. The SynDiag patent, courtesy of Dr Giulio Cattano – Polytechnic School – University of Turin.

The SynDiag method and performance: in the pre-processing phase the DICOM file is initially imported as a stack of 2D planar slices. This can be done in any of the three coordinate directions, as the algorithm does not depend on the position of the foetus. Ultrasound wave scattering damages the images by introducing a type of noise called *speckle*, so in order to enhance segmentation performance, noise is removed through filtering in the first phase. Current algorithms performing this task are based on statistical analysis, inverse PSF filtering, and log separation. In the SynDiag algorithm, a standard 3D low-pass Gaussian filtering was accurate enough for a preliminary speckles removal. After this pre-processing step, the image improves in terms of quality and helps to enhance the performance, although it is not yet clean enough for achieving complete surface extraction. The second phase is the surface reconstruction through 3D histogram processing. Both volume and surface reconstruction are demanding tasks, due to the coexistence of different tissues in the same image (from both mum and foetus). Edge extraction is even trickier when the foetuses' head lays directly on the mother's uterus, hence in this scenario, the two tissues are virtually merged from the ultrasound imaging standpoint. To overcome this problem the SynDiag algorithm has been developed, it is based on a statistical analysis of local and 3D histograms that automatically combine slice and volumetric processing. The following phase is known as data fusion. Potentially, the model extracted after the second phase is complete enough to recognize the

shape of the foetuses' face, but to enhance detection and improve the accurateness a data fusion step has been added to the workflow. The previous 3D shape extraction from all three directions has been repeated by permuting the dimensions of the DICOM stack, and combine the extracted surfaces evaluating the logical AND of the three binary arrays. Consequently, this operation increases the robustness of the SynDiag algorithm. Moreover, this kind of procedure heavily reduces the number of false positives (i.e. edges that do not actually belong to the desired surface). After the data fusion, the output is fairly "clean", but can still be refined by using a post-processing phase in which the three main operations: edge detection, island removal and point cloud and mesh generation take place. Finally, the surface is reconstructed by the *Poisson surface reconstruction* algorithm, exploiting the publicly-available *pointCloud2rawMesh* function and the resulting vertices and faces are written in the final PLY file[16-24]. The resulting 3D quantitative model (a mathematical object) has also been 3D printed as shown in the following images.

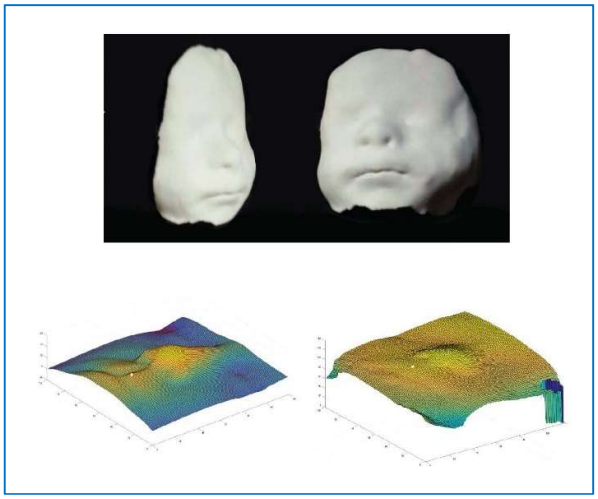

Figure 8. The 3D quantitative model.

The 3D printed foetus face (in white colour), it is the 3D printed version of the quantitative model produced with MeshLab that is the triangular mesh obtained by the SynDiag algorithm.

The surface of the foetus face (in yellow colour) is a mathematical elaboration of it. Courtesy of Dr Daniele Conti – SynDiag inventor.

Figure 9. 3D qualitative images: these images are three examples of 3D ultrasound images exported by using ultrasound full console machines currently used in clinics and hospitals. These images have the best achievable quality nowadays, but they cannot be 3D processed and consequently they cannot give a printable 3D model because they are only qualitative. Courtesy of Dr Daniele Conti – SynDiag inventor.

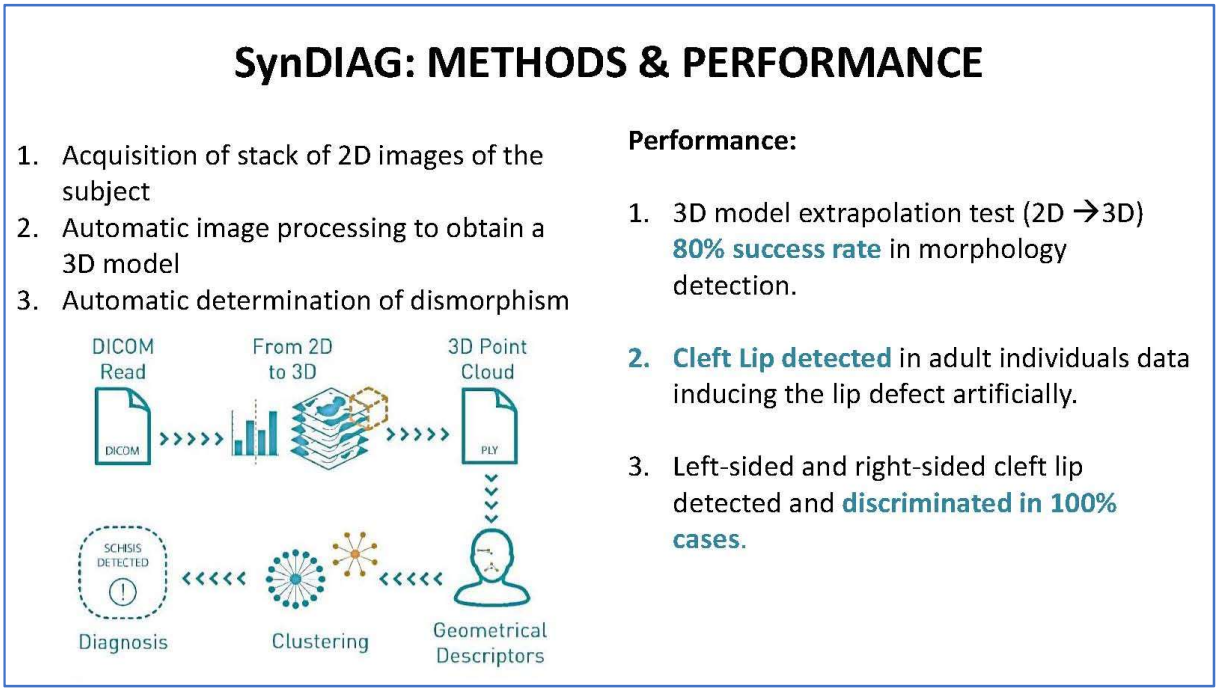

Figure 10. The SynDiag methods and performance, courtesy of Dr Daniele Conti – SynDiag inventor.

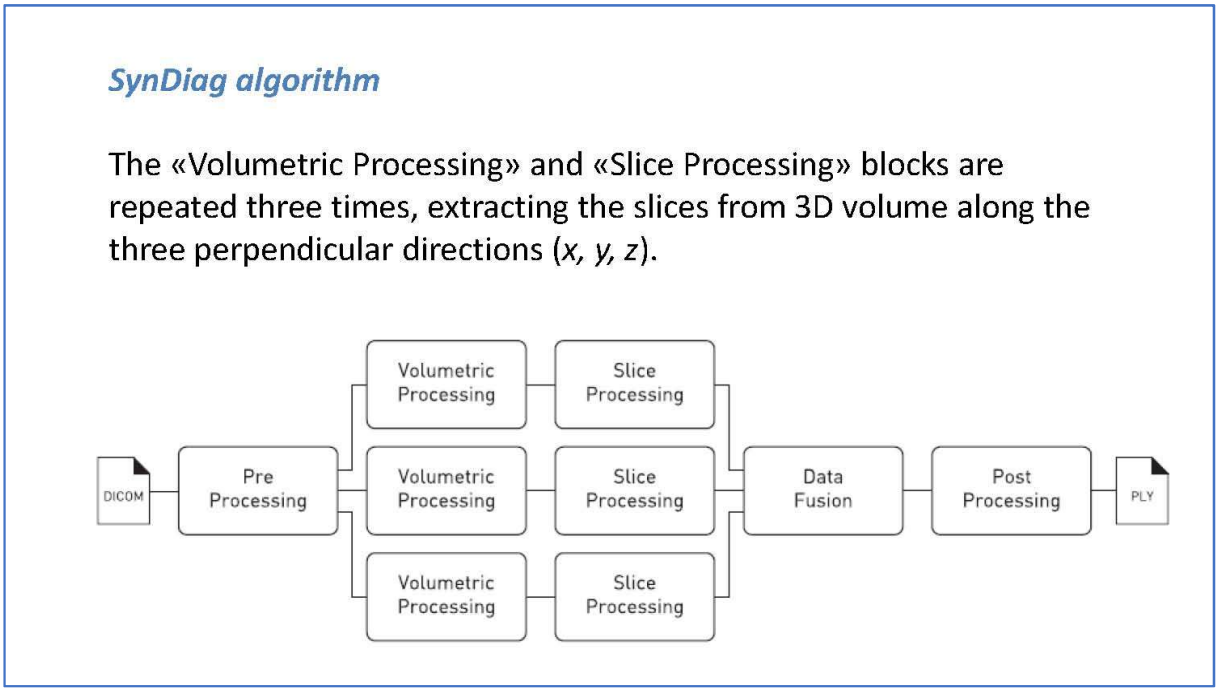

Figure 11. The SynDiag algorithm workflow, courtesy of Dr Daniele Conti – SynDiag inventor.

1.1.3. CONCLUSION

The SynDiag project started in 2012 and was patented at Polytechnic School – University of Turin during the academic year 2015 – 2016 when I joined the project. Working at this project really challenged me as I helped my colleagues with my clinical and pharmaceutical background to improve our new patent in the field of foetal diagnosis by 3D ultrasound imaging technology. I had to fully understand the algorithm methods and performances working closely with the inventors of it. Then I had to collect from gynaecologists and physicians every daily clinical problem related to the pre-natal diagnosis of foetuses' malformations by using the existing ultrasound imaging technology. At the end I understood how to tailor the SynDiag algorithm according to the clinical needing, and consequently how was its own potential in the ultrasound devices market. In my opinion the great advantage of this new technology is that the method automatically extracts relevant 3D information of the foetuses' face from a set of planar 2D ultrasound slices, outputting a high-resolution mesh of the facial surface. It is very easy to use by physicians, also by ones at the beginning of their career, because the method is fully automatic. In addition to this, the whole procedure has been designed and tested with DICOM files as input and a triangular mesh in PLY files as output to achieve the maximum interoperability. This algorithm has also been implemented using MATLAB® and it is easily portable to any other language. In conclusion, I can confirm that SynDiag has been appreciated across the world (U.S.A., Australia, Singapore, Russian Federation, UAE, and Europe).

1.1.4. ACKNOWLEDGEMENTS

I would like to acknowledge for the SynDiag project and patent my PhD Coordinator and Supervisor Prof Mario Morino, my PhD Vice-Coordinator Prof Alberto Arezzo, my SynDiag project Supervisor Prof Emilio Paolucci and his colleague Prof Giuseppe Scellato. I acknowledge the inventors of SynDiag algorithm Dr Luca Bonacina, Dr Antonio Froio, Dr Daniele Conti and Prof Enrico Vezzetti and Dr Federica Marcolin for their collaboration in the project. I acknowledge my colleagues Arch. Stefano Fantucci and Dr Giulio Cattano for being very kind and helpful while working with me at the SynDiag patent. I am also grateful to gynaecologists of S. Anna University Hospital of Turin and some colleagues from the Royal Pharmaceutical Society of Great Britain for their kind help and contribution.

1.2. Proton Therapy

1.2.1. INTRODUCTION

In the field of medical procedures, Proton Therapy is a type of external beam radiotherapy that uses a beam of protons to irradiate diseased tissue, most often in the treatment of cancer. It is also called proton beam therapy, it painlessly delivers radiation through the skin from a machine outside the human body. Protons can be accelerated inside a machine called synchrotron or cyclotron that speeds up the protons, the speed determines the energy level. At high energy, protons can destroy cancer cells because high-energy protons can travel deeper in the body than low-energy ones. With proton therapy, radiation does not go beyond the tumour. In contrast, with photon-based external-beam radiation therapy, x-rays continue depositing radiation as they exit the human body. This means that the radiation leaving the body may damage nearby healthy tissue and that damage can cause side effects. The chief advantage of proton therapy over other types of external beam radiotherapy is that as a charged particle, the dose is deposited over a narrow range and there is minimal exit dose. These charged particles damage the DNA of cells, ultimately killing them or stopping their reproduction. Cancerous cells are particularly vulnerable to attacks on DNA because of their high rate of division and their reduced abilities to repair DNA damage. Some cancers with specific defects in DNA repair may be more sensitive to proton radiation. [ ] Furthermore, the dose delivered to tissue is maximized only over the last few millimetres of the particle's range; this maximum is called the Bragg peak, often referred to as the SOBP (the SOBP is the sum of several individual Bragg peaks at staggered depths). To treat tumours at greater depths, the proton accelerator must produce a beam with higher energy, typically given in eV or electron volts. Accelerators used for proton therapy typically produce protons with energies in the range of 70 to 250 MeV. Adjusting proton energy during the treatment maximizes the cell damage the proton beam causes within the tumour. Tissue closer to the surface of the body than the tumour receives reduced radiation, and therefore reduced damage. Tissues deeper in the body receive very few protons, so the dosage becomes immeasurably small. In most treatments, protons of different energies with Bragg peaks at different depths are applied to treat the entire tumour. The total radiation dosage of the protons is called the spread-out Bragg peak (SOBP). It is important to understand that, while tissues behind (or deeper than) the tumour receive almost no radiation from proton therapy, the tissues in front of (shallower than) the tumour receive radiation dosage based on the SOBP. [w] After the end of the Second World War, building on discoveries made during work on the Manhattan Project and other activities, a group of scientists and physicists developed particle

accelerators of much higher energy and began applying what they had learned to help benefit mankind. They focused on the application of nuclear medicine for diagnostic purposes and the treatment of certain diseases. One particular interesting possibility had to do with improving the treatment of cancerous tumours, especially those previously unreachable or not treatable without inducing significant damage to healthy surrounding tissues. The first suggestion that energetic protons could be an effective treatment method was made by Robert R. Wilson in a paper published in 1946 while he was involved in the design of the Harvard Cyclotron Laboratory. Today the larger proton therapy centre in the world is the Roberts Proton Therapy Center in Philadelphia, PA (USA). This centre is a part of Penn's Abramson Cancer Center, University of Pennsylvania Health System. In August 2013, the UK government confirmed that £250 million would be made available to build two UK proton therapy centres – one at the Christie Hospital in Manchester, the other at UCL Hospital in London. They're due to open in 2018, and there's also an option on the table to have a third facility in Birmingham at some point in the future. This is a big sum of money for just two treatment centres that are expected to treat around 1,500 patients per year between them – many more people than are currently sent abroad (mainly in the USA) for proton therapy.

Another centre of excellence for both proton therapy and neutron therapy, is located in Obninsk, Kaluga Oblast (Russia) at about 2 hours by car from Moscow airport Domodedovo (about 110 km southwest of Moscow), where is also based the World's First Nuclear Power Plant since 27 June 1954. The nuclear reactor, used to generate electricity, heralded Obninsk's new role as a major Soviet scientific city, a status it retains in the Russian Federation where it carries the sobriquet of First Russian Science City. In Obninsk is based the *Medical Radiological Research Center A.F. Tsyba* - a branch of the federal state budgetary institution "National Medical Research Center for Radiology" of the Ministry of Health of the Russian Federation (the Tsyba MSC - a branch of the NMI of Radiology of the Ministry of Health of Russia) that is one of the oldest radiological centers in Russia. The MRRC A.F. Tsyba, originally was the Institute of Medical Radiology of the Academy of Medical Sciences of the USSR and, was founded in 1962 to develop and improve methods of radiation diagnosis and radiation therapy, prevent, and treat radiation damage, and study the biological and medical effects of ionizing radiation. The Center is the head on the problem of radiology and radiation medicine, the leading institution in the Russian Federation to develop and apply high-tech radiological methods for the diagnosis and treatment of patients with oncological and non-oncological diseases. The basis of most of the Center's development of methods for treating patients is the principles of increasing the effectiveness of treatment, organ preservation and improving the quality of life. The Center's advantage is an integrated approach that allows to

conduct necessary examinations and treatment and to provide the patient with access to innovative technologies for the prevention, diagnosis, and treatment of malignant neoplasms. The staff of the Center consists of 1779 people of which about 310 researchers (mainly physicists), including about 59 doctors.[ ]

1.2.2. EXPERIMENTAL

1.2.3. CONCLUSION

…….

In my opinion the great advantage of this technology …..

Konstantin Eduardovich Tsiolkovsky, known also as K. E. Tsiolkovskii, Jurij Alekseevič Gagarin and Stanislav Evgrafovič Petrov.

1.2.4. ACKNOWLEDGEMENTS

I would like to acknowledge for this project my PhD Coordinator and Supervisor Prof Mario Morino because allowed me to go to Obninsk. It is a pleasure to acknowledge the assistance of Prof Marina Filmonova – Head of the Radiopharmacology Laboratory, her wonderful PhD students Victoria, Katia and Tatiana and all her staff for their hospitality in Russia, and Prof Sergey Ivanov – Acting Director of MRRC, for the kind invitation and permission to visit the A. Tsyb Medical Radiological Research Center (branch of the National Medical Research Radiological Center of the Ministry of Health of the Russian Federation, Obninsk, Russia). I acknowledge Prof Albert Browin for explaining me lots of clinical details about the Proton Therapy and the Neutron Therapy. I acknowledge the Embassy of the Russian Federation of London for the visa, the Russian National Tourist Office of London for the kind assistance and the insurance, and the UCLU student desk for their advices to apply for a Russian visa. I am also grateful to Dr Roberto Alessio – official translator of Turin Court for helping me translating all the documents written in Cyrillic alphabet.

Figure. The monument at Konstantin Eduardovich Tsiolkovsky in Obninsk – Kaluga – Russia (own pictures).

Figure. The monument at Konstantin Eduardovich Tsiolkovsky outside the Brisbane Planetarium in Brisbane – Queensland – Australia.
(International Conference: Innovate Medicine, 29th–30th November 2017 – Brisbane).
The statue, by Sergei Bychkov, was donated to Queensland during Russia Week in Australia in 2007, the 150th anniversary of the birth of Tsiolkovsky. Source: Google Library.

Chapter 2

New Materials to improve diagnosis, therapy and surgery

2.1. A new polyurethane for an in vitro model of the cardiac tissue

2.1.1. INTRODUCTION

The aim of this work is firstly to overcome the current lack of models for the study of the physiological conditions through the development of an *in vitro* dynamic model, able to reproduce the myocardial tissue. The idea to develop alternatives methods to the practice of animal experimentation was officially presented to the European Parliament on 26th June 2013. The way to proceed will be to make non-animal alternative methods, wherever applicable, compulsory, and to encourage their further development, in a concerted drive towards the rapid abolition of the useless and risky practice of animal experimentation. The practice of animal experimentation and testing have never formally undergone the process of "validation", which is currently required of all new testing methods. Polyurethanes today have the realistic potential to be advantageous materials due to their high versatility that, according to the selected starting reagents, allows to adapt their physical, thermal, mechanical, and biological properties to the final application.

To satisfy the target an elastomeric biodegradable polyurethane (K-BC 2000) was synthesized through a two steps procedure starting from poly-ε-caprolactone diol (Mn = 2000Da), 1,4-butane diisocyanate and L-lysine ethyl ester. Then this polyurethane was processed via Thermally Induced Phase Separation (TIPS) under application of a cooling gradient in order to obtain oriented fibers

texture, like the cardiac muscle tissues topography. Polyurethane scaffolds obtained with TIPS were functionalized with fibronectin, one of the main components of the cardiac ECM proteins. The functionalization was performed by plasma treatment with argon and acrylic acid, followed by the activation of carboxylic groups by N'-(3-dimethylaminopropyl)-N-ethylcarbodiimide in combination with N-hydroxysuccinimide, and the coupling with fibronectin. The constructs were characterized by SEM, contact angle, XPS and mechanical test, showing mechanical properties and morphology similar to those of native tissue (Fig.). Functionalized scaffolds were seeded with cardiac cells prepared from neonatal Sprague-Dawley rats. To evaluate the cardiomyocyte self-beating activity, scaffolds were analyzed from four days after cell seeding every two days, by using fluorescent microscopy. Time lapse analysis demonstrated that cells beat synchronously from day 7 and for over 50 days.

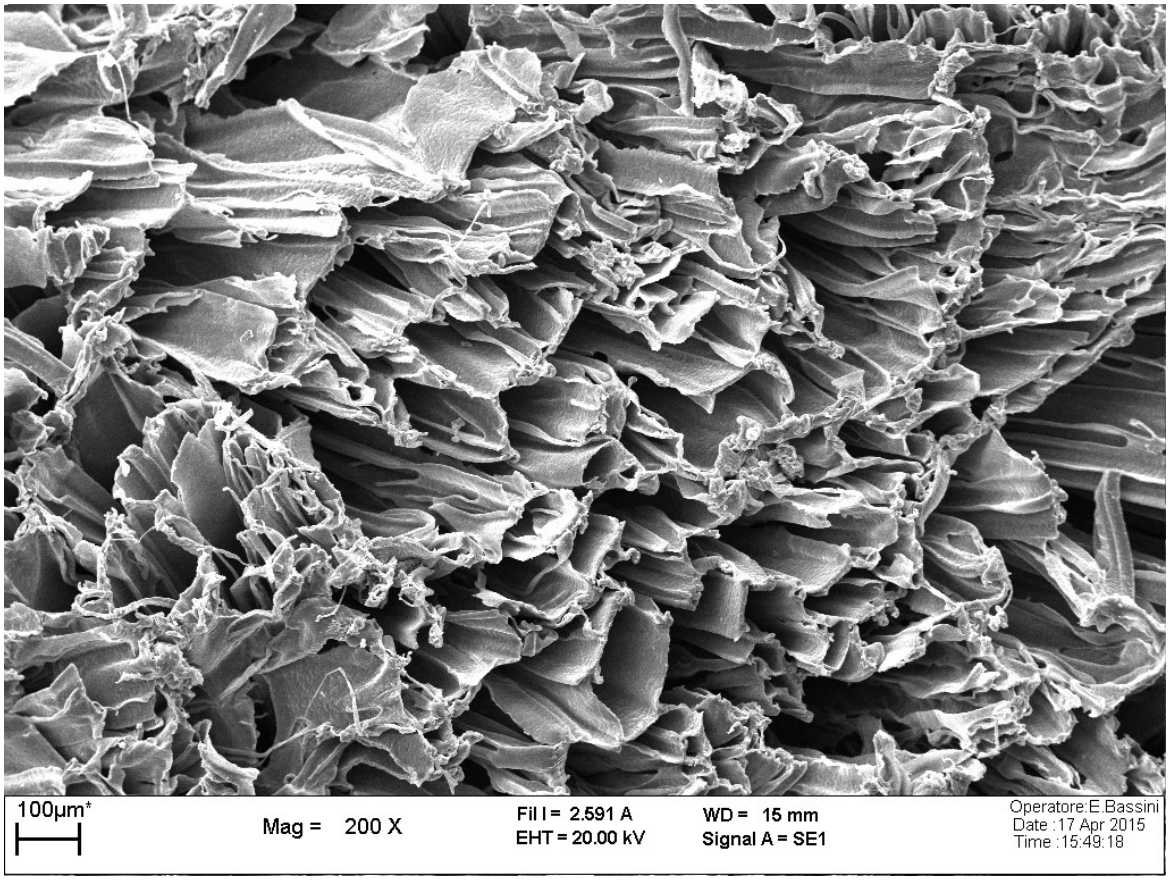

Figure . The SEM micrograph of my scaffold.

2.1.2. EXPERIMENTAL

The MIND project started in 2010, it was fully financed by the Italian Ministry of Education (MIUR) and it involved five Italian universities: Polytechnic School – University of Turin, Polytechnic School – University of Milan, University of Turin – Molecular Biotechnology Center, University of Genoa – Dibris Dept., CNR of Pisa – Institute of clinical physiology and University of Rome – Biomedical campus. The MIND project aims at overcoming the current lack of models for the study of the physiological conditions associated with aging through the development of *in vitro* dynamic models, able to reproduce the physio-pathological conditions of aged tissues, while respecting the principle of animal testing. [ ] Polyurethanes today have the realistic potential to be advantageous materials due to their high versatility that, according to the selected starting reagents, allows to adapt their physical, thermal, mechanical and biological properties to the final application. A new elastomeric biodegradable polyurethane for an *in vitro* model of the cardiac tissue was synthesized and processed in order to obtain oriented fibers texture, like the cardiac muscle tissues topography. [ ]

Materials and methods: It is well known the importance of reproducing the mechanical anisotropy of cardiac tissue. The application of isotropic scaffolds for the regeneration of anisotropic tissues might confer isotropic properties to the newly formed tissue that prevent its structural and mechanical integration in the native environment. [ ]

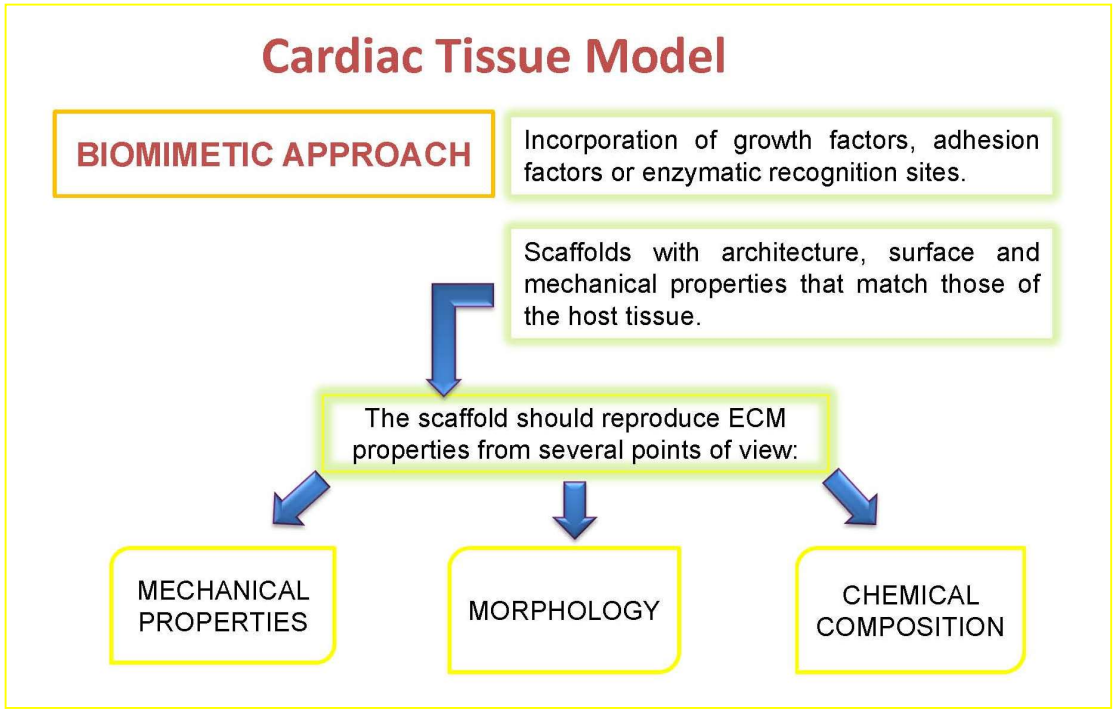

Figure . The Cardiac tissue model.

The elastomeric biodegradable polyurethane (acronym K-BC 2000) used in this work was synthesized through a two steps procedure starting from14g of PCL or *poly-ε-caprolactone diol (Mn = 2000 Da),* 2,014g of *1,4-butanediisocyanate* and 1,776g of *L-lysine ethyl ester* (as chain extender) as shown in the picture below. Solvents used for the synthesis: DCE anhydrous, DCE, DMF and methanol. All the ingredients have been purchased from Sigma-Aldrich®.

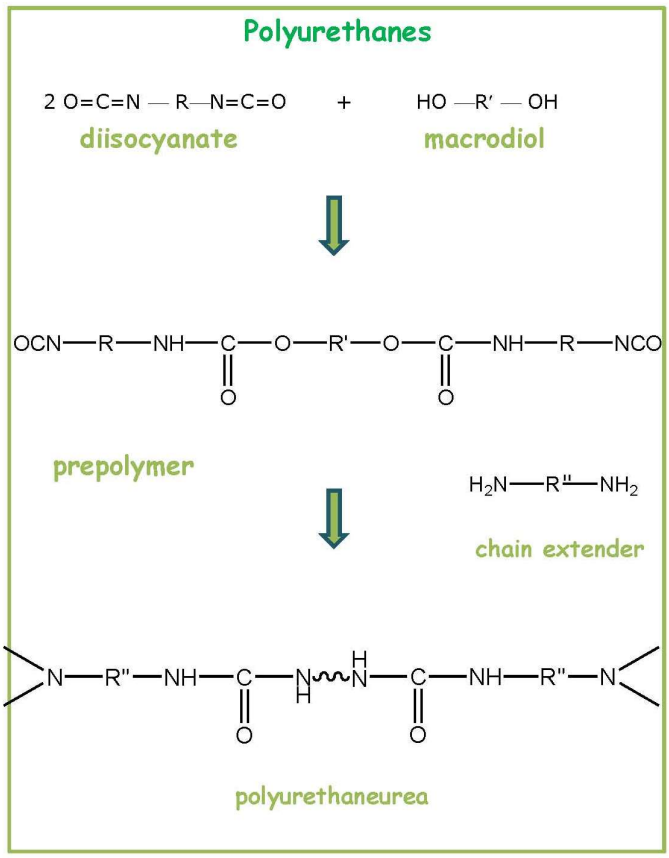

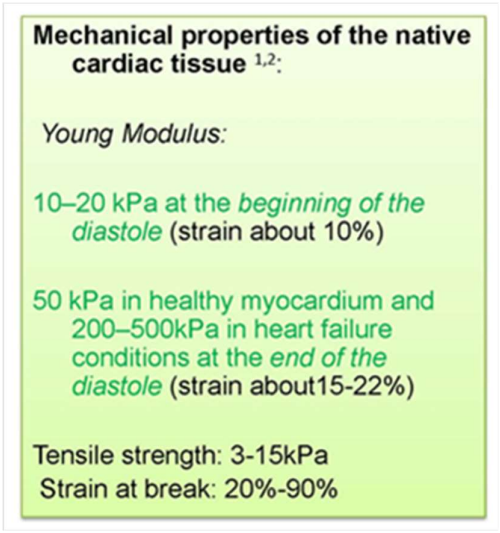

Figure . The PU synthesis through a two steps procedure and the mechanical properties it aims to reproduce.

After the PU synthesis, the following step has been the scaffold fabrication by using a technique called Thermally Induced Phase Separation (TIPS) under application of a cooling gradient.

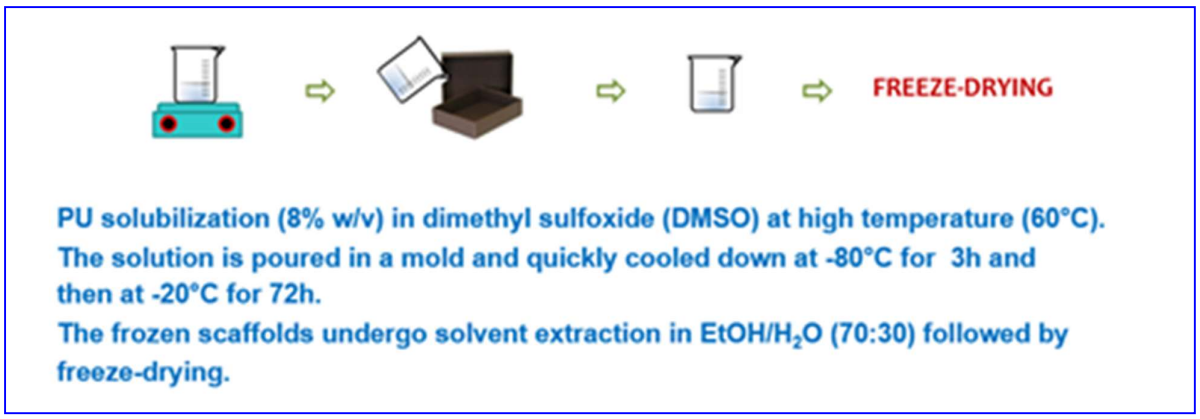

Figure . The Scaffold Fabrication (morphology).

The final step has been the scaffold functionalization with fibronectin, one of the main components of the cardiac ECM proteins. It has been performed through a plasma treatment with argon and acrylic acid, followed by the activation of carboxylic groups by using 5mg of EDC or *N'-(3-dimethylaminopropyl)-N-ethylcarbodiimide* in combination with 1,25mg of NHS or *N-hydroxysuccinimide* for 1ml of water solution (pH 5), and finally coupling with 5mg of human fibronectin protein (it has been purchased from YO Proteins, Sweden) in 5ml PBS solution at 37°C (pH 5), filtered through a 0,2µm membrane filter. All details are shown in the following picture.

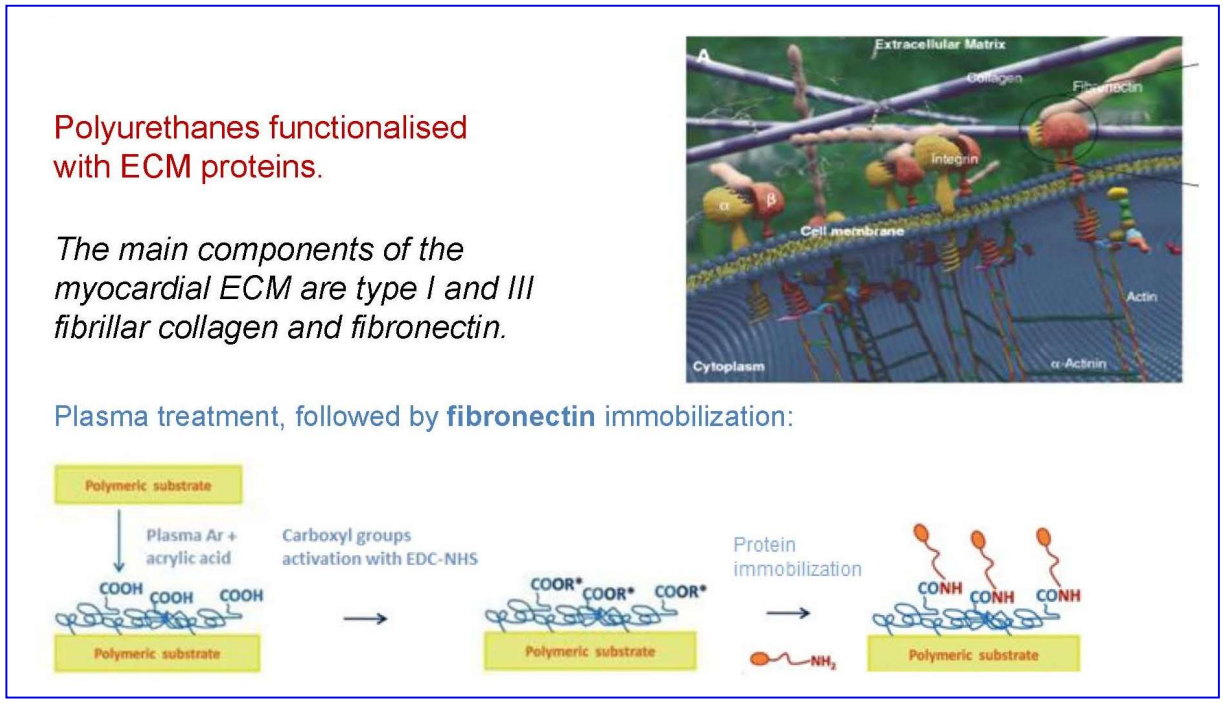

Figure . The scaffold functionalization with human fibronectin, conc. 1mg/ml (chemical composition).

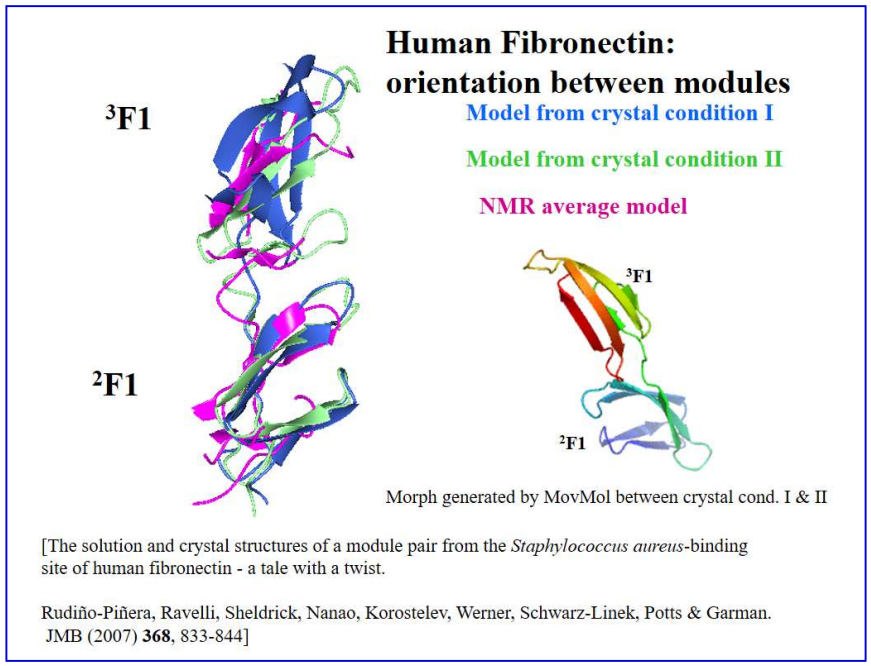

Figure . The Human Fibronectin, courtesy of Prof Elspeth Garman – Dept. of Biochemistry, Oxford University (UK).

The characterization of Polyurethane (PU) scaffolds. The microstructural morphology of *young* and *aged* samples will be compared in terms of porosity, mean pore radius and mean pore roundness. By using a cryotome, PU slices with a thickness of 80μm were cut. Samples were embedded in a proper medium before cutting. Sections were obtained both from the top face (top section) of the scaffold and from the lateral face (transverse section). The results for 1 top section and 8 transversal sections will be presented for both a *young* and an *aged* sample. The height maps of each slice have been obtained by means of a laser scanning confocal microscope (LEXT-OLS4100, Olympus) and a MATLAB script has been used for segmentation purposes. Specifically, a binary image has been obtained out of each height map, specifying a height threshold as a fraction of the maximum height value obtained in a slice. Height data were considered voids (white) if below the aforementioned threshold, while matrix (black) otherwise. Since the choice of the height threshold affects the segmentation results, the influence of this parameter will be discussed in the results session. Finally, a MATLAB script has been used to compute the following morphological quantities (porosity, roundness and mean pore radius) and the wall thickness (t_w) was also measured by direct measurement on reflected intensity confocal images. Since this measurement was not automated by means of a script, while operated manually, only 1 slice out of the 8 slices available for transverse sections was considered for the measurement of an average value of the wall thickness of *young* and *aged* samples. Among the available slices, those showing sharper cuts were selected.

$$porosity, \quad \rho = \frac{voids\ (white\ data)\ area}{Field\ of\ View\ area} = \frac{A_v}{A_{FoV}}$$

$$roundness, \quad c = \langle 4\pi \frac{i-th\ void\ area}{i-void\ squared\ perimeter} \rangle = \langle 4\pi \frac{A_i}{P_i^2} \rangle$$

$$mean\ pore\ radius, \quad R = \langle \sqrt{\frac{A_i}{\pi}} \rangle$$

were, $\langle a \rangle = \frac{1}{N} \sum_{i=1}^{N} a_i$

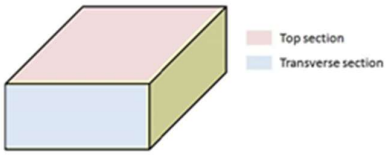

Figure . The sketch of the orientation of cryotome cuts on the PU scaffold samples. Courtesy of Prof Pasquale Vena – Polytechnic School – University of Milan.

The characterization results: on the influence of the segmentation threshold on the morphological quantities. In order to discuss the influence of the height threshold on segmentation results, the case of a top section of an aged sample will be presented in continue. When segmentation is pursued as described in the Methods section, the height threshold would have no influence on the final binary image in the ideal case featuring (i) a perfectly flat cutting plane and (ii) microstructural wall

perfectly orthogonal with respect to the cutting plane. Indeed, the top surface of the slice is heterogeneous (Figure), suggesting that the material was partially drawn by the blade during the cut. Furthermore, the walls of the microstructure are at an angle with respect to the cutting plane (Figure). This might be either due to the overall orientation of the sample with respect to the blade or due to the inherent heterogeneous microstructural arrangement of the pores. The influence of the segmentation threshold was investigated comparing the values of the morphological quantities computed for threshold values (t) between 0 and 1, with 0.05 increment. Intuitively, one can imagine that increasing the segmentation threshold leads to thinner matrix walls (Figure).

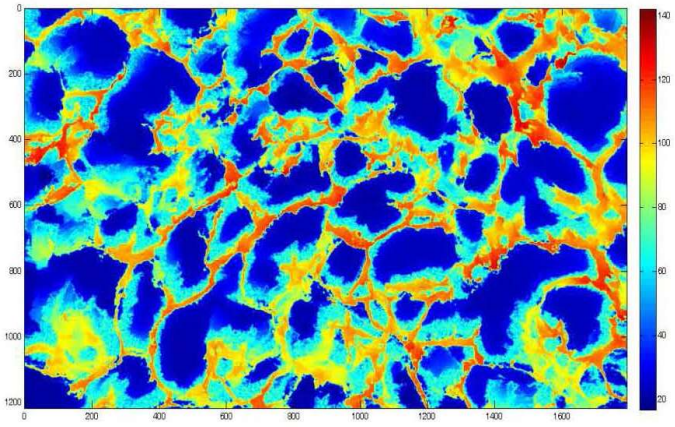

Figure . Height map of a top section of an aged sample. Courtesy of Prof Pasquale Vena – Polytechnic School – University of Milan.

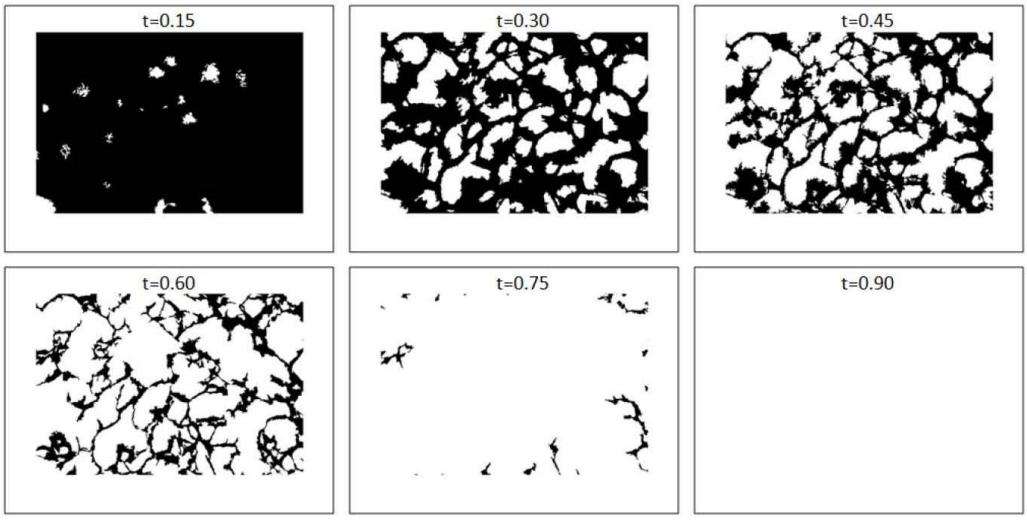

Figure . Example of binary image of the same height map for different segmentation threshold choices. Courtesy of Prof Pasquale Vena – Polytechnic School – University of Milan.

A quantitative picture of the influence of the segmentation threshold is given by the following figures. The choice of the threshold highly affects the porosity. It was not possible to identify a range of segmentation values resulting in a constant value of computed porosity (Figure). This reliability of the porosity values computed with this approach is then judged poor.

A relatively stable value of roundness and mean pore radius was found for segmentation thresholds between 0.2 and 0.6 (Figure and Figure , respectively). The roundness value range between 0.3 and 0.4, meaning that most of the pores are far from being circular (i.e. $c = 1$).

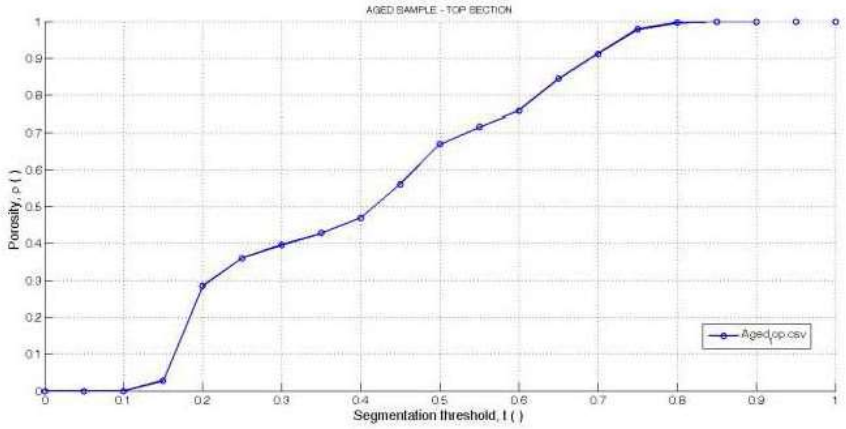

Figure . Porosity values computed for the same slice segmented with different height thresholds. Courtesy of Prof Pasquale Vena – Polytechnic School – University of Milan.

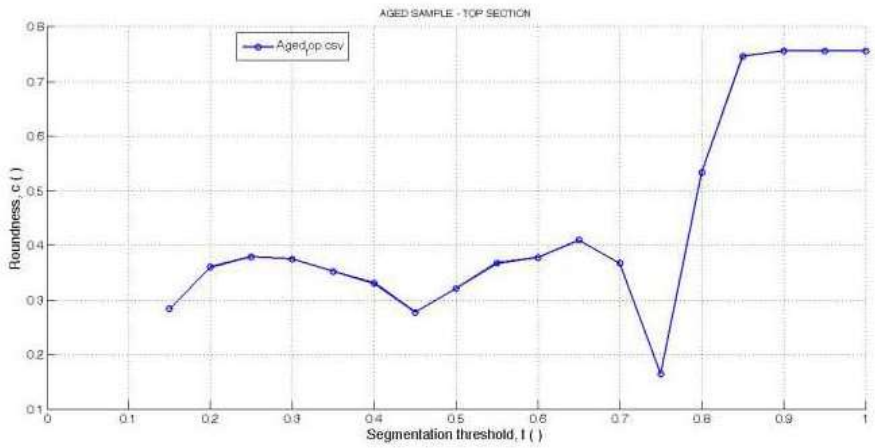

Figure . Roundness values computed for the same slice segmented with different height thresholds. Courtesy of Prof Pasquale Vena – Polytechnic School – University of Milan.

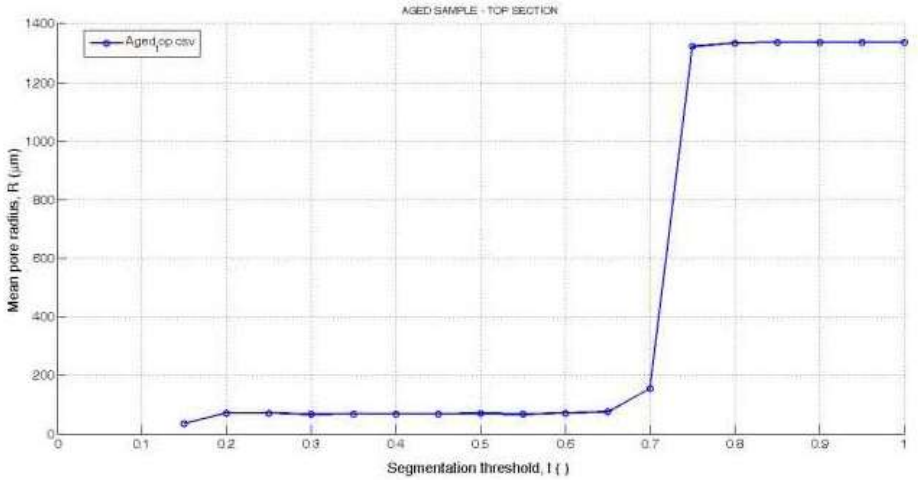

Figure . Mean pore radius computed for the same slice segmented with different height thresholds. Courtesy of Prof Pasquale Vena – Polytechnic School – University of Milan.

A detail on the mean pore radius computed between $t = 0.2$ and $t = 0.6$ shows that R is in the range of 70μm.

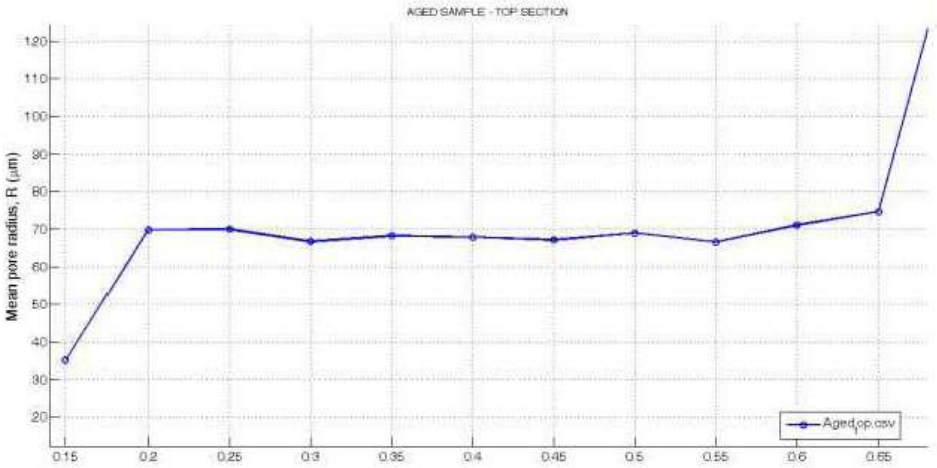

Figure . Detail of the plateau value obtained for the mean pore radius. Courtesy of Prof Pasquale Vena – Polytechnic School – University of Milan.

A similar behavior was found for the top section of a young sample (Figure) and for the transverse sections of both aged and young samples (Figure and Figure , respectively). When comparing curves of different slices belonging to the same sample, a further comment is suggested on the definition of the segmentation threshold: besides showing a similar trend, an offset seems to affect the results of some slices. Since the threshold is defined as a fraction of the maximum height of each height map, the same threshold value may correspond to different values in terms of absolute

height, depending on the specific slice which is queried. To investigate the influence of the segmentation threshold in terms of absolute height values would be a more proper choice.

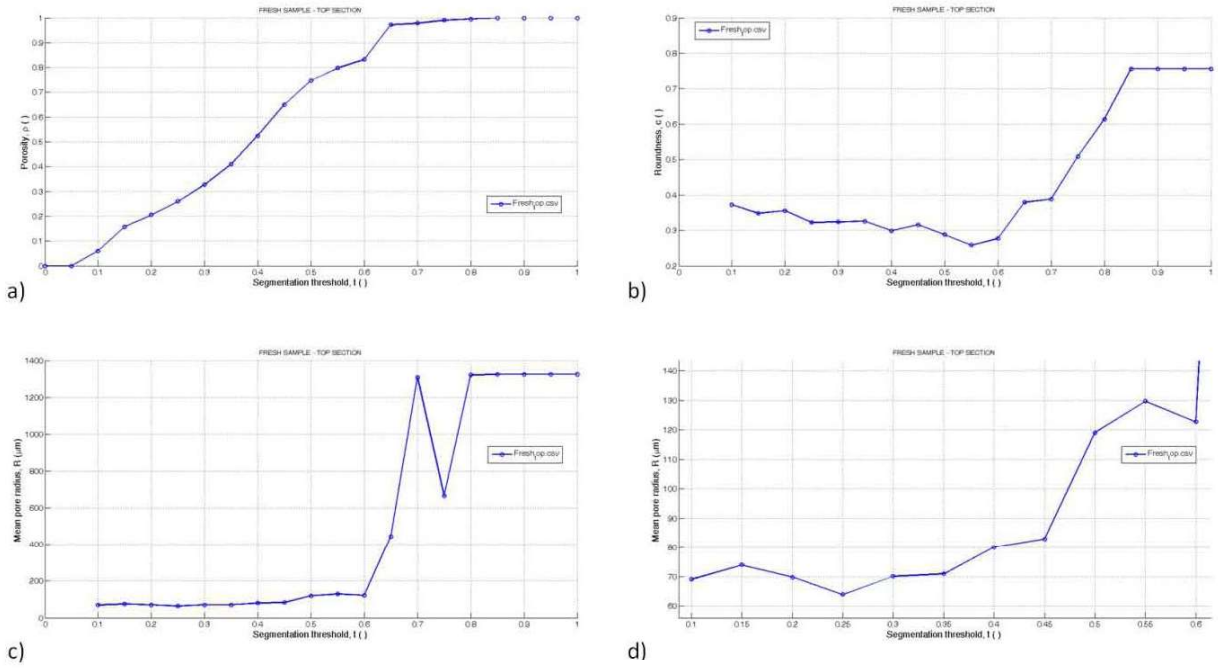

Figure . Results of the morphological characterization on the *top section of a fresh sample*. The plots show the values of (a) porosity, (b) roundness and (c) mean pore radius computed for segmentation thresholds varying between 0 and 1. A detail on the region of relatively stable values of the mean pore radius is shown in the inset (d). Courtesy of Prof Pasquale Vena – Polytechnic School – University of Milan.

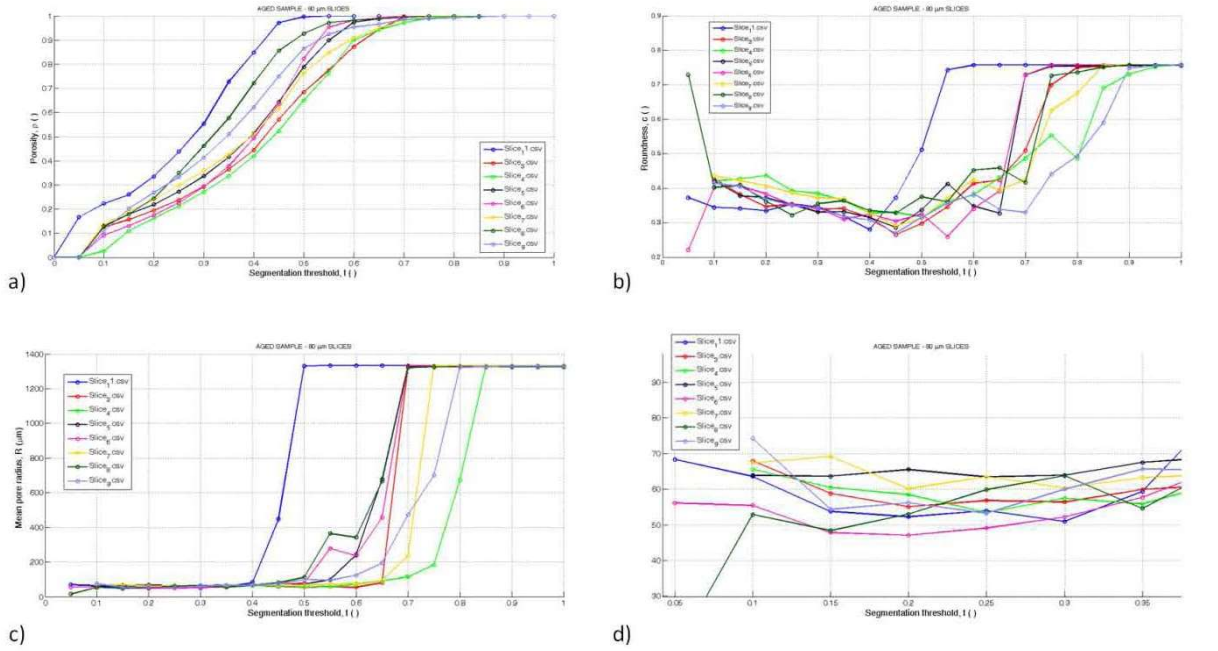

Figure . Results of the morphological characterization on the *8 transverse sections of an aged sample*. The plots show the values of (a) porosity, (b) roundness and (c) mean pore radius computed for segmentation thresholds varying between 0 and 1. A detail on the region of relatively stable values of the mean pore radius is shown in the inset (d). Courtesy of Prof Pasquale Vena – Polytechnic School – University of Milan.

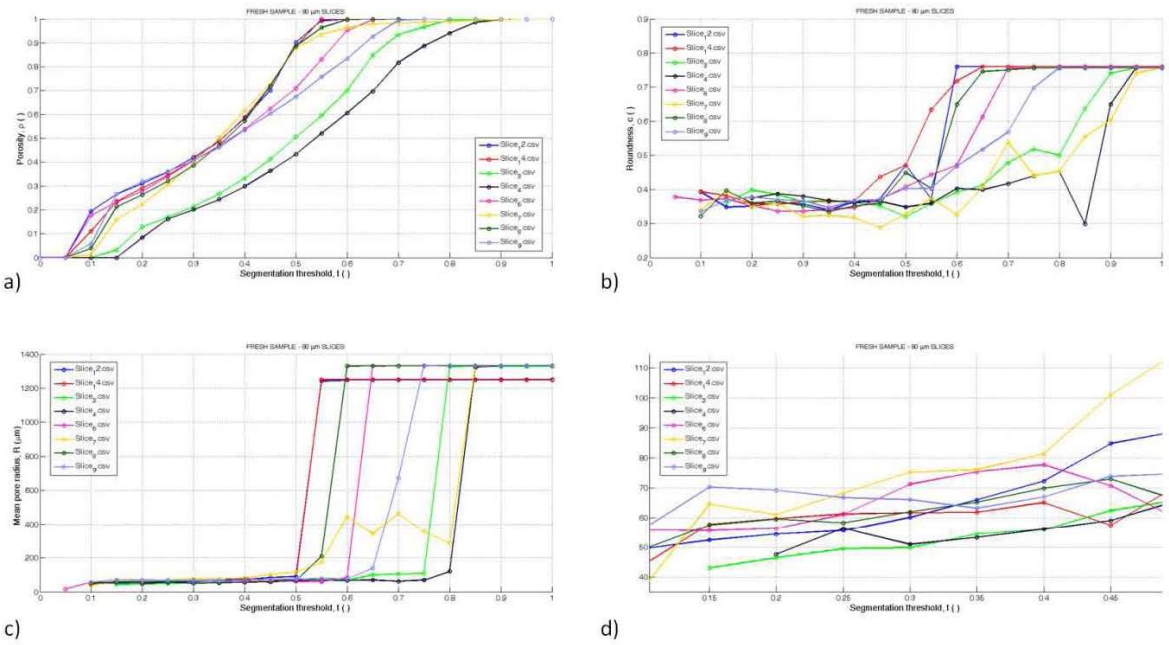

Figure . Results of the morphological characterization on the *8 transverse sections of a fresh sample*. The plots show the values of (a) porosity, (b) roundness and (c) mean pore radius computed for segmentation thresholds varying between 0 and 1. A detail on the region of relatively stable values of the mean pore radius is shown in the inset (d). Courtesy of Prof Pasquale Vena – Polytechnic School – University of Milan.

Although the present segmentation method didn't show promising results in terms of reliability, a comparison between young and aged samples in terms of morphological parameters will be presented in the following paragraph. Based on previous comments, a segmentation threshold t = 0.40 has been selected to compare different samples, this value falling within the range of segmentation parameters providing stable mean pore radius estimates for all the processed slices.

The characterization results: on the comparison between *young* and *aged* samples. A qualitative comparison between representative height maps of fresh and aged samples is reported in Figure .

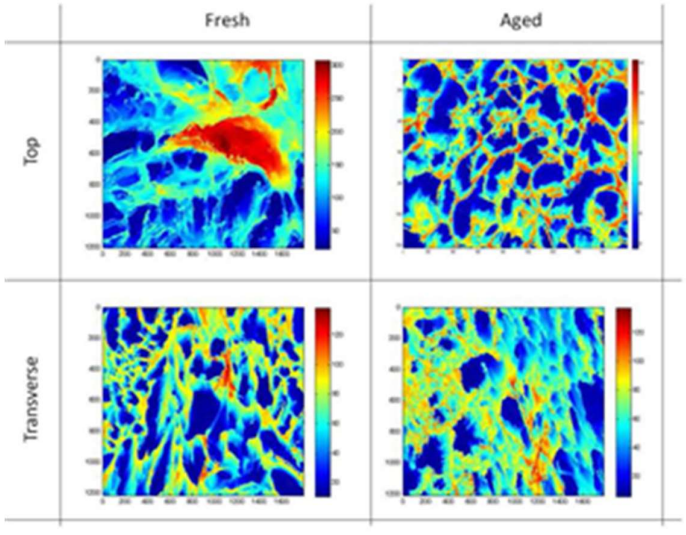

Figure . Qualitative comparison between height maps of young (indicated as fresh) and aged samples. Courtesy of Prof Pasquale Vena – Polytechnic School – University of Milan.

In continue, a quantitative comparison of morphological quantities is presented. Since only 1 top slide was available for each sample type, the corresponding results were computed as defined in the Methods section. Since 8 transverse slides were available for each sample type, results for the transverse sections were further averaged among the results of each single slide. Thus, the standard deviation values are reported only in the case of transverse sections. As concerns porosity (Figure), aged samples displayed lower porosity (-11.3%) as compared to young samples when comparing top sections, while the inverse trend (+11.8%) appeared when comparing the transverse sections. Nevertheless, when the standard deviation values are considered for the transverse section, no significant difference can be identified. Such a wide scattering of experimental results is assumed to be due to the current definition adopted for the segmentation threshold. As already mentioned, the same segmentation threshold corresponds, at the moment, to different absolute height values, which results in a horizontal shift of the curves describing the behavior of porosity vs segmentation threshold (see Figure and Figure). Switching to a definition of segmentation threshold to absolute height values is expected to improve results reliability and is recommended as a future task.

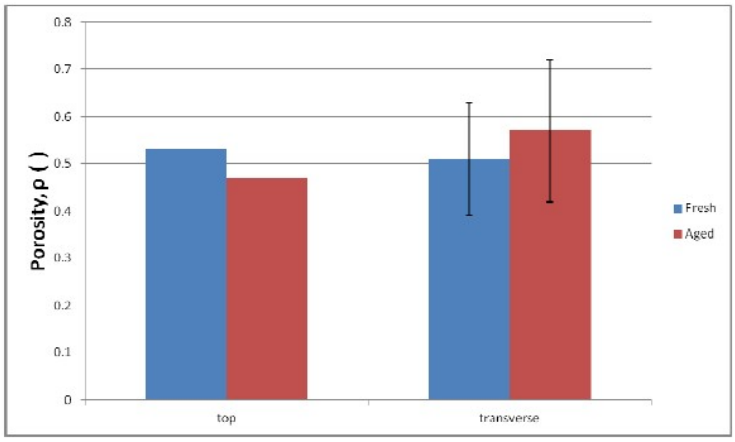

Figure . Quantitative comparison between the values of *porosity* computed for young (indicated as fresh) and aged samples, both in top and transverse sections. Courtesy of Prof Pasquale Vena – Polytechnic School – University of Milan.

Similar arguments apply for the roundness of pores (Figure). Nevertheless, in this case it can be argued that, while the roundness of aged samples does not seem sensitive to the orientation of the cut, for young samples the pores display a slightly higher roundness in the transverse sections as compared to the top sections.

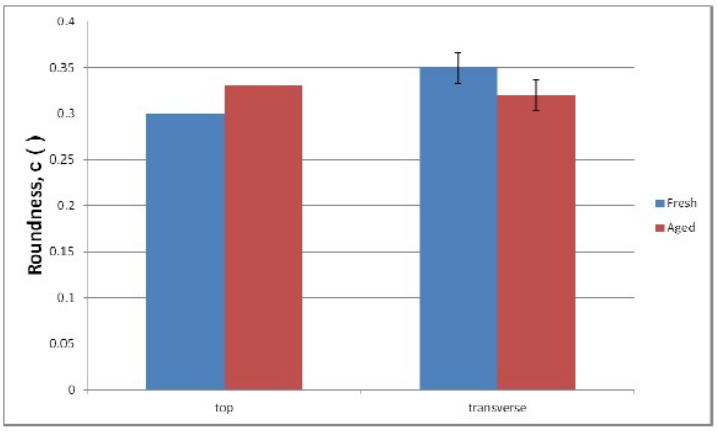

Figure . Quantitative comparison between the values of *roundness* computed for young (indicated as fresh) and aged samples, both in top and transverse sections. Courtesy of Prof Pasquale Vena – Polytechnic School – University of Milan.

The difference in terms of mean pore radius seems also sensitive to the orientation of the cut. Pores in young top sections were found to be bigger (80µm) as compared to young transverse sections and aged sections (Figure).

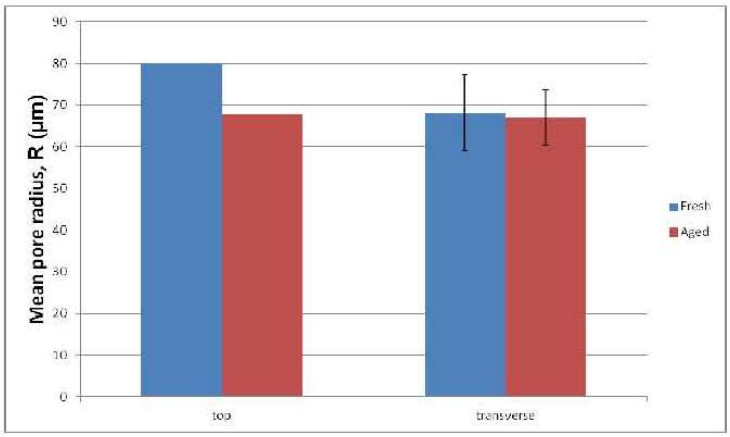

Figure . Quantitative comparison between the values of *mean pore radius* computed for young (indicated as fresh) and aged samples, both in top and transverse sections. Courtesy of Prof Pasquale Vena – Polytechnic School – University of Milan.

As concerns the wall thickness, measurements were performed on a sub-region of the original field of view of the corresponding slices, were a sharper cut was found and the cross-section of the matrix walls was more visible. For this reason, the pictures reported in Figure X are magnified as compared to previous views and the scale bar indicates the correct pixel proportion.

The difference in terms of wall thickness values was more evident as compared to previous morphological quantities. The walls of aged samples were found to be 27,1% thinner as compared to young samples when top sections were considered. The same trend and a higher difference (-43,5%) was found for transverse sections. The standard deviation is again significant, most likely due to a combination of material heterogeneity and operator uncertainty.

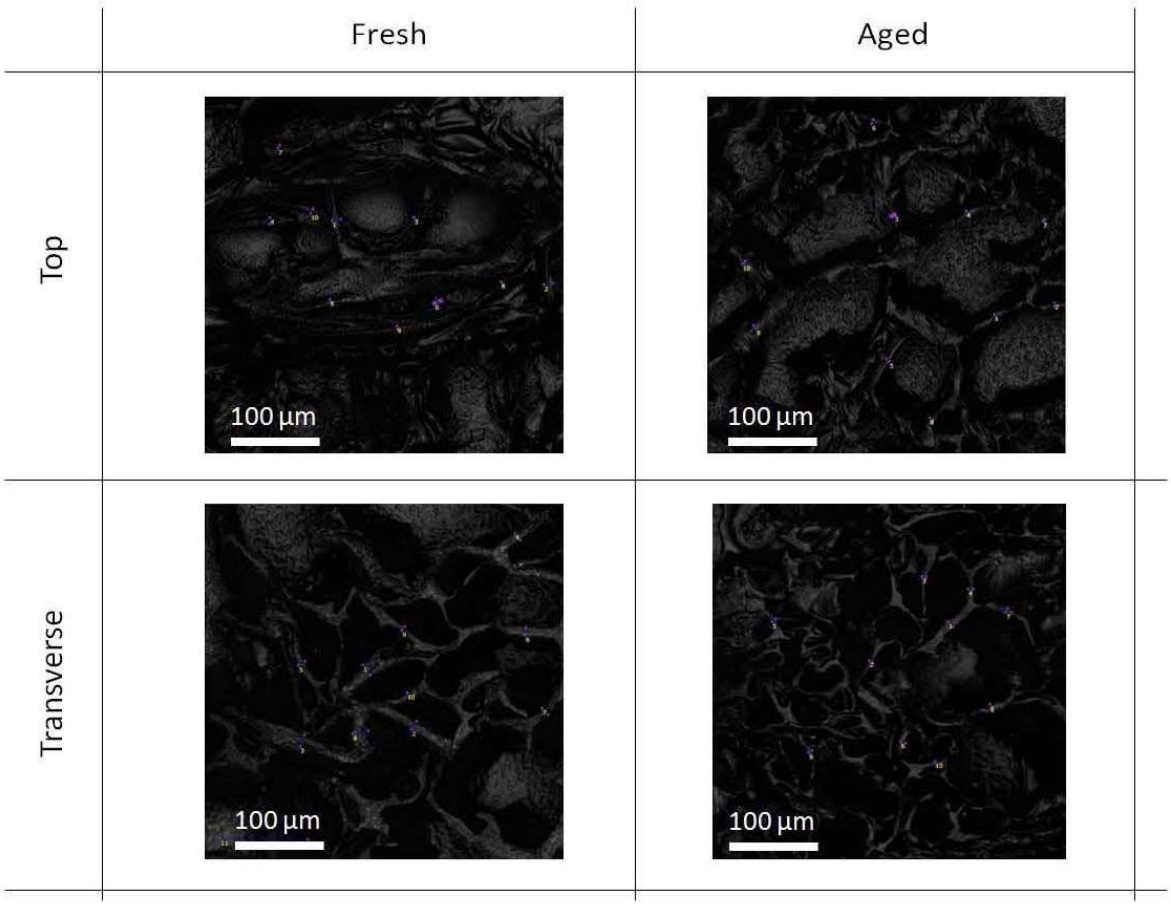

Figure X. Reflected intensity confocal images showing the regions were the wall thickness was manually evaluated, for both young (indicated as fresh) and aged samples. Courtesy of Prof Pasquale Vena – Polytechnic School – University of Milan.

As already mentioned, the cut is usually at an angle with respect to the scaffold walls, thus the use of the height profile to discriminate the thickness of the walls is rather unreliable. This is consistent with the reliability issues observed for the estimation of the porosity values: as long as only height maps data are concerned, measuring porosity or wall thickness can be practically considered complementary tasks, thus it is reasonable to meet similar issues. When considering reflected intensity images, the contrast between a cross section exposed by a sharp cut and the surrounding scaffold matrix is expected to be higher than in the case of height maps and profiles. For this reason, the wall thickness measurements were performed on reflected intensity images rather than height maps.

Table 1 and Table 2, respectively summarize the quantitative comparison shown in previous plots, for both top and transverse sections.

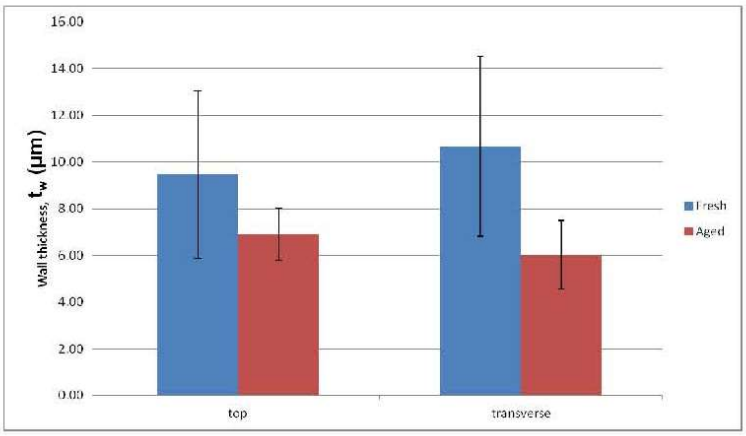

Figure . Quantitative comparison between the values of *wall thickness* computed for young (indicated as fresh) and aged samples, both in top and transverse sections. Courtesy of Prof Pasquale Vena – Polytechnic School – University of Milan.

Table 1. Summary of quantitative comparison between morphological quantities of young (indicated as fresh) and aged samples. Values refer to the *top sections*. Courtesy of Prof Pasquale Vena – Polytechnic School – University of Milan.

Quantity	Fresh sample	Aged sample	Aged vs Fresh difference
Porosity, ρ ( )	0.53	0.47	-11.3%
Roundness, c ( )	0.30	0.33	+10.0%
Mean pore radius , R (µm)	80.07	67.86	-15.3%
Wall thickness, t_w (µm)	9.46±3.59	6.90±1.11	-27.1%

Table 2. Summary of quantitative comparison between morphological quantities of young (indicated as fresh) and aged samples. Values refer to the *transverse sections*. Courtesy of Prof Pasquale Vena – Polytechnic School – University of Milan.

Quantity	Fresh sample	Aged sample	Aged vs Fresh difference
Porosity, ρ ( )	0.51±0.12	0.57±0.15	+11.8%
Roundness, c ( )	0.35±0.02	0.32±0.02	-8.6%
Mean pore radius , R (µm)	68.12±9.18	67.05±6.67	-1.6%
Wall thickness, t_w (µm)	10.67±3.86	6.03±1.46	-43.5%

Table 3. Ingredients for scaffolds fabrication (young and aged samples).

scaffold fabrication	PU	PCL	DMSO
young	1,76g	0,00g	22ml
aged	0,88g	0,88g	22ml
	50%	**50%**	**8% w/v**

Results and Discussion: polyurethanes were successfully synthesized as confirmed by Attenuated Total Reflectance Fourier Transform Infrared Spectroscopy and Size Exclusion Chromatography (Mn =70.000 g/mol). SEM results: scaffolds SEM micrographs show oriented fibers texture, like the cardiac muscle tissues topography. All the samples examined show a range of porosity between 59 – 64% calculated by using the Image J software. The measured diameter of single pores is between 100,2mm – 152,6mm.

XPS analysis results: XPS analysis of scaffolds confirmed the surface immobilization of ECM protein by changes in both chemical composition and C1s signal deconvolution. *The O/C ratio is maximum for polyacrylic acid (PAA) grafted polyurethane (PUR)*, according to the presence of the PAA layer, rich in carboxyl group. *The N/C ratio is higher in fibronectin immobilized surface*, according to the presence of several amide groups. The protein treated surface shows also the highest percentage of C–N and C–O bond and a peak attributed to amide bond, according to the protein chemical composition.

Water contact angle results: plasma activation led to a considerable reduction in the contact angle value; a decrease in wettability was observed after fibronectin immobilization.

Mechanical tests results: polyurethane film is about 14MPa. Dynamic Mechanical Analysis (DMA) of scaffolds shows a storage modulus in the dry state of about 1MPa. The elastic modulus remains constant within a wide range of frequencies, indicating a good material pliability in different physiological or pathological states (stress-controlled DMA, Frequency Sweep conditions: f =1-100 Hz; e = 1%; T = 37°C; Stress/Strain conditions: load cell = 18N, stress rate = 1N/min, T = 37°C).

Biological test results: to evaluate the cell adhesion to the polyurethane scaffolds, primary neonatal rat cardiomyocytes were stained with an Acridine Orange. Then, cardiomyocytes were seeded on scaffolds and allowed to adhere for two days. From 4 days after cell seeding, constructs were analyzed using fluorescent microscopy. As shown in Figure X, primary cells colonized the scaffold surface and remained adherent to the scaffold for more than 50 days. To evaluate the cardiomyocyte self-beating activity, scaffolds were analyzed from 4 days after cell seeding every two days using fluorescent microscopy. Time lapse analysis demonstrated that cells beat synchronously from day 7 and for over 50 days.

Porous substrates showing anisotropic properties were successfully produced through TIPS under application of a cooling gradient. Further work will be necessary to study and evaluate the cell adhesion on an aged model of the same polyurethane scaffolds.

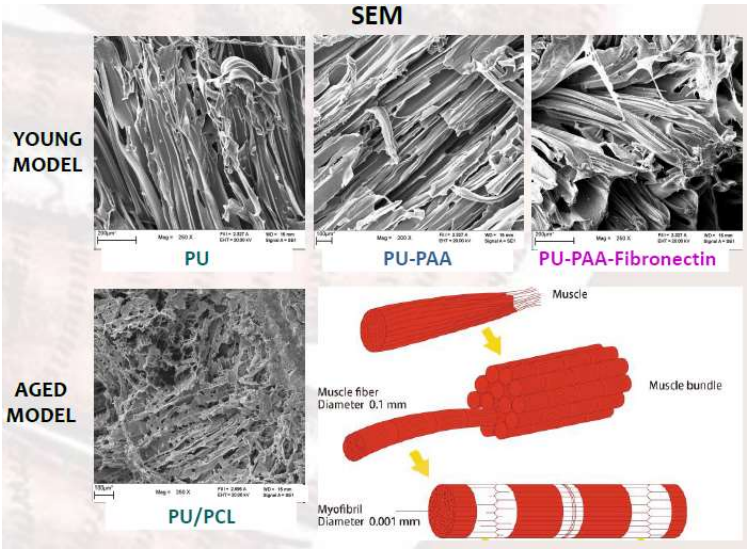

Figure . SEM micrograph of the scaffold young and aged model. The obtained polyurethane shows oriented fibers texture, like the cardiac muscle tissues topography.

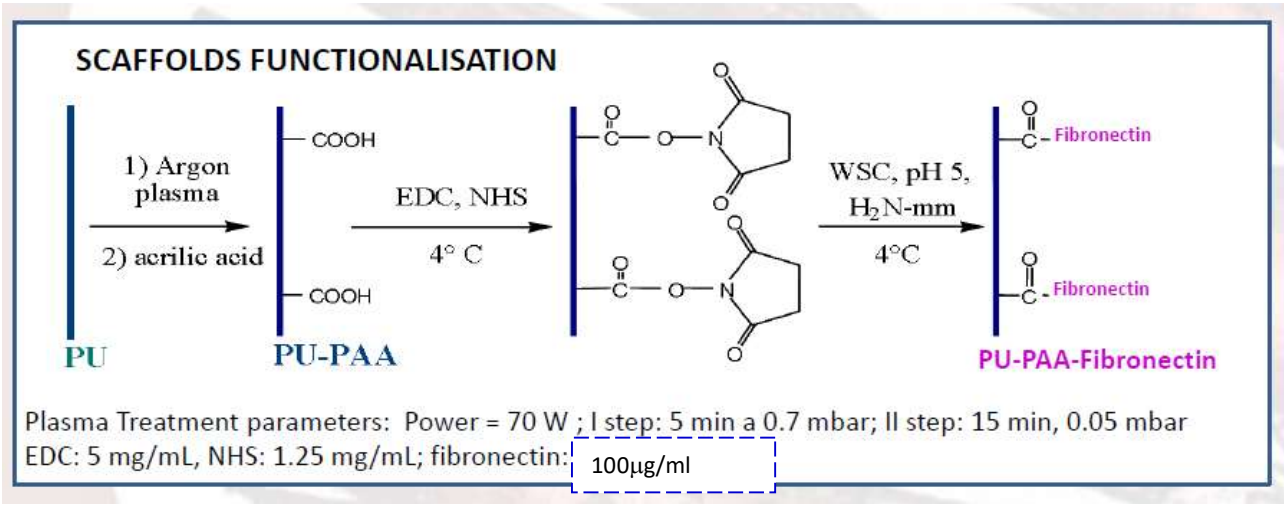

Figure . Scaffolds functionalization procedure.

Table 4. XPS analysis results.

SCAFFOLDS	C (%)	O (%)	N (%)
PUR	71.6	21.6	5.4
PUR-PAA	67.0	27.5	2.4
PUR-PAA-Fibronectin	63.4	22.0	11.8

SCAFFOLDS	C			
	C-C, C-H	C-O, C-N	CONH	COOH, COOR
PUR	15.6	29.6	-	54.9
PUR-PAA	14.2	26.4	-	59.4
PUR-PAA-Fibronectin	8.4	35.7	12.3	43.6

XPS Analysis

Table 5. Water contact angle results.

Scaffold	Angle (°)
PUR	133.3±0.8
PUR-PAA	84.0±0.5
PUR-PAA-Fibronectin	101.9±0.7

Water contact angle

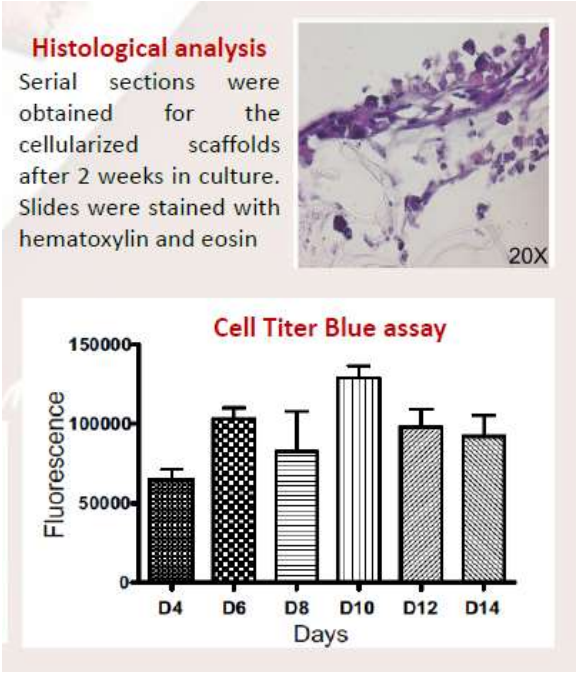

Figure . Histological analysis and Cell Titer Blue assay, courtesy of Prof Mara Brancaccio's team – MBC Dept. University of Turin (Italy).

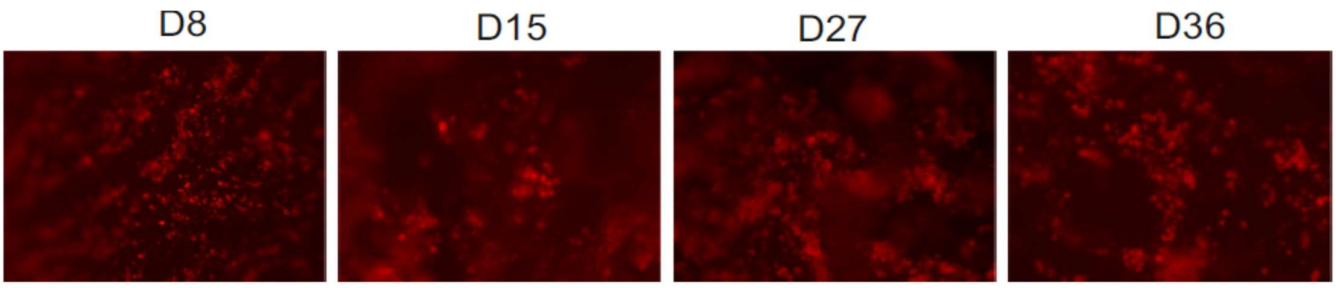

Figure . Cardiomyocyte culture after 8, 15, 27,36 days; courtesy of Prof Mara Brancaccio's team – MBC Dept. University of Turin (Italy).

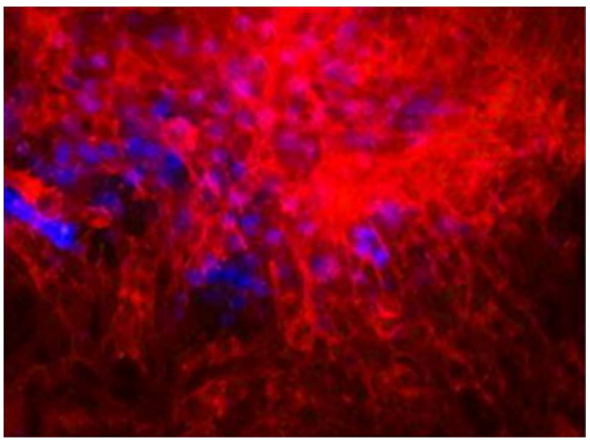

Figure . Actin cytoskeleton of myoblasts cultured for 7 days on the synthesized polyurethane (K-BC 2000); courtesy of Prof Mara Brancaccio's team – MBC Dept. University of Turin (Italy).

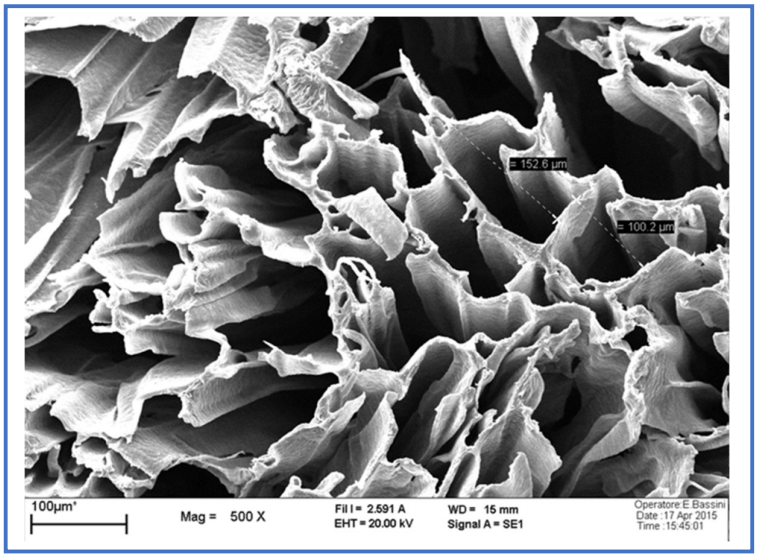

Figure . The SEM micrograph of my scaffold showing the pores size.

2.1.3. CONCLUSION

The MIND project started in 2010 and was fully financed by the Italian Ministry of Education for 5 academic years. I joined the project during the academic year 2014 – 2015 and I had nice results. Working at this project gave me the chance to synthesize a new material, a new polyurethane with precise characteristics and the target to overcome the lack of laboratory models to study the heart ageing. After the kind invitation received from the Central European Institute of Technology (CEITEC) Brno – Czech Republic, the international conference committee selected my poster for a platform presentation in the category of Biomaterials. During the event "Frontiers in material and life sciences: Creating life in 3D" International Conference on 2-4 Sept 2015, hosted in Brno (Czech Republic) my talk has been awarded by the conference committee, the Executive director of CEITEC Dr Markus Dettenhofer and also by the international press and public.

At present Myocardial Tissue Engineering and Regenerative Medicine represent a good strategy in order to revolutionize the treatment of cardiac diseases and the management of cardiac surgery. However, today there is the experimental evidence that following a good nutrition plan it will be possible to prevent common aging diseases. Prof Valter Longo – Longevity Institute, School of Gerontology, Department of Biological Sciences, University of Southern California (3715 McClintock Avenue, Los Angeles, CA 90089, USA), in one of his fascinating manuscripts explained that immune system defects are at the center of aging and a range of diseases[53]. He continues giving the experimental evidence that prolonged fasting reduces circulating IGF-1 levels and PKA activity in various cell populations, leading to signal transduction changes in long-term hematopoietic stem cells (LT-HSCs) and niche cells that promote stress resistance, self-renewal, and line-age-balanced regeneration. Multiple cycles of fasting abated the immunosuppression and mortality caused by chemotherapy and reversed age-dependent myeloid-bias in mice, in agreement with preliminary data on the protection of lymphocytes from chemotoxicity in fasting patients. The pro-regenerative effects of fasting on stem cells were recapitulated by deficiencies in either IGF-1 or PKA and blunted by exogenous IGF-1. These findings link the reduced levels of IGF-1 caused by fasting to PKA signaling and establish their crucial role in regulating hematopoietic stem cell protection, self-renewal, and regeneration[52-56]. At this point, in my opinion, it is widely clear that fasting inhibits IGF-1/PKA to promote stem-cell based regeneration in mice and humans.

1.2.4. ACKNOWLEDGEMENTS

I would like to acknowledge my PhD Coordinator and Supervisor Prof Mario Morino, my PhD Vice-Coordinator Prof Alberto Arezzo, Dr Roberto Passera – Division of Nuclear Medicine, San Giovanni Battista Hospital, University of Turin (Italy), Prof Mauro Rinaldi – Director of the Cardiac Surgery Division, San Giovanni Battista Hospital, University of Turin (Italy), and Prof Elspeth Garman – Dept. of Biochemistry, University of Oxford (UK). I acknowledge the Italian Ministry of Education (MIUR), the universities involved in the project, and Polytechnic School – University of Turin Laboratories (DIMEAS Laboratory of Turin and Biomedical Laboratory of Alessandria). It is a pleasure to acknowledge Prof Mara Brancaccio – Department of Molecular Biotechnology and Health Sciences, University of Turin, Italy and her PhD students Federica Logrand and Nicoletta Vitale for the biological tests and results on cardiomyocytes grown on my scaffolds. I acknowledge Prof Pasquale Vena – Polytechnic School – University of Milan, for the characterization of my polyurethane scaffolds and Prof Sergio Martinoia – University of Genoa – Dibris Dept., for the measures on cardiomyocytes grown on my scaffolds. I am also grateful to Dr Markus Dettenhofer – Executive director of CEITEC, and his colleagues for awarding my poster and platform presentation at the International Conference *"Frontiers in Life and Materials Sciences: Creating life in 3D"* hosted in Brno (Czech Republic)[57]. Finally, I would like to thank Dr Ugo Saini (my GP) for his kindness while I was ill and, Atty. Paola Pinciaroli and Atty. Elena Secchi for their kind support.

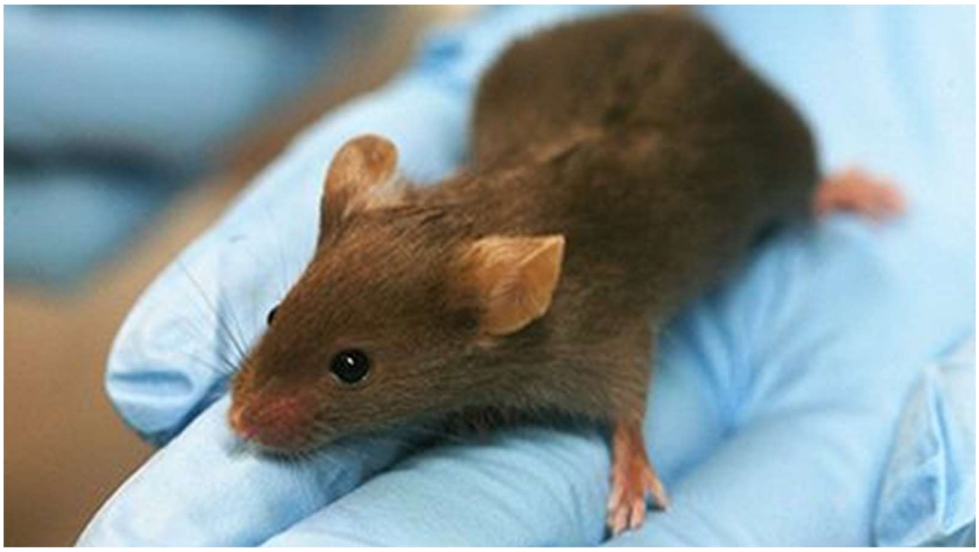

2.2. A novel bactericidal surface to reduce nosocomial infections

2.2.1. INTRODUCTION

As antibiotic resistance continues to threaten the treatment of various infections, the aim of this work concerns the design of a new coating film containing light activated antimicrobial chemicals and nanoparticles to avoid microbes spread across hospitals. This work involves developing research areas that did not exist previously, such as the light activated polymers which have been studied at Chemistry Department UCL and in some cases commercialized[58].

It is well known that methicillin-resistant Staphylococcus aureus (MRSA) is a substantial public health problem not restricted to any geographic area, but worldwide. The same is true for the opportunistic pathogen Pseudomonas aeruginosa. Micro-organisms selected for this study were Epidemic MRSA 4742 representative of a Gram-positive epidemic bacteria isolated at UCL Hospital and Pseudomonas aeruginosa PAO1 as well as the clinical strand isolated at UCL Hospital representative of Gram-negative bacteria resistant to the majority of currently used antibiotics. Concerning this one a complementary study of its biofilm-mediated resistance to antibiotics has been followed supported by Prof E. Sapi (USA) and her team; [See Chapter 3 of this thesis].

To satisfy the target the dye selected was crystal violet or gentian violet because it has been demonstrated that in vitro it can disrupt Pseudomonas aeruginosa biofilms and it can kill MRSA. The nanoparticles (NPs) used for this study were silver ions because the antimicrobial activity of Ag+ ions is well documented and reviewed. The antimicrobial polyurethane coating films produced were tested against these micro-organisms to demonstrate their efficacy[59]. It has been also studied the critical importance of the presence of silver nanoparticles to improve the functional property of the inanimate surface following Prof. N. Carlone (Italy), Prof. M. Vasil (USA) and Prof. E. Pohl (UK) suggestions. Antimicrobial activity of control and treated polyurethane samples on 4742 MRSA and PAO1 after 5 hours of incubation at 500 lux has been examined. There is no MRSA growth with crystal violet (CV) solution and CV + Silver NPs solution in 5 hours. The situation changes in the case of PAO1 where the growth is reduced only by the solution containing silver NPs in 5 hours. However, after an incubation time of 24 hours in the dark a significant antimicrobial activity was observed.

Silver NPs used for this work remain inside of the polyurethane matrix – they stay into the bulk and not on the surface and exhibit potent antimicrobial activity. In addition to this, the combination of silver NPs and a light activated agent (CV) can provide a dual kill mechanism also under dark conditions. These surfaces are promising candidates for use in healthcare environments to reduce the incidence of hospital-acquired infections.

2.2.2. EXPERIMENTAL

The Smart Surfaces project started at Chemistry Department University College London few years ago following the passionate research studies of Prof Michael Wilson – emeritus Professor of Microbiology at University College London. Among his main research interest there was the antibiotic resistance and the development of new antimicrobial strategies. He showed a great interest in translational research and has applied for 13 patents for inventions in the fields of light-activated antimicrobial agents and water purification. The first article on Smart Surfaces entitled "*Efficacy of a novel light-activated antimicrobial coating for disinfecting hospital surfaces*" was published in November 2011 by Prof Michael Wilson, Prof Ivan P. Parkin, and their students[60].

It is well known that healthcare-associated infections are infections acquired from the result of a person's treatment by health care providers and are caused by a variety of micro-organisms. These infections include: gastrointestinal infections (22%), urinary tract infections (20%), low respiratory tract infections (20%), surgical site infections (14%), skin and soft tissue infections (10%), bloodstream infections (7%) and others (7%). Unfortunately, every year there are at least 300 000 incidents of healthcare-associated infections in hospitalized patients in England, costing the UK's National Health Service (NHS) > 1 billion pounds a year. In recent years, significant effort has been devoted to preventing healthcare-associated infections attributed to methicillin resistant *Staphylococcus aureus* (MRSA), and *Clostridium difficile* because they have caused multiple fatalities[60-65]. The World Health Organisation (WHO) has published in 2017 a list of the 12 bacteria which pose the greatest threat to human health because they are resistant to antibiotics. *Pseudomonas aeruginosa* is the first one of the list of the three bacteria considered to be of critical priority. Methicillin-resistant *Staphylococcus aureus* is the second one in the list of the other six bacteria considered to be of high priority. If antibiotics lose their effectiveness, key medical procedures – including organ transplantation, caesarean sections, joint replacements, and chemotherapy – could become too dangerous to perform. The bacteria on WHO list can cause severe and often deadly infections such as bloodstream infections and pneumonia. The most critical

group of them includes multi-drug resistant bacteria that pose a particular threat in hospitals and nursing homes[67]. In the daily practice *P. aeruginosa* and *S. aureus* are the two most common causes of chronic wound infections and are frequently found together[68]. It has been experimentally demonstrated that exist synergistic interactions between *P. aeruginosa* and *S. aureus* in fact this one can produce lactate that is a carbon source that *P. aeruginosa* preferentially consumes over medium-supplied glucose[69]. In 2017 the Kazan Federal University (Volga Region, Russia), discovered that *S. aureus* survives in *P. aeruginosa* biofilm under antimicrobial treatment conditions[70]. In addition to this, the evidence suggests that *P. aeruginosa – S. aureus* infections are more virulent than monoculture infection with either species[68]. The big problem of Antibiotic Resistance will be fully described in Chapter 3 of this thesis.

According to Hwang et al. 2016, contaminated surfaces in hospital serve as bacterial reservoir which can contribute to transmission of health care-associated pathogens *via* touch by patients and hospital workers[59]. Cleaning and disinfection of the surface have been used in hospitals to prevent surface contamination. Although cleaning may decrease the levels of surface contamination, it is difficult to eradicate entirely because firstly, the bacteria may be strongly adherent to the surface and even a small number of residual bacteria will quickly reproduce to significant numbers if environmental conditions are favourable. Secondly, it is not easy to implement the cleaning and disinfection schemes thoroughly. Thus, it is necessary to develop effective and applicable alternatives to inhibit pathogen transmission in hospitals[71-77].

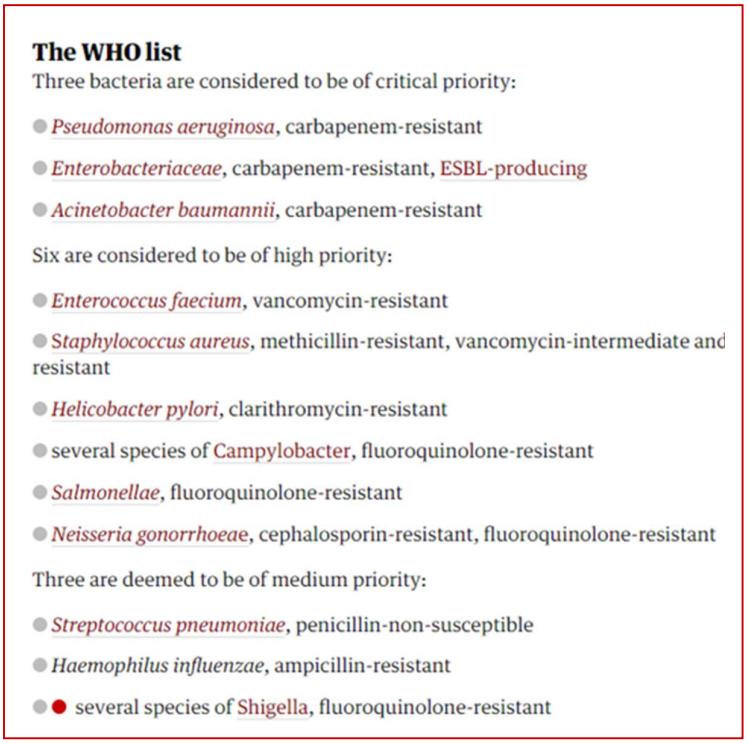

Figure . The WHO list of the 12 superbugs published in February 2017. Source: www.who.int/mediacentre/news/releases/2017/bacteria-antibiotics-needed/en/

Materials and methods: In order to prevent hospital surface contamination, at Chemistry Dept. UCL have been developed research areas that did not exist previously, such as the light activated polymers. To satisfy the target the dye selected was crystal violet or gentian violet because it has been demonstrated – by Wang et al. 2008, that *in vitro* it can disrupt *Pseudomonas aeruginosa* biofilms[78] and it can kill MRSA[80]. The clinical utility of gentian violet was first demonstrated – by Saji 1992, in a series of patients with decubitus ulcers by using an ointment containing 0.1% gentian violet. In 12 cases of patients with the MRSA infected skin lesions, MRSA was eliminated completely from the infected areas of the skin within 4 weeks. The side effects of gentian violet were not observed in all cases during the use of the ointment containing gentian violet[79-80]. The efficacy of gentian violet has been also demonstrated – by Okano et al. 2000, while studying a broad range of MRSA skin and soft tissue infection and clearance of nasal carriage. In the 8 cases of impetigo, the mean time to eradication was 7 days and the *in vitro* minimum inhibitory concentration (MIC) of gentian violet was 0,0225μg/mL. The dye agent was well tolerated in all 37 patients, with no significant side effects being reported[81]. Synthesis of gentian violet was attributed French chemist Charles Lauth in 1861 under the name of "Violet de Paris" and was popularized by George Grubber, a German pharmacist in 1880. In 1912, Churchman noted the bacteriostatic action of gentian violet against Gram-positive bacteria both *in vitro* and in animal studies. Based upon results from Churchman, in 1925 Hinton used gentian violet intravenously in 12 patients with severe sepsis from Gram-positive bacteria, of which seven patients improved[82]. Separate studies by Bakker and Fung have found that gentian violet inhibited growth of Pseudomonas, an extremely virulent Gram-negative rod, *in vitro*. Gentian violet was found to be more active than brilliant green at pH 7.4, particularly against *Pseudomonas aeruginosa*. The spectrum of activity of gentian violet was not increased by the addition of brilliant green. An aqueous solution of gentian violet 0.5% turned out to be an adequate topical anti-infective drug[83-84]. Recently, a report by Wang et al. 2008 showed that gentian violet disrupts and inhibits *Pseudomonas aeruginosa* biofilm in flow chambers and, also has some efficacy against planktonic *Pseudomonas aeruginosa*. The efficacy of gentian violet *in vitro* suggests that it may disrupt biofilm *in vivo*[78]. It is well known that many pathogens have developed systems that are controlled by the iron concentration to secret virulence factors, in *Pseudomonas aeruginosa* the ferric uptake regulator (Fur) is the protein that controls the iron uptake system and, consequently the expression of the virulence factor known as *Exotoxin A*[85]. Both excess iron and iron restriction have been implicated in reducing *Pseudomonas aeruginosa* biofilms[78]. More details about *Pseudomonas aeruginosa* and methicillin resistant *Staphylococcus aureus* (MRSA) will be given in Chapter 3 of this thesis.

The nanoparticles used for this study were silver ions because the antimicrobial activity of Ag^+ ions is well documented and reviewed. Silver has been recognized for its antimicrobial properties for centuries. The Phoenicians used silver water vessels to keep water, wine, and vinegar pure during their long voyages. Hippocrates, the "Father of Medicine", wrote that silver has healing and anti-disease properties. Greeks, Romans, and Egyptians used silver to purify and preserve water[86]. In North America, pioneers put silver dollars coins in their water flasks and barrels before journeying west. At the beginning of the twentieth century (1900-1940) surgeons routinely used silver sutures to reduce the risk of infection and promote healing[87]. Silver, a naturally occurring element, is non-toxic, hypoallergenic, does not accumulate in the body to cause harm and is considered safe for the environment. After testing 23 methods of purifying water, NASA has also chosen silver as the purifying agent on the Space Shuttle program. Positively charged silver particles literally seek out, oxidize, and destroy negatively charged bacteria and, in general all pathogens. In fact, silver is anti-bacterial, anti-microbial, anti-viral, and anti-fungal[88].

A series of samples were prepared for microbiological testing using a novel two-step dipping method. A simple swell-encapsulation-shrink process was employed to incorporate crystal violet (CV) dye and silver nanoparticles (Ag NPs) into polyurethane using acetone as a swelling solution. In the swell-encapsulation process, the CV molecules and Ag NPs in the acetone penetrate the polyurethane matrix as it swells, and the polyurethane then shrinks when it is removed from the solution. The CV molecules and Ag NPs remain inside of the polyurethane matrix.

Preparation of chemical stock solutions. The crystal violet solution – solution A was prepared dissolving 60mg of crystal violet powder (CV, Sigma-Aldrich, St. Louis, MO, USA) in 100ml of a solution containing 10ml of DI water and 90ml of acetone. The solution was sonicated in an ultrasound bath for 5 min in order to ensure complete dissolution of CV powder. The solution B was prepared dissolving 45mg (0.26mM) of $AgNO_3$ (Silver nitrate, Sigma-Aldrich, St. Louis, MO, USA) in 50ml of DI water to produce an approximately 5mM solution. The solution C was prepared dissolving 294.7mg (1mM) of $Na_3C_6H_5O_7{\cdot}2H_2O$ (tri-sodium citrate dihydrate, Hopkin & Williams Ltd, London, UK) in 50ml of DI water to form a 20mM solution. Synthesis of silver nanoparticles was prepared mixing 10ml of solution B with 180ml of DI water and heated with constant stir. After the mixture was boiled for ~ 2 min, 10ml of solution C was added. With constant stir, the mixture was boiled for a further 30 min and then allowed to cool. The development of a yellow colour was observed during the process.

Preparation of white light-activated antimicrobial surface. Polyurethane squared samples (1.0×1.0cm) were immersed in 10ml of acetone solution and left to swell in the dark for 24 h and

then left to dry in the air. Polyurethane dried samples were immersed in solution A (CV solution) and left to swell in the dark for 24 h. The samples were recovered from the CV solution and washed using a DI water bath sonicator for 2 times and then air-dried for 24 h in the dark. The samples were prepared as follows: CV only, CV with Ag NPs. Additionally, NPs encapsulated polyurethane samples without CV were prepared as follows: polyurethane with Ag NPs.

Material characterization. TEM (JEM-2100, JEOL Inc., Peabody, MA, USA) with EDS was used to confirm the size, morphology, and chemical composition of synthesized NPs. (Figure 0)

The UV-vis absorption spectra against NPs suspensions, control and treated samples were measured using UV-vis Spectrometer (PerkinElmer Inc., Winter St., CT, USA). Absorption was measured from 350 to 900nm. To determine NPs uptake from NPs suspension to polyurethane, the UV-vis spectra of NPs suspension were measured before and after swell-encapsulation-shrink process. The polymer sample was immersed in a mixture of acetone (9ml) and NPs (1ml) for 24 h. The comparison of absorbances *before* and *after* at 409nm (Ag NPs) was enable determination of the amount of silver NPs absorbed in the polymer. The uptake rate of NPs from NPs suspension to polyurethane sample was calculated as follow;

$$\text{Uptake rate } (\%) = 100 \times \left(\frac{(\text{AU}_{\text{before}} - \text{AU}_{\text{after}})}{\text{AU}_{\text{before}}} \right)$$

where AU_{before} represents the absorbance of NP suspension before polyurethane immersion in the solution and AU_{after} shows the absorbance of NPs suspension after the polymer removal.

Wetting properties. Equilibrium water contact angle measurements on: untreated polyurethane, acetone treated polyurethane (control), crystal violet-coated polyurethane, crystal violet-coated nano-silver encapsulated polyurethane, and nano-silver encapsulated polyurethane, were also obtained. A droplet of deionised water was dispensed by gravity from a gauge 27 needle and the samples were photographed side on. The data were analysed using Surftens 4.5 software.

Table 6. Average water contact angle measurements (°) ± standard deviation, of water on a range of polyurethane samples.

Polyurethane Sample	Water contact angle (°) ± Standard deviation
Untreated	99.9 ± 0.7
Control	70.5 ± 0.9
CV only	97.8 ± 0.9
CV-Ag	98.9 ± 0.8
Ag only	99.6 ± 0.9

Antimicrobial tests. To examine the antimicrobial activity, a range of polyurethane samples (1.0×1.0cm) was used to perform the experiments: acetone treated polyurethane (control), crystal violet-coated polyurethane, crystal violet-coated nano-silver encapsulated polyurethane, and nano-silver encapsulated polyurethane. These samples were tested against Epidemic MRSA 4742 representative of a Gram-positive epidemic bacteria isolated at UCL Hospital and *Pseudomonas aeruginosa* PAO1 as well as the clinical strand isolated at UCL representative of Gram-negative bacteria resistant to the majority of currently used antibiotics. These organisms were stored at –70°C in Brain-Heart Infusion broth (Oxoid Ltd, Hampshire, England, UK) containing 20% (v/v) glycerol and propagated on Columbia Agar Base (Lab M Ltd, Lancashire, England, UK) + 5% defibrinated horse blood (E&O Laboratories Ltd, Bonnybridge, Scotland, UK).

BHI broth (10ml) was inoculated with one bacterial colony and cultured in air at 37°C for an incubation of 18 h with shaking, at 200 rpm. The bacterial pellet was recovered by centrifugation (21°C, 2000×g, 5 min), washed in phosphate buffered saline (PBS) and centrifuged again to recover the bacteria, which were finally re-suspended in PBS (10ml). The 2 times washed suspension was diluted 1000-fold in PBS to obtain the inoculum. The inoculum contained 4.6×10^6 colony forming units per mL (CFU mL^{-1}). The inoculum in each experiment was confirmed by plating ten-fold serial dilutions on agar for viable counts. Duplicates of each polymer sample type were inoculated with 25µL of the inoculum (containing 1.1×10^5 CFU) and covered with a sterile cover slip (22mm×22mm) to ensure good contact between the bacteria and the sample surface. The samples were placed into plastic petri dishes containing moistened filter paper to maintain humidity at room temperature. The samples were then irradiated for up to ~5 hours using a white light source, the white light intensity was measured using a lux meter (LX-101, Lutron Inc., Coopersburg, PA, USA) at a distance of 30cm from the light source. The intensity of the light ranged from 390 to 530 lux. A further set of samples (in duplicate) was maintained in the dark for the duration of the irradiation time. In the dark, the light was completely blocked (0 lux). After light exposure, the inoculated samples and cover slips were placed into 450µl of PBS, and mixed using a vortex mixer for 1 min. The neat suspension and ten-fold serial dilutions were plated on Columbia blood agar for viable counts. The plates were incubated aerobically at 37°C for 24 h. Finally, the colonies grown on these plates were counted. All experiments were reproduced three times for each bacterial type.

Results and discussion: In this work it has been used a simple "two-step" method to develop a polymer encapsulated with a phosensitiser dye in addition to silver nanoparticles. In the first step, the polyurethane samples were immersed in an acetone swelling solution. In the subsequent step, the same samples were immersed half in a crystal violet solution for 24 h and the other half in a 9:1

crystal violet solution : nano-silver solution for 24 h. Upon exposure to the solvent, the polymer swells enabling the dye molecules to diffuse through the polymer. Although the mechanistic details are not so clear, it is clear that the CV dye strongly attaches to the polymer surface under aqueous dipping conditions, as the polymer sections showed no detectable leaching of crystal violet.

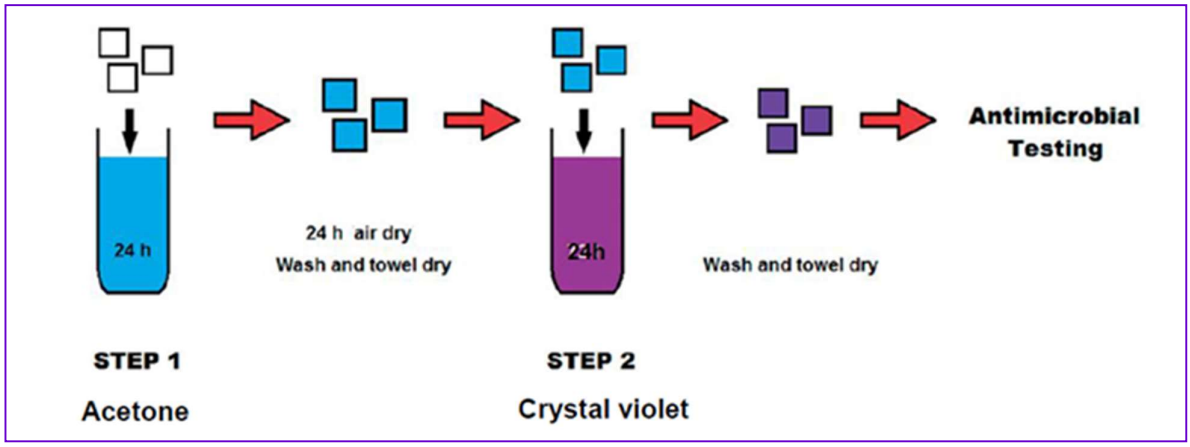

Figure . The simple "two-step" dipping method: the bactericidal surface was prepared by incorporating crystal violet and silver nanoparticles into the polyurethane using a simple dipping technique.

The NPs were made by citrate reduction of boiling aqueous solution of $AgNO_3$. The mean size of Ag NPs was 22.4 ± 16.7nm with median of 22nm, and interquartile range (IQR) of 24nm. They showed at TEM a spherical morphology as shown in figure 0. EDS analysis confirmed that all of peaks were assigned to Ag and impurities were not detected. Transmission electron microscopy (TEM) and energy-dispersive X-ray spectroscopy (EDS) were used in order to characterize the NPs.

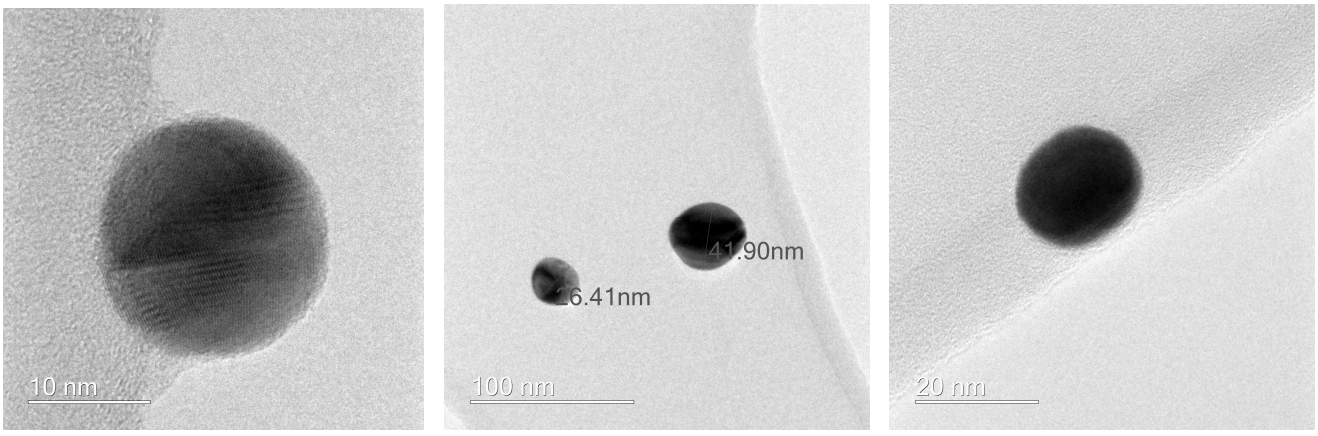

Figure 0. TEM photos selection of my silver nanoparticles. These photos have been taken under the kind guidance of Dr Steven Firth – Chemistry Dept. UCL.

The UV-vis absorption spectra of the Ag NPs suspension exhibited a peak at 409nm. Absorption was measured from 350 to 900nm. To determine the total amount of NPs encapsulated inside the polyurethane samples, the UV-vis absorbance spectra of nanoparticles suspension were measured *before* and *after* swell-encapsulation-shrink process. The polyurethane sample was immersed in a mixture of acetone (9mL) and NPs (1mL) for 24 h. Only the 8% of Ag NPs in the suspension was absorbed to polyurethane sample. The Ag NPs uptake rate from the NPs suspension to polyurethane sample was 8 ± 0.5% (average water contact angle ± standard deviation).

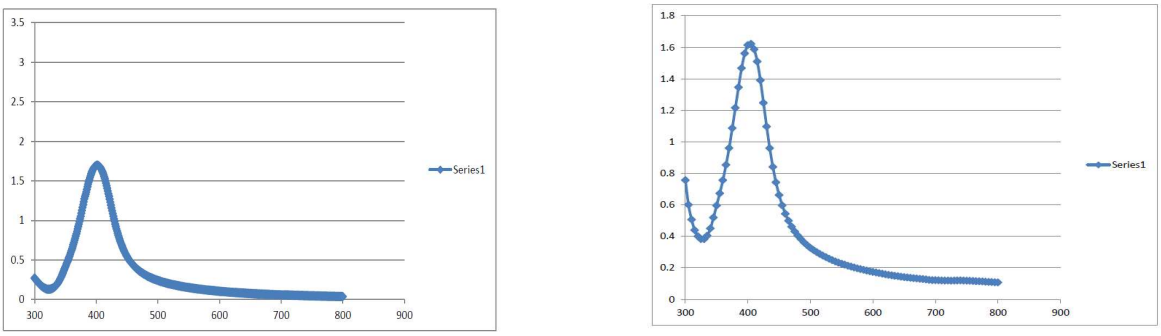

Figure !. The UV-vis absorbance spectra of the Ag NPs suspension *before* and *after* swell-encapsulation-shrink process respectively. Comparison of absorbances before and after at 409nm of Ag NPs.

To examine modified polyurethane functional properties, some samples of it were wiped rigorously with 70% alcohol. There was no visual evidence of dye removal from the treated polymer surface under these cleaning conditions, indicating the modified polymers should be stable with respect to standard hospital cleaning protocol. This test is considered a very important one, since despite the potent antimicrobial nature of these polymers, it is anticipated that surfaces treated by this method may still undergo the regimented hospital cleaning protocol and thus, must be stable to robust wiping using an alcohol-based, anti-infective wipe.

Table 7. Recommended light intensities for different areas in the UK healthcare environments.

Environment	Light intensity/lux
Operating theatre	10 000-100 000
A&E examination room	1000
Ward corridors	≥200
Typical dental chair	250
Measurement performed at UCLH (NHS)	

The lighting condition used in this study can be considered in relation to the brightness of various areas in the UK healthcare environments, as recommended by the Department of Health (Table 7)[89] and it was found that they were similar to those typically found in hospital corridors and wards; areas in which microbial contamination is prevalent. It is anticipated that the dye degradation is correlated to the light-flux levels and thus, the samples tested indicate a strong stability and suitability for these antimicrobial surfaces to be employed in a clinical environment such as hospital wards, where they would be expected to maintain the full potency for about 2 years (based on light-flux level used).

The antimicrobial activity of the control, CV dyed polyurethane samples, CV dyed and nano-silver encapsulated polyurethane samples and nano-silver encapsulated polyurethane samples under white light and dark conditions was tested against a representative strain of the Gram-positive bacterium, MRSA and, against a representative strain of the Gram-negative bacterium *Pseudomonas aeruginosa*. The data show that the antimicrobial activity of the polymers was promoted by exposure of the samples to a white hospital light source; a compact fluorescent lamp which emits light across the visible region of the spectrum and is similar to those commonly found in the UK NHS hospitals. In all experiments, a control sample set was maintained under dark conditions for the same period of time as the samples exposed to light and in a further experiment, a sample set was incubated under dark conditions for an extended time period (24 h). The antimicrobial activity of crystal violet-coated polyurethane (CV only), crystal violet-coated nano-silver encapsulated polyurethane (CV Ag) and nano-silver encapsulated polyurethane (Ag only) was compared to that of a control, solvent treated polyurethane sample. The lethal photosensitization induced by these samples when exposed to a white light source emitting an average light intensity of ~500 lux at a distance of 30 cm from the samples for ~5 h is shown in Figure .

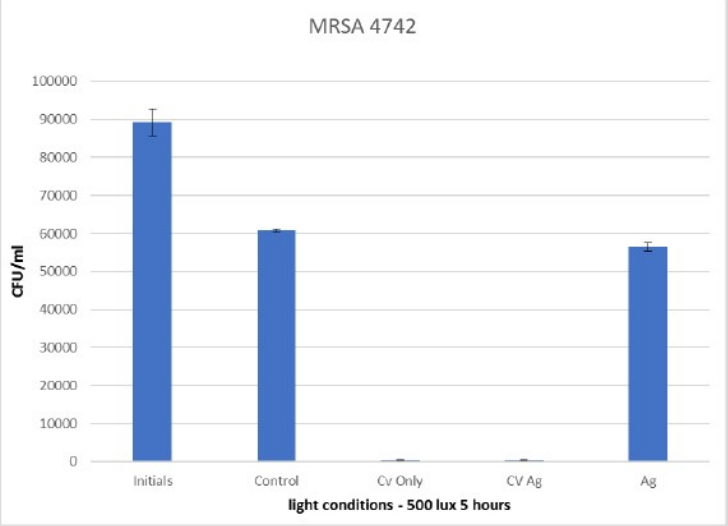

Figure !. Antimicrobial activity of control and treated polyurethane (PU) samples on *4742 methicillin-resistant S. aureus* at 500 lux for 5 hours of incubation.

After 5 h at 500 lux, no reduction in the numbers of viable bacteria of MRSA 4742 was observed on the surfaces of the control material (polyurethane alone) and the nano-silver encapsulated polyurethane (Ag only). However, a statistically significant (*P*-value < 0.01) decrease in the number of viable bacteria was observed on the material containing crystal violet alone (2.08 log reduction in bacterial numbers) and crystal violet with Ag NPs (2.08 log reduction). After 5 h in dark conditions no significant reduction has been found in all samples, however after 24 h in the dark polyurethane containing CV alone and CV with Ag NPs showed a significant reduction in the numbers of bacteria below the limit of detection (*P*-value < 0.01, detection limit: below 10^2 CFU mL^{-1}). Additionally, in experiments of polyurethane containing Ag NPs only, no reduction in the number of viable bacteria was confirmed after 5 h incubation in the dark. However, after 24 h in dark condition, a significant reduction was observed on polyurethane with Ag NPs only (*P*-value < 0.01, detection limit: below 10^2 CFU mL^{-1}).

Concerning the antimicrobial activity of the polyurethane samples against the Gram-negative bacterium *P. aeruginosa*, at the same light and dark conditions used for the MRSA, the following data has been found as shown in Figure .

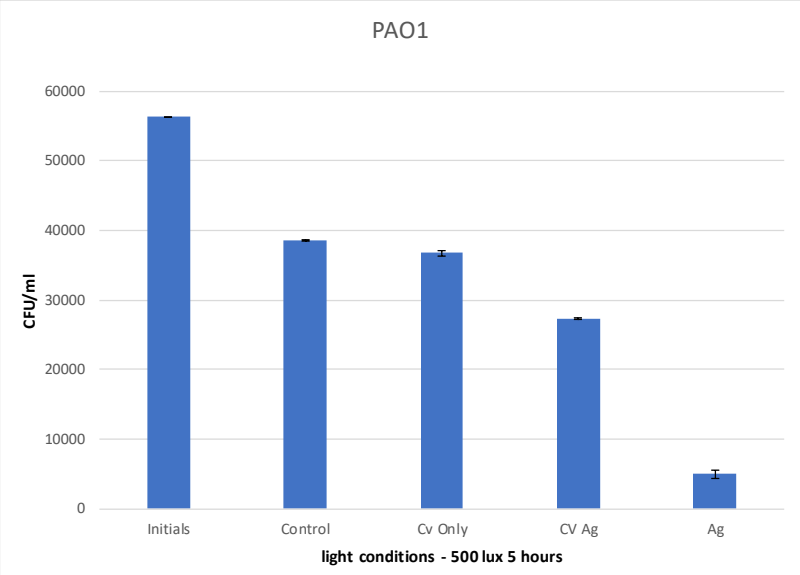

Figure !. Antimicrobial activity of control and treated polyurethane (PU) samples on *PAO1 Pseudomonas aeruginosa* at 500 lux for 5 hours of incubation.

After 5 h at 500 lux, no reduction in the numbers of viable bacteria of PAO1 was observed on the surfaces of the control material (polyurethane alone), polyurethane with only CV and polyurethane containing CV and Ag NPs. However, a statistically significant (*P*-value < 0.01) decrease in the number of viable bacteria was observed on the material containing Ag NPs alone (0.89 Log reduction). After 5 h in dark conditions no significant reduction has been found in all samples,

however after 24 h in the dark polyurethane containing only Ag NPs showed a significant reduction in the numbers of bacteria below the limit of detection (*P*-value < 0.01, detection limit: below 10^2 CFU mL^{-1}). Additionally, in experiments of polyurethane containing only CV and CV with Ag NPs, no reduction in the number of viable bacteria was confirmed after 5 h and 24 h of incubation in dark conditions. An identical situation has been found performing the same experiments for the clinical strand isolated at UCL Hospital of the bacterium *Pseudomonas aeruginosa*.

The XPS analysis of these samples – acetone treated polyurethane (control), crystal violet-coated nano-silver encapsulated polyurethane, and nano-silver encapsulated polyurethane, confirmed that silver NPs remain inside of the polyurethane matrix, consequently nothing has been found on the samples surface.

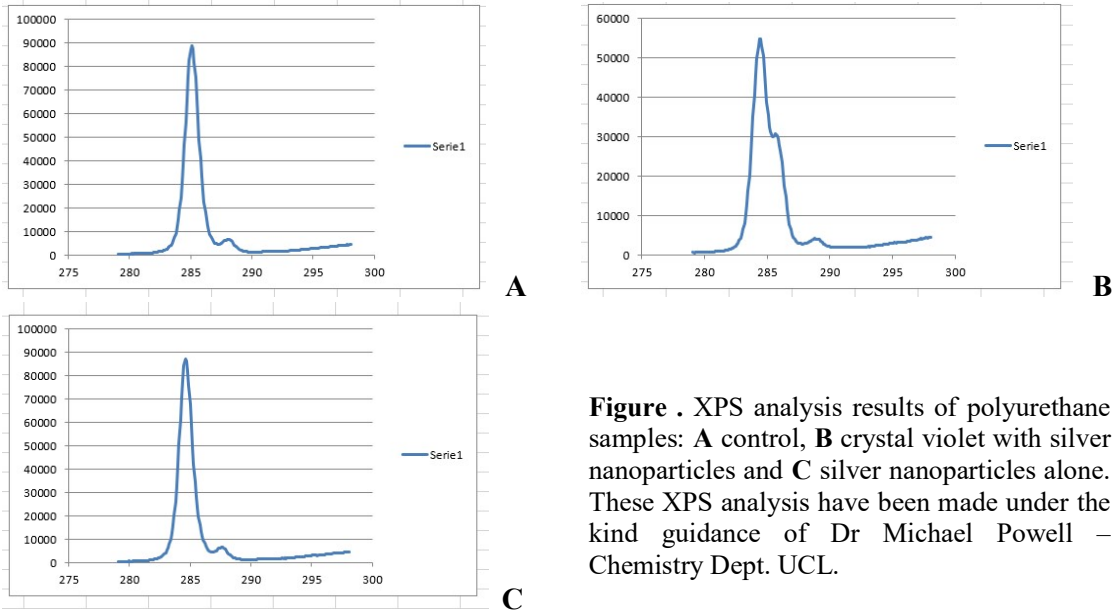

Figure . XPS analysis results of polyurethane samples: **A** control, **B** crystal violet with silver nanoparticles and **C** silver nanoparticles alone. These XPS analysis have been made under the kind guidance of Dr Michael Powell – Chemistry Dept. UCL.

The photo-bactericidal activity of polyurethane samples can be explained as follows; under white light condition, CV molecules in polyurethane are excited to a high energy triplet state from a low ground state. The triplet state dye reacts *via* type I (biomolecular reaction) or/and type II (reaction of molecular oxygen) photochemical pathways to produce ROS and $^1O_2$ leading to bacterial death. It was speculated that NPs incorporation enhances type I or type II photochemical reaction of the dye molecules[90]. To determine enhancement of $^1O_2$ generation, measurement of singlet oxygen was conducted at UCL Chemistry Dept. Laboratories. It has been estimated that the reactive oxygen species, singlet oxygen, has a very short diffusion distance of around 0.2 microns within the polymer[91]. Only dye embedded near the polymer surface will act in the photosensitisation of bacteria, as only the reactive oxygen species generated near to the polymer surface, rather than that

generated within the bulk, will act to photo-damage bacteria. With high concentrations of photosensitiser on the crystal violet-coated polymer surfaces, there is a greater probability of the generation of cytotoxic reactive oxygen species within range of "attack" against bacteria colonising the surface, subsequently contributing to the increased bacterial kills. These samples demonstrate efficacious antimicrobial activity when tested against both Gram-positive and Gram-negative bacteria, commonly associated with nosocomial infections. It is anticipated that these bactericidal surfaces can be employed in hospitals for use in touch surfaces, including but not limited to: tablet and mobile phone covers and screen protectors[92], computer keyboards, hand-dryers and paint films, to help maintain low bacterial levels and hence, potentially reduce the risk of spreading infections. In addition, this technology has been recently applied at UCL Hospitals for use in medical devices such as catheters[58-59]. It is expected that Ag incorporated polymers could be used to develop antimicrobial surfaces for clinical environments and also for various appliances such as keyboards, mobile phones and tablet covers, and also toilet and kitchen surfaces. However, for a real and daily application of the polymer, adverse effects on human health should be considered. As Ag NPs used in this study have been widely used in food industry, medicine, and water quality control, studies of their toxicity have been extensively conducted[93-99]. The toxicity of Ag NPs depends on many factors including size, dosage, and exposure time. Tests against mammals conducted *in vivo* demonstrated that Ag NPs only had toxic effects at long term (28-90 days) and high concentration dosages (inhalation: $>10^4$ particles per cm^3, ingestion: >30 mg kg^{-1})[100-101].

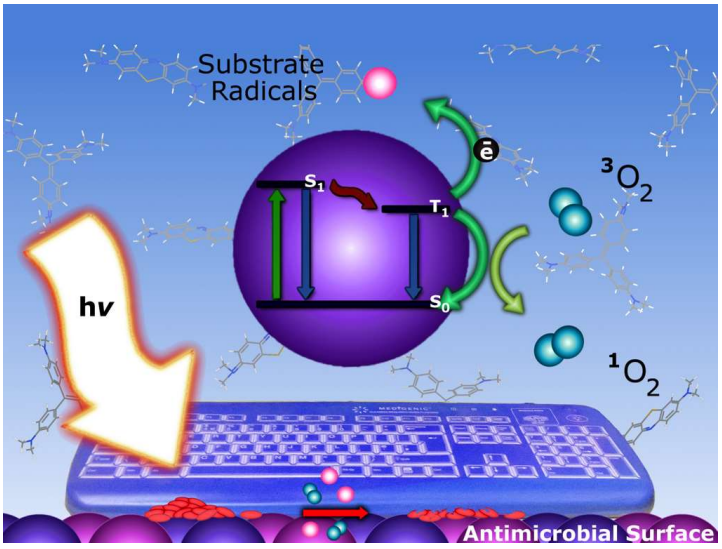

Figure . The photo-bactericidal activity of polyurethane samples: under white light condition, CV molecules in polyurethane are excited and so, ROS and $^1O_2$ are produced, leading to bacterial death. Courtesy of Dr S. Noimark and Dr K. Page – Chemistry Dept. UCL.

2.2.3. CONCLUSION

For the first time at Chemistry Dept. UCL have been developed Smart Surfaces made of a potent light-activated antimicrobial polyurethane – using polymers incorporated with multi-dye-nanoparticles combinations, that also demonstrated an effective killing power under dark conditions. It has been enough to use a standard hospital white light source to activate the photobactericidal power of the crystal violet-coated polymers. The samples were obtained following a simple swell-encapsulation-shrink process, crystal violet alone and in combination with silver nanoparticles was incorporated inside a polyurethane used in healthcare applications. This incorporation resulted in a potent white light-activated antimicrobial surface that demonstrated also a good bactericidal activity under dark conditions (24 h), reducing bacterial viability and, consequently bacterial number, below the detection limit. The multi-mechanism antimicrobial activity proves attractive in terms of potential applications for use in a variety of hospital surfaces, as low bacterial levels will be maintained under non-optimal lighting conditions (*i.e.* at night, or when lights are dimmed), with a boost in antimicrobial activity achieved with increasing illumination intensity. It is anticipated that these smart surfaces because of the fact that silver nanoparticles remain inside of the polyurethane matrix, exhibited a potent antimicrobial activity and in combination with a light-activated agent – crystal violet, are promising candidates for being used in healthcare applications, healthcare environments to reduce the surface bacterial contamination and thus, the incidence of hospital-acquired infections. In particular concerning my samples, the final target will be to develop a bactericidal surface able to kill at the same time both methicillin-resistant *Staphylococcus aureus* and *Pseudomonas aeruginosa* for using it in healthcare environments to reduce the spreading of nosocomial infections (*i.e.* hospital floors are heavily contaminated[102]). The possible applications of my polyurethanes are shown in the picture below.

Figure . The possible applications of my antimicrobial polyurethanes: screen protectors and keyboards for ultrasound full console machines, aerosol therapy devices and hospital shoes.

In the academic year 2017 the UCL Smart Surfaces project has been really appreciated by the public and the press (The Times) and the other media (BBC radio and TV and, RAI London TV). In particular, this project has been selected to represent the innovation in the field of chemistry[103] during the prestigious event managed by the Royal Society of London on 4th – 9th July 2017 entitled "*The Royal Society SUMMER SCIENCE EXHIBITION 2017*". The UCL Smart Surfaces exhibition stand was the n°20 at The Royal Society 6-9 Carlton House Terrace, London SW1Y 5AG. It has been described as follows: *"Touch the new self-cleaning materials, based on lily pads, that can kill bacteria and prevent infection*". In conclusion, I can confirm that the UCL Smart Surfaces project and my work on it, has been very appreciated across the world (U.S.A., Australia, New Zealand, Singapore, UAE, and Europe).

Figure . The UCL Smart Surfaces Exhibition stand ready on the day before the beginning of the event (Sunday 3rd July 2017). Courtesy of Dr S. Noimark and Dr K. Page – Chemistry Dept. UCL.

Scientists cook up self-cleaning kitchens

Jonathan Leake
Science Editor

Scientists have come up with the ultimate dream kitchen – one which is capable of self-cleaning and destroying bacteria without a hint of soap or sprays.

The researchers, from University College London (UCL), have created paints and plastics that react with anything landing on them, driving off stains, repelling water or producing micro-doses of toxic molecules to assassinate microbes.

"We are creating self-cleaning and self-sterilising materials for use in hospitals and in homes – especially kitchens and bathrooms," said Kris Page of UCL.

He will reveal the materials at the Royal Society summer exhibition in London this week.

Page and his colleagues were partly inspired by the self-cleaning glass used in modern buildings, which is coated with titanium dioxide catalysts that destroy dirt.

They have combined this with a "fluorinated silane" with properties similar to Teflon, which makes any water landing on it form a sphere, rather than soaking in. The spheres then pick up specks of dirt and carry it away, cleaning the surface.

UCL has already patented the materials which Page believes could help to clean the filthiest objects that most people possess – their mobile phones. Most are coated in a toxic mix including faecal bacteria, sundry body fluids and grease.

"Whenever I think of the best place to deploy self-cleaning materials, mobile phones – plus cases and screen protectors – come to mind," said Page, emphasising that he meant other people's.

Figure . The Sunday Times article about UCL Smart Surfaces (2nd July 2017, 12:01 am). Courtesy of Dr S. Noimark and Dr K. Page – Chemistry Dept. UCL.

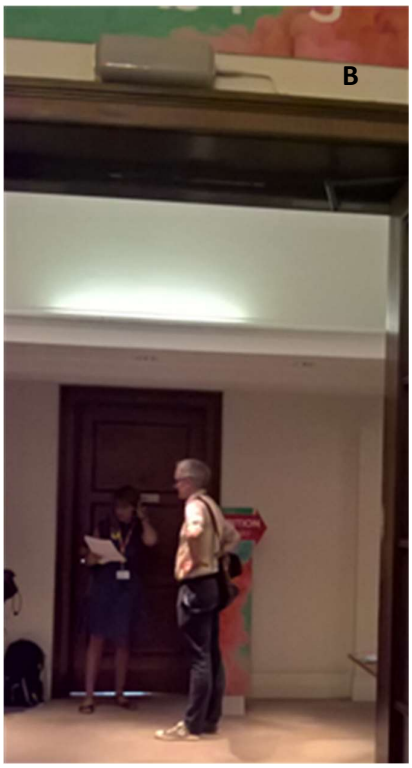

Figure . The Press (E), the radio (B), and the television (A, C, D) at the Royal Society Summer Science Exhibition 2017 – London, UK. Courtesy of Dr S. Noimark and Dr K. Page – Chemistry Dept. UCL.

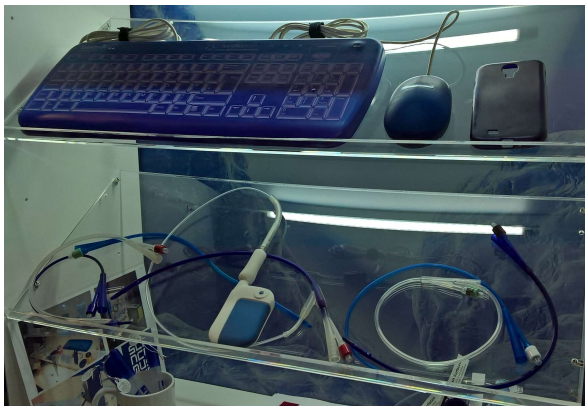

A

B

Figure . The Smart Surfaces prototypes (A): antimicrobial keyboard, mouse, smartphone cover and the antimicrobial catheters. The teaching station with microscope (B). Courtesy of Dr S. Noimark and Dr K. Page – Chemistry Dept. UCL.

Figure . The long queue of people coming at the Royal Society Summer Science Exhibition 2017 – London, UK. Courtesy of Dr S. Noimark and Dr K. Page – Chemistry Dept. UCL.

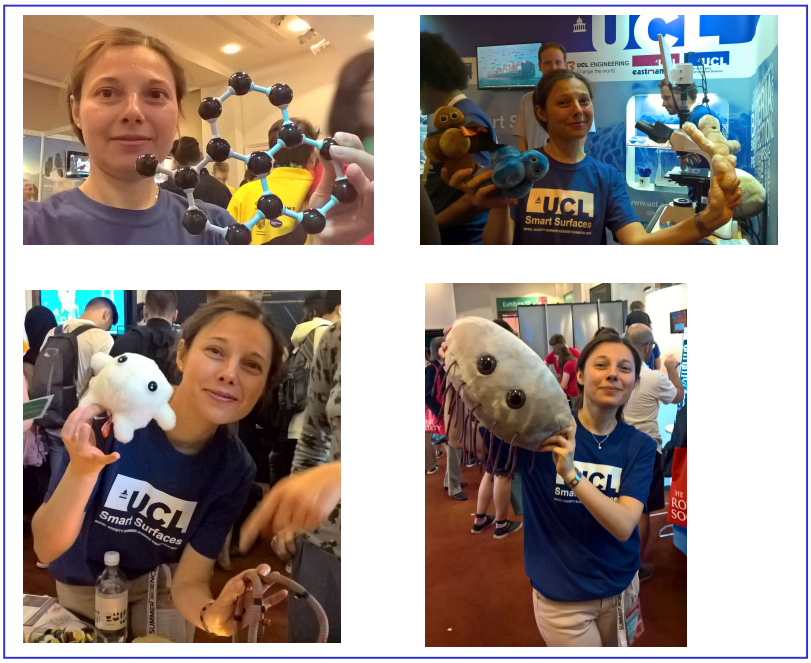

Figure . My own teaching moments at the Royal Society Summer Science Exhibition 2017 – London, England, UK.
In particular, in this small selection of personal photos, I was explaining to kids, high school students and adults the chemistry of UCL Smart Surfaces and their antimicrobial power and, of course the benefits for the human health.

2.2.4. ACKNOWLEDGEMENTS

I would like to acknowledge my PhD Coordinator and Supervisor Prof Mario Morino and my PhD Vice-Coordinator Prof Alberto Arezzo because they allowed me to go to London for completing my PhD programme. It is a pleasure to acknowledge Prof Andrea Sella and Prof Paul F. McMillan for managing my interview process at UCL and Prof Ivan P. Parkin – Dean of Mathematical and Physical Sciences at UCL, for hosting me and letting me work on the Smart Surfaces project. I acknowledge my colleagues Gi Byoung Hwang and Claudio Lourenco for being very kind and helpful while working with me inside the laboratory, and also Ladan Khodadoost, Ekrem Ozkan, Adnan Patir, Yao Lu, Ke Wu and Ethel Koranteng. The post-docs of the Chemistry Dept. UCL Dr Sacha Noimark, Dr Kristopher Page, Dr Raoul Quesada, Dr Michael Powell, and Dr Haitam Hussain for his precious guidance in the microbiology laboratory. The staff of the Chemistry Dept. UCL Dr Jadranka Butorac and her colleagues of the administration office, Dr Steven Firth, Brian Kavanagh, and Tony Field. I am also grateful to Prof Eva Sapi – Chair of the department of biology and environmental science at University of New Haven (USA), Prof Ehmke Pohl – Professor in the Dept. of Biosciences and in the Dept. of Chemistry Durham University, Co-Director in the Biophysical Sciences Institute, Member of the Durham X-ray Centre and Fellow of the Wolfson Research Institute for Health and Wellbeing Durham University (UK), Prof Michael Vasil – Emeritus Professor at the Dept. of Microbiology School of Medicine University of Colorado Denver (USA), Prof Nicola A. Carlone – Emeritus Professor at the Dept. of Microbiology School of Medicine University of Turin (Italy) for their experienced and professional suggestions on the bacterium *Pseudomonas aeruginosa*. I acknowledge the Royal Family of the United Kingdom and in particular, Her Royal Highness The Princess Royal – Chancellor of the University of London for economically supporting UCL research projects. Finally, I would like to thank Dr Marco Varvello – RAI London and his troupe for their visit at our stand during The Royal Society Summer Science Exhibition 2017, Dr Tiziana Ferrario and Dr Giovanna Botteri – RAI New York, Dr Marco Clementi – RAI Rome and Bav Heer MRPharmS – BBC for their kind compliments.

Figure . *Her Majesty The Queen* of the United Kingdom and the other Commonwealth Realms *Elizabeth II* during her visit at UCL Francis Crick Institute on 9th November 2016. Courtesy of the University College London.

Chapter 3

New Materials and Strategies to overcome the upcoming problem of antibiotic resistance

3.1 Silver nanoparticles to improve control of nosocomial infections

3.1.1. INTRODUCTION

The rise of the Superbugs and the Antibiotic Resistance is the big problem of our time, in fact the WHO has come up with a list of antibiotic-resistant "priority pathogens" – 12 families of bacteria that pose the greatest threat to human health. The WHO said the 12 bacteria have built-in abilities to find new ways to resist treatment and can pass along genetic material that allows other bacteria to become drug-resistant as well. "Antibiotic resistance is growing, and we are fast running out of treatment options. If we leave it to market forces alone, the new antibiotics we most urgently need are not going to be developed in time" said Dr Marie-Paule Kieny, WHO's assistant director-general for health systems and innovation[114]. In order to give a comprehensive tractation of the problem I fully reported the Reuters article written by Yasmeen Abutaleb, Ryan McNeill and Deborah J. Nelson on 18th November 2016 entitled *"One life, two donated organs and $5.7 million in bills – a tale of superbugs' deadly costs".* The deadly epidemic America is ignoring – The Uncounted, a Reuters Investigation[115].

Recovering from transplant surgery, Dan Greulich fell prey to a drug-resistant infection. What happened over the next five months shows the terrible human and financial price of an epidemic raging through the U.S. healthcare system.

LOS ANGELES – With good reason, Dan Greulich's doctors called him "the miracle man." In the span of a decade, the insurance company executive engaged not once, but twice, in a race with death as he awaited replacements for failing organs. And twice, just as death was poised to win, he made it to the top of the national transplant list – ahead of thousands of other dying people. Donor organs became available, he was rushed into surgery, and he emerged with a new lease on life. After Greulich's second combined liver-and-kidney transplant in early 2012, his wife, Rae, sent a letter to the donor's family. "You not only saved a man," she wrote, "you saved a family." But then, less than three weeks into his recovery at University of California-Los Angeles Medical Center, Greulich contracted an antibiotic-resistant infection – a common and often lethal hazard of hospital stays. Over the next five months, according to thousands of pages of medical and billing records reviewed by Reuters, Greulich was attacked by no fewer than half a dozen different "superbugs," most of them strains that are encountered almost exclusively in healthcare facilities. Greulich's immune system, suppressed by medications to prevent organ rejection, had no way to fight the bacteria. When the usual antibiotics failed to snuff them, he was pumped full of powerful alternatives, sometimes as many as half a dozen a day. Some had alarming side effects — hearing loss, severe pain, nausea. The infections kept coming. Sepsis, a dangerous inflammatory response to infection, set in. Confined to an intensive-care unit (ICU), Greulich was frequently placed on mechanical ventilation, itself a common source of infection. He wavered in and out of consciousness. Doctors cut him open again to seek the source of the problem. At one point, they considered putting him back on the transplant list, but only if they could clear him of infection. They couldn't. On June 30, 2012, Greulich died, age 64. Dan Greulich is one of the uncounted – the tens of thousands of people in the United States whose infections and deaths by superbug are not tracked by public health agencies. As revealed in the first article in this series, deaths related to drug-resistant infections often aren't recorded as such on death certificates. Greulich's death certificate blames "cardiac arrhythmia," or an irregular heartbeat. Even when superbug deaths are recorded, tens of thousands a year go uncounted because federal and state agencies are doing a poor job of tracking them. Today, the lack of a unified national surveillance system makes it hard to fight a scourge that officials 15 years ago declared to be a grave threat to public health. Deaths like Greulich's speak to the high human toll of superbugs. But Greulich's death and, in particular, the effort to prevent it also speak to the enormous waste caused by the infections: two precious organs

in a country where 22 people die every day waiting for one; thousands of hours put in by dozens of doctors, nurses and other medical workers to save a life; and big sums of money spent on drugs, surgery and hospital care, contributing to the billions of dollars superbugs add to the U.S. healthcare bill every year. “Two people that could have gotten those organs died waiting for those organs,” Rae Greulich said. “To see it become a failure is certainly devastating,” said Dr David Klassen, chief medical officer of the United Network for Organ Sharing (UNOS), the Richmond, Virginia, nonprofit group that coordinates all U.S. transplants. It isn’t clear how Greulich contracted the superbugs that killed him. UCLA Medical Center declined to make anyone available to discuss his illness and hospitalization. In a statement emailed to Reuters, the hospital said: “We treat many severely ill patients who require complex care, and we have detailed procedures and protocols in place to prevent, detect and treat infections.” Beyond the loss of viable organs that could have saved other lives, Greulich’s infections added to the growing national tab for treating them. Records show that from the time he first entered UCLA Medical Center in December 2011, until he died seven months later, Dan Greulich racked up a total bill of $5.7 million. How much of that went toward treating Greulich’s superbug infections and how much went toward his transplant surgery and related treatments is hard to determine precisely. Too many other variables are at play. However, at $5.7 million, the charges for Greulich’s seven-month hospitalization were nearly five times what the National Foundation for Transplants says are the average first-year charges for a liver-and-kidney transplant. Charges for antibiotics he was given in a failed attempt to beat his infections were at least $230,000, exceeding the $200,000 in charges for obtaining and transplanting a liver and kidney. Charges for seven months of “accommodations” at UCLA Medical Center totaled $2 million.

AN ELUSIVE NUMBER. Lack of reliable data hinders any effort to calculate how much superbugs add to overall U.S. healthcare costs. The Centers for Disease Control and Prevention (CDC) cites figures from a 2009 study sponsored by the Alliance for Prudent Use of Antibiotics that put the annual cost of antibiotic-resistant infections at more than $20 billion. But that figure is extrapolated from data from a single hospital. And it uses infection rates from 2000, which were far less than what they are now. Dr Stuart Levy, director of Tufts University’s Center for Adaptation Genetics and Drug Resistance in Boston and an author of the 2009 study, acknowledged the limitations of the analysis. “The important point was we were supposed to show this was a very costly consequence of doing hospital care,” he said. Reuters undertook its own analysis to get an idea of how much superbug infections cost. Using national inpatient data from the federal Agency for Healthcare Research and Quality for 2013, the analysis of millions of records focused on infections from two

superbugs: methicillin-resistant *Staphylococcus aureus* (MRSA) and *Clostridium difficile*. It found that an infection can add thousands of dollars to the cost of a patient's hospital stay. The average MRSA infection added about $11,000 per inpatient stay, while *C. difficile* added about $5,200. In all, Reuters found that the two infections combined added about $6 billion in charges to hospital stays nationwide in 2013. MRSA infections added about $4.1 billion, and *C. difficile* added about $1.9 billion. To calculate those numbers, Reuters used a method called propensity score matching to compare costs for patients with and without infection who are otherwise similar in terms of demographic characteristics, other illnesses, hospital setting and so on.

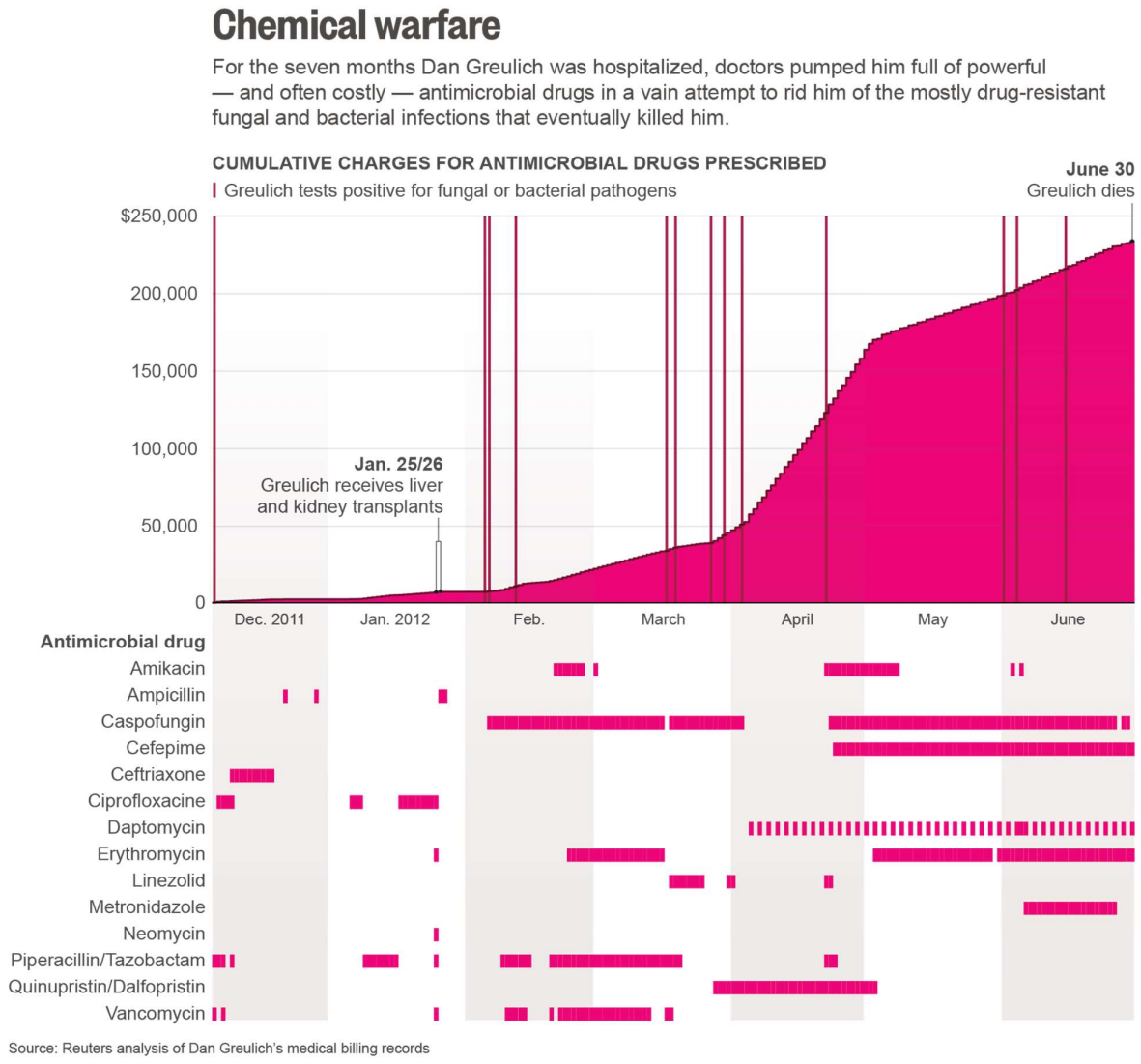

Figure . The analysis of Dan Greulich's medical billing records – the Uncounted, a Reuters Investigation[115].

While MRSA and *C. difficile* are two of the most common and well-known drug-resistant pathogens, they are only two of 18 superbugs the CDC considers to be a threat to public health, suggesting a total cost much higher than $6 billion. Some of those other infections, while not as widespread, can be far more costly to treat. Most superbug infections are contracted in hospitals and other medical facilities. The big bills that result are most often covered by health insurers and other third-party payers. This means that ultimately, the costs are passed to consumers in the form of higher insurance premiums, said David Cutler, a Harvard University economist who specializes in healthcare. “There is no other way to do it,” he said. Private insurers generally do not deny reimbursement for treatment related to superbug infections. Even in cases where hospitals are held legally liable for the infections, they are often shielded from eating the full cost. James Woodard contracted a MRSA infection at age 64 while in the University of New Mexico Hospital for back surgery in 2012. The infection led to a dozen more surgeries over four years and left him wheelchair-bound and with memory loss. But he hasn’t forgotten the pain as the infection spread: “It felt like someone was hacking my body in half,” he said. In a malpractice suit Woodard and his wife brought against the hospital, a jury earlier this year found the hospital at fault and awarded Woodard and his wife $4.25 million for medical costs, Woodard’s injuries and other damages. But New Mexico caps malpractice awards. Within those limits, the hospital is asking the court to set the award at $700,000, said hospital spokesman Luke Frank. That is less than the $973,000 that Frank said the hospital received in payments from Woodard’s insurer. Hospitals “make money on those complications,” said Woodard’s lawyer, Amalia S. Lucero. And Woodard could end up with even less if his own insurer recovers some of the money it paid to the hospital from whatever award Woodard receives. More than half the states have imposed caps on malpractice awards in response to medical and insurance industry concerns that multi-million-dollar verdicts were driving up the cost of healthcare and premiums. The Centers for Medicare & Medicaid Services (CMS) penalizes hospitals for high infection rates by reducing payments from the huge Medicare government health-insurance program for the elderly. And the agency does not pay the added costs of some types of preventable infections, such as catheter-associated urinary tract infections, if they are contracted in the hospital. Hospitals have found a way to get around the CMS payment restrictions. Several studies have shown that hospitals sometimes use a strategy called “upcoding,” whereby they manipulate the codes for submitting reimbursement claims so that they receive payment for infection-related treatments. For instance, a hospital could claim an infection was present when the patient was admitted, rather than acquired in the hospital. Or it could not mention an infection at all.

A 2015 study from the Stanford Graduate School of Business estimated that CMS reimbursed for more than 10,000 "upcoded" claims from 2009 to 2010, costing Medicare a total of $200 million. As for Dan Greulich's $5.7 million bill, his widow, Rae, said the couple paid about $10,000 themselves. Most of the balance was covered by Dan's employer-sponsored insurance with Anthem Inc. The insurance company declined to comment. Hospital charges are typically a starting point that insurers end up negotiating down. Payment records for Greulich's seven-month stay at UCLA Medical Center show that Anthem paid at least $2.9 million.

LONG ODDS. One day in February 2000, Dan Greulich failed to show up for work as a senior vice president of property and casualty insurer Western Mutual at the company's Agoura Hills, California, office. His son, Tim, found him lying unconscious on the floor at home. At the hospital, doctors told Greulich that his liver and kidneys were failing, damaged beyond repair from his years of heavy drinking. He probably wouldn't live more than a couple of months. His alcoholism disqualified him for a life-saving transplant. Greulich began attending Alcoholics Anonymous meetings while undergoing dialysis four times a week. "He completely gave up [alcohol] the second he went to that hospital," Tim said. "He never picked up a drink after that." By the end of 2000, he was on the transplant waiting list. The hospital entered his information into a computer system run by UNOS, the transplant coordinator, which uses information from hospitals and organ-procurement groups across the country to match donors with recipients. The odds were against him. In 2001, the 6,080 people who died and became donors didn't come near to covering the 86,000 people waiting for organs. As Greulich waited, his health deteriorated. He struggled to make it through each workday. He spent lunch hours napping in his car. Then, in July 2002, he got his first transplant. Recovery, according to Rae, was complicated by his first encounter with superbugs: He contracted a MRSA infection, which kept him in the hospital until September. A month later, after about two years as a couple, Dan and Rae got married. Tim, Dan's son from a previous marriage, lived with them. Dan returned to work, paring down his hours from 60 to 45 a week. He and Rae bought their dream home in Simi Valley, in the mountains 40 miles outside of Los Angeles. They had fruit trees in their backyard – lemon, orange, pomegranate – and kept horses. For nine years, Dan remained healthy and was "very religious" about taking his transplant medications, according to medical records. In 2011, he began taking an herbal remedy called St. John's wort to cope with stress at work. He didn't know the plant could block the effects of anti-rejection drugs. On Dec. 6, nearly a decade after his first double transplant, Dan was back in UCLA Medical Center, his donated liver and kidney failing. He was soon relisted for a transplant. Again, as he waited, his health declined. On Jan. 5, 2012, medical records show, he was vomiting blood, and he was moved

to an intensive-care unit. He was charged the next day for his first night in the intensive-care bed: $10,400. His skin grayed. He spent more time sleeping. Every day, it seemed more likely that he would die before he made it to the top of the transplant list. In the early morning hours of Jan. 25, Rae received a call in her hotel room: A 40-year-old woman had died, and she was an organ donor. Dan was at the top of the waiting list. “Everything’s going to be OK,” Rae said she was thinking hours later, as Dan was wheeled into surgery. A second transplant is far more complicated and risky than the first, said Dr Fady Kaldas, an associate professor of surgery at UCLA specializing in liver transplants who was part of Dan’s medical team. Dan was losing so much blood during the operation that doctors spread the procedure over two days to give his body time to stabilize. At one point, Rae recalled, doctors told her they were losing Dan. He survived — one of 462 people to get a double transplant that year. His new liver soon began working on its own. His sister, Pat Herbert, said he told her he would make it to Florida for her birthday in May. His rosy colour returned. Even when his new kidney didn’t take, meaning he would have to rely on dialysis, he remained optimistic. Then, in early February, as nurses were removing post-surgical drains from Dan’s abdomen, a nauseating stench filled the ICU room, Rae recalled. Rae suspected something was awry. She was right. Dan’s medical records show that lab tests of fluid from the drains found two drug-resistant pathogens, *Citrobacter freundii* and *Aeromonas*. And they weren’t Dan’s first infections. He was already fighting a fungus called *Candida albicans*, which can be especially dangerous in transplant patients.

MODERN DANGERS. Modern medical advances – complex organ transplants, drug therapies, devices such as ventilators and dialysis machines – sustain life for people who would otherwise die. But they come at a cost. They leave many people – cancer patients, people with HIV, premature infants, anyone with a suppressed or weakened immune system – particularly vulnerable to bacteria. At the same time, many of the bacteria that thrive in the hospitals where these people are concentrated have developed resistance to antibiotics. Dan Greulich was the perfect target. Transplant patients take drugs for the rest of their lives that suppress their immune systems so that their own bodies don’t reject the donor organs. That leaves them vulnerable to opportunistic pathogens like the two that showed up in Dan’s lab tests. Both rarely cause illness in otherwise healthy people; for the immune-compromised, they can be deadly. Hospitals have well-established protocols to contain the threat. At UCLA Medical Center, once Greulich tested positive for drug-resistant infections, everyone – doctors, nurses, technicians, Rae, other relatives – had to don a gown and gloves before entering his room and discard them when leaving. Rae said she repeatedly asked nurses about Dan’s post-operative drains. They told her only that he had a fungal infection,

she said. No one told her the names of the pathogens, or that they were resistant to multiple drugs, or how dangerous they were. UCLA Medical Center declined to comment. Dan was now battling sepsis – life-threatening inflammation that is triggered throughout the body in a haywire response to infection. His blood pressure was abnormally low. His heartbeat was rapid and weak. Breathing was difficult, and he was often placed on mechanical ventilation, inserted through a tracheostomy, a hole surgeons cut into his windpipe. He was receiving dialysis through a port in his groin. He received fluids and drugs – including increasing amounts of ineffective antibiotics – through multiple tubes inserted into his veins and arteries. He was seldom lucid. Occasionally he would utter an "I love you" to Rae or ask how his recovery was going. Rae usually lied. "You're doing so much better," she would say, to encourage him to keep fighting. Doctors were desperate to locate the infection behind Dan's sepsis. On Feb. 22, they wheeled him into surgery again and opened his abdomen, distended with retained fluid. This was risky in a patient so ill. "It's not necessarily the easiest thing to take somebody who's so stressed and sick and take them back to surgery," Kaldas said. The surgery failed to reveal a definitive site of infection. Dan's medical bills show at least $20,000 in related charges – for the operating room, the procedure, anesthesia and a liver biopsy. In March, Dan tested positive for a drug-resistant strain of *Enterococcus*. Unrelenting sepsis caused his body to swell. His skin was stretched tight and easily punctured. When Rae tried to clip his fingernails one day, he bled. Doctors had put Dan on drugs called vasopressors, which constrict blood vessels and thus raise the dangerously low blood pressure that sepsis causes. But that same mechanism also decreases essential blood flow to new organs, putting them at risk. "That's what makes sepsis such an evil process … It just wreaks havoc on your body, including a delicate transplanted liver," Kaldas said. "It's always a game of what's going to happen first. Are these organs just going to fall apart from being on vasopressors for a week, or is the infection going to go away first?" Another month, another infection. In early April, it was vancomycin-resistant *Enterococcus* (VRE), another common menace to hospital patients with weakened immune systems. A few days later, Rae recalled, two of Dan's doctors sat down with her for a talk. Imaging showed that his new liver was a potential site of infection and a probable source of his sepsis. If they could clear Dan of the infections, they would consider him for a third liver-and-kidney transplant. In notes dated April 18, 2012, Dr Leonard Irwin Goldstein wrote that another transplant would provide "his best chance for long-term survival." Only now, Rae said, did she realize that Dan's struggle was not to recover from transplant surgery, but from a barrage of infections. "Nobody said he had a laundry list of infections," she said. She started researching infection control and keeping a close eye on the nurses caring for Dan. In the ensuing weeks, she wrote three letters to the ICU's nurse manager to urge vigilance against further infection and to list lapses she noticed

in her husband's care. In a May 7 letter, she described stopping a nurse from starting an intravenous line when she saw that the nurse wasn't going to change gloves after touching cabinet drawers and other potentially contaminated surfaces. UCLA Medical Center declined to comment. Since February, Dan had undergone increasingly aggressive antibiotic therapy. By the end of March, records show, he had been charged about $45,000 for the drugs. Then, for April alone, the amount ballooned to more than $110,000. Of that, $93,000 covered charges for 169 doses of Synercid, a combination of quinupristin and dalfopristin that is one of the few drugs that can beat back VRE. In just one day — May 2, 2012 — Dan was given six different antimicrobial drugs: amikacin, cefepime, daptomycin and Synercid, all of them commonly used to treat multi-drug-resistant infections; Bactrim; and caspofungin, an anti-fungal. Many of these drugs are hard on the body. The Synercid caused severe bone pain. Dan, who for months hadn't complained about his pain, uttered to his wife, "I'm in agony," according to Rae. At Rae's request, doctors eventually stopped the drug. "Antibiotics beat you up," said Kaldas. "Imagine somebody on nuclear weapons of antibiotics, and they're on 10 of them, or five of them, or three of them. It's a lot to ask." By June, the continuing antibiotic therapy had left Dan nearly deaf. His hair had fallen out. On and off a ventilator, he had suffered several bouts of pneumonia. Unrelenting sepsis and the phenomenon known as ICU delirium – confusion and cognitive impairment associated with acute-care settings – left him incapable of recognizing little around him other than Rae and Tim. Doctors now said Dan would never be well enough for another transplant. He was going to die. They urged him to sign a "do not resuscitate" order. He refused. Rae posted a sign above his bed: "Mr. Greulich very clearly stated NO DNR and wants aggressive treatment." For Dan's medical team, giving up on a third transplant was an admission of defeat. "What we worry about is putting yet another organ into somebody that's going to go the same way as the last organ," said Kaldas. "You've developed a relationship with this patient … There's nothing you want more than to see them get better. But you have to take a step back and say, well, a third liver will not make this person get better." After months of illness, pain and confinement, Dan began to lose his will to live. He told Rae he felt worthless and that he knew he wasn't ever going to recover. On June 29, Rae walked into his hospital room a little before 9 a.m., as she had nearly every day for the past seven months. He was sitting up in bed, alert and almost perky, she said. "I want to die," he told her. The next day, Rae and Dan's son, Tim, 24 years old at the time, stood at Dan's bedside, holding his hands. They said their goodbyes. Just before 11:30 a.m., doctors turned off Dan's dialysis machine. He soon lost consciousness. Rae and Tim watched as the tracing on Dan's heart monitor slowed and slowed and then flat-lined. Greulich's death certificate did not mention sepsis or the infections that caused it. His autopsy report, however, lists at least five pathogens present in samples taken from his body,

most of them drug-resistant. The report states: “The autopsy findings and microbiology studies support the clinical diagnosis of septic shock, which appears to be the immediate cause of death.” “It was clearer than anything that he died of septic shock,” Rae said. “When I got the death certificate, I was staggered.” [115]

3.1.2. EXPERIMENTAL

It is nowadays widely clear that antibiotic resistance is one of the biggest threats to global health, food security, and development today. Unfortunately, antibiotic resistance can affect anyone, of any age, in any country across the world. It can occur naturally, but misuse of antibiotics in humans and animals is accelerating the process. A growing number of infections – such as pneumonia, tuberculosis, gonorrhoea, and salmonellosis – are becoming harder to treat as the antibiotics used to treat them become less effective. According to facts reported in the introduction section of this chapter, antibiotic resistance leads to prolonged hospital stays, higher medical costs and, increased mortality. In my project, as mentioned in chapter 2 of this thesis, all the efforts have been focused on MRSA and *Pseudomonas aeruginosa*. In addition to this, a set of tests have been performed against *Streptococcus mutans*, the bacterium mainly responsible of tooth decay.

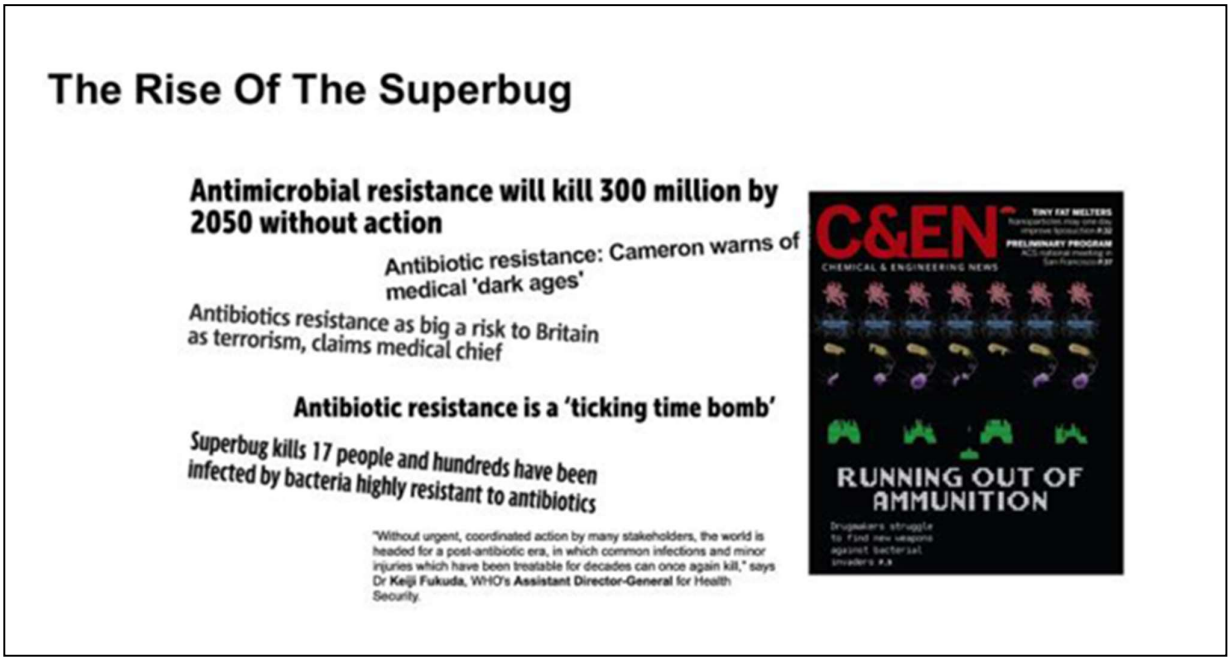

Figure . The rise of the Superbug. Courtesy of Dr S. Noimark and Dr K. Page – Chemistry Dept. University College London (United Kingdom).

P. aeruginosa is a multidrug resistant pathogen recognized for its ubiquity, its intrinsically advanced antibiotic resistance mechanisms, and its association with serious illnesses – especially hospital-acquired infections such as ventilator-associated pneumonia and various sepsis syndromes.

Fig. P. aeruginosa is a Gram-negative opportunistic pathogen that is commonly associated with hospital-acquired infections (HAIs).

Figure . The bacterium *Pseudomonas aeruginosa*. Source: Google Library, PubMed – NCBI.

The organism is considered opportunistic insofar as serious infection often occurs during existing diseases or conditions – most notably cystic fibrosis and traumatic burns. It is also found generally in the immunocompromised but can infect the immunocompetent as in hot tub folliculitis. Treatment of *P. aeruginosa* infections can be difficult due to its natural resistance to antibiotics. When more advanced antibiotic drug regimens are needed adverse effects may result.

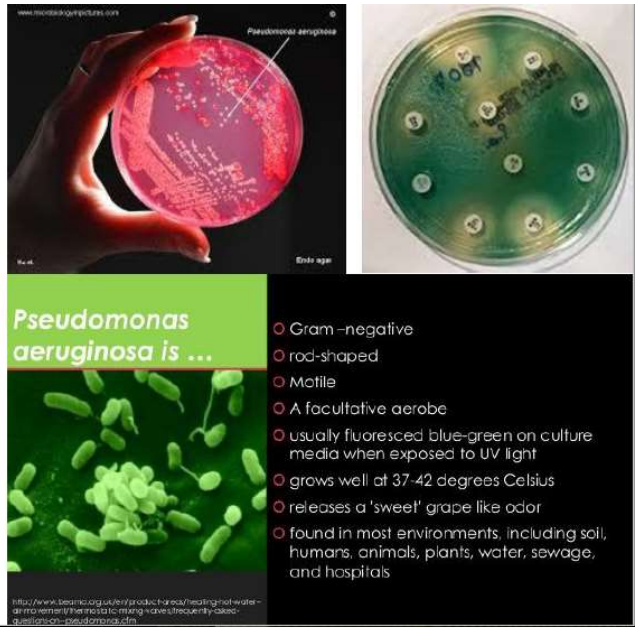

Figure . The bacterium *Pseudomonas aeruginosa*. Source: Google Library, PubMed – NCBI.

S. aureus is a bacterium responsible for several difficult to treat infections in humans. MRSA is any strain of Staphylococcus aureus that has developed, through horizontal gene transfer and natural selection, multi-resistance to beta-lactam antibiotics, which include the penicillins (methicillin, dicloxacillin, nafcillin, oxacillin, etc.) and the cephalosporins. MRSA evolved from horizontal gene transfer of the *mecA* gene to at least five distinct *S. aureus* lineages.

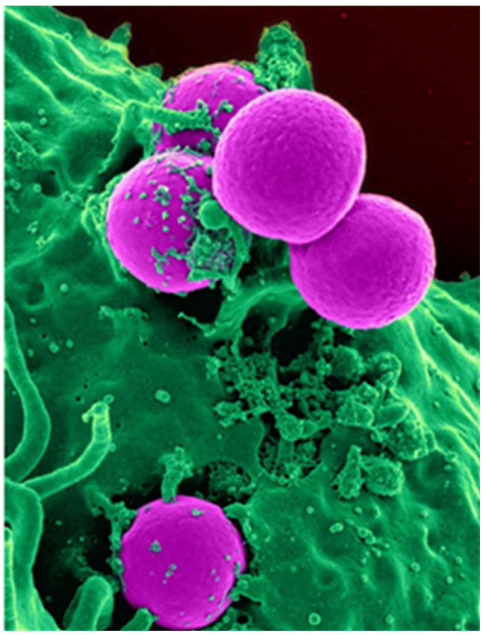

Figure . The bacterium *Staphylococcus aureus*. Source: Google Library, PubMed – NCBI.

Methicillin-resistant S. aureus can live for months in hostile environments and is thereby transmitted from surfaces long after it is initially deposited.
The evolution of such resistance does not cause the organism to be more intrinsically virulent than strains of S. aureus that have no antibiotic resistance, but resistance does make MRSA infection more difficult to treat with standard types of antibiotics and thus more dangerous. MRSA is especially troublesome in hospitals and nursing homes, where patients are at greater risk of nosocomial infection also known as hospital acquired infection.

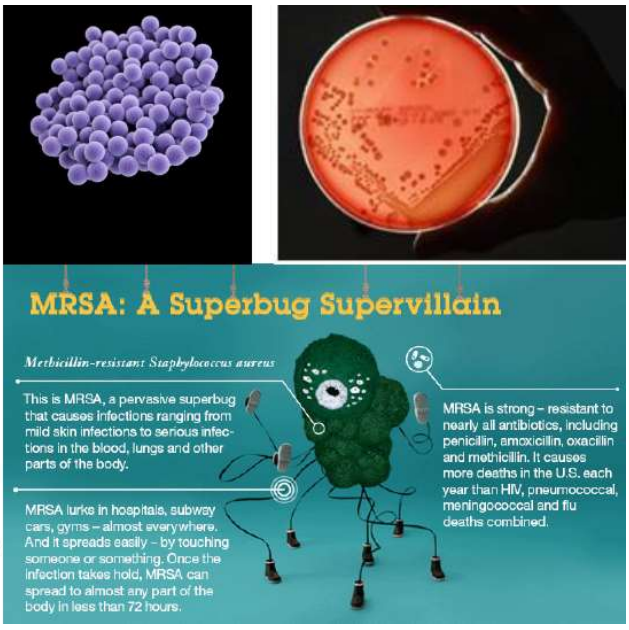

Figure . The bacterium *Staphylococcus aureus*. Source: Google Library, PubMed – NCBI.

Materials and methods: In order to prevent antibiotic resistant bacteria spreading not only inside hospitals, nurse houses but also public transports and schools; my research has been focused on the antimicrobial power of silver nanoparticles. In fact, in a study conducted in Lisbon – the capital of Portugal following a previous one in the city of Oporto (Portugal), has been documented the MRSA contamination of hand touched surfaces of public buses. The majority of the isolates belonged mainly to EMRSA-15 clone, MRSA New York/Japan clone and, MRSA USA300 or related clones. The first two clones are currently the two major lineages circulating in Portuguese hospitals! The conclusion of the study was that public buses in two major cities in Portugal are often contaminated with MRSA representing the dominant clones in hospitals in the particular geographic area. It has been clear that MRSA contamination of public transport and the transfer of the bacteria to the hands of passengers may represent a route through which hospital-acquired MRSA clones may spread to the community[116]. The spread of pandemic methicillin-resistant Staphylococcus aureus (MRSA) clones such as USA300 and EMRSA-15 is a global health concern. As a part of a surveillance study of three long-term care facilities in the Greater Chicago area, phenotypic and molecular characterization of nasal MRSA isolates was performed. In this American study it has been identified 22 EMRSA-15 isolates from 14 patients in three nursing homes that were sharing patients with some 40 acute care facilities in the region. Further, 12 of these 14 patients were residents of one nursing home, and their nasal carriage surveillance isolates accounted for 5.8% of all MRSA isolates identified at that facility. This study represents the evidence of the largest identified cluster of EMRSA-15 isolates observed in the United States, which is of concern since EMRSA-15 has been shown to replace previously predominant MRSA strains in Germany, Spain, Portugal, and Singapore[117-120]. In 2017 the Kazan Federal University (Volga Region, Russia), discovered that *S. aureus* survives in *P. aeruginosa* biofilm under antimicrobial treatment conditions[70]. It has been experimentally demonstrated that exist synergistic interactions between *P. aeruginosa* and *S. aureus* in fact this one can produce lactate that is a carbon source that *P. aeruginosa* preferentially consumes over medium-supplied glucose[69]. In addition to this, the evidence suggests that *P. aeruginosa – S. aureus* infections are more virulent than monoculture infection with either species[68].

As detailed in chapter 2, silver has been recognized for its antimicrobial properties for centuries. Silver exerts a broad-spectrum antimicrobial effect against bacteria and, the development of bacterial resistance is rare and sporadic. Lots of studies on the antibacterial efficacy of silver, with particular emphasis on would healing, have been performed on planktonic bacteria[121]. With respect to chronic infections, however, the failure to achieve bacterial eradication with antimicrobial

measures is, as published by Bjarnsholt et al. 2007, due to the lifestyle bacteria adopt during chronic infections, namely the biofilm mode of growth. In this study it has been investigated the action of silver on mature *in vitro* biofilms of *Pseudomonas aeruginosa* (PAO1), a primary pathogen of chronic infected wounds. The experimental results showed that silver is very effective against mature biofilms of *P. aeruginosa*, but that the silver concentration is important. In fact, the bactericidal concentration of silver required to eradicate the bacterial biofilms was 10-100 times higher than that used to eradicate planktonic bacteria[121].

Interestingly, it has been discovered that within minutes of when a bacterium attaches to a surface it undergoes a remarkable change in gene function. Many operating genes (e.g. flagellae) are down regulated while others (slime production) are upregulated. How do we know it?
We can get a picture of cellular activity by examining the proteins produced by cells at a particular time by using a SDS-PAGE.
Here, we can see proteins from the outer membranes of planktonic (outlined in blue, Lanes 1-4 and 6) and biofilm (outlined in red, Lane 5) bacteria, of a single strain.

We can clearly see that the bands of proteins are strikingly different, telling us that the planktonic and biofilm forms of a single species are expressing different genes, and therefore carrying out different activities.

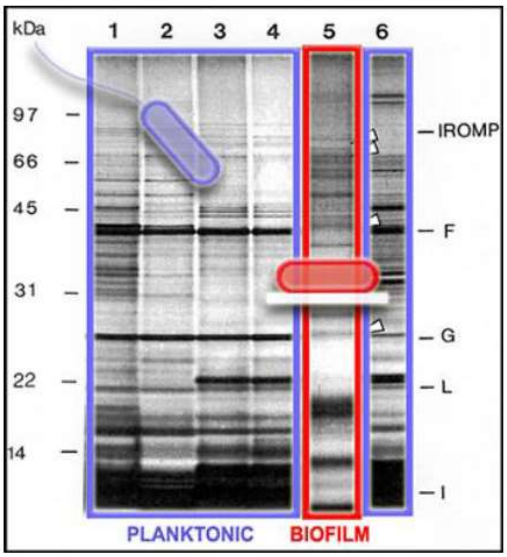

SDS PAGE preparation of the outer membrane proteins (OMPs) of Pseudomonas aeruginosa cells in planktonic and biofilm states.

Courtesy of Alfred B. Cunningham, John E. Lennox, and Rockford J. Ross - Montana U.S.A. Eds. 2001-2010.

Figure . The SDS page of *P. aeruginosa* cells in planktonic and biofilm states[122]. Courtesy of Alfred B. Cunningham, John E. Lennox and, Rockford J. Ross – Montana U.S.A. Eds. 2001-2010.

The antimicrobial activity of silver has been fully described by Dr J.A. Farwell in 1970, in his own manuscript entitled *Sensitivity of Pseudomonas aeruginosa to silver*, it has been reported that aqueous silver nitrate was effective against virulent pseudomonads invading burns (in burn therapy) and the results of such therapy were improved when non-viable tissue was continually removed from the burn area. A relationship between lethal action and concentration of silver ions was established and reported in 1932. Later, in 1940 it has been found that an organo-metallic complex was formed and that metallic oxides were also active and, the adsorption of the silver onto the cell surface lead to the formation of a metal-protein complex which was lethal to the bacterial cells. The action of silver is identical to that one proper of heavy metals, in fact they act in two stages: first,

adsorption onto the cell and second, reaction with essential cell components causing breakdown of metabolism followed by death[123]. Dr Farwell demonstrated that a direct relationship was shown between silver concentration and the percentage survival after 20 mins (*P. aeruginosa* suspensions). This relationship held over the range 5×10^{-6}M – Ag^{+} to 3×10^{-5}M – Ag^{+}. Above this level a maximum die-off was obtained. The time taken for a 30% drop in viable count also decreased with increased silver concentration to a minimum at similar concentrations to that at which the die-off was maximum. It was clear that *P. aeruginosa* stored suspensions of non-depleted cells and, magnesium depleted suspensions survived better than those cells depleted of the carbon source – glucose (the adsorbed magnesium on the cell wall aided survival of stored suspensions). In fact, it has been found that *P. aeruginosa* did not lay down storage products even when conditions favoured this and also that, when the cells became carbon or nitrogen depleted in the growth medium, ribosomal degradation occurred. These depleted cells, stored in buffer, showed loss of viability as well as decrease in RNA and DNA but non-depleted cells showed an initial rise in count under the same conditions. Preliminary experiments with silver treated cells suggested that leakage occurred, and that this leakage was a result of silver action (and not of cell death). This implied that silver had an effect on the permeability mechanism of the cell and this had been reported in 1963 when it has been attributed the stimulation of *Neurospora* respiration by silver to increased permeability[123]. More recently, on Nature in 2015 it has been explained the antibacterial activity of silver-killed bacteria. It has been reported a route for the prolonged action of silver (biocidal agent) that has not been previously recognized and, that Wakshlak RB. et al. 2015 called the "zombies effect": bacteria which were killed by silver show significant biocidal activity towards viable population of the same bacterium. The origin of this phenomenon is in two characteristics of the metal-induced biocidal action: first, the metallic species are not deactivated by the killing mechanism and, therefore can carry on their biocidal effect repeatedly; and second, the dead bacteria serve as an efficient sustained release reservoir for releasing the lethal metallic cations for further action against other living bacteria. It has been experimentally demonstrated that biocidally-killed bacteria are capable of killing living bacteria. This concept is demonstrated by first killing *Pseudomonas aeruginosa* (PAO1) with silver nitrate and then challenging, with the dead bacteria, a viable culture of the same bacterium: an efficient antibacterial activity of the killed bacteria is observed. A mechanism is suggested in terms of the action of dead bacteria as a reservoir of silver, which, due to Le-Chatelier's principle, is re-targeted to the living bacteria[124]. The so-called "zombies effect" of *Pseudomonas aeruginosa* is shown in the following figure.

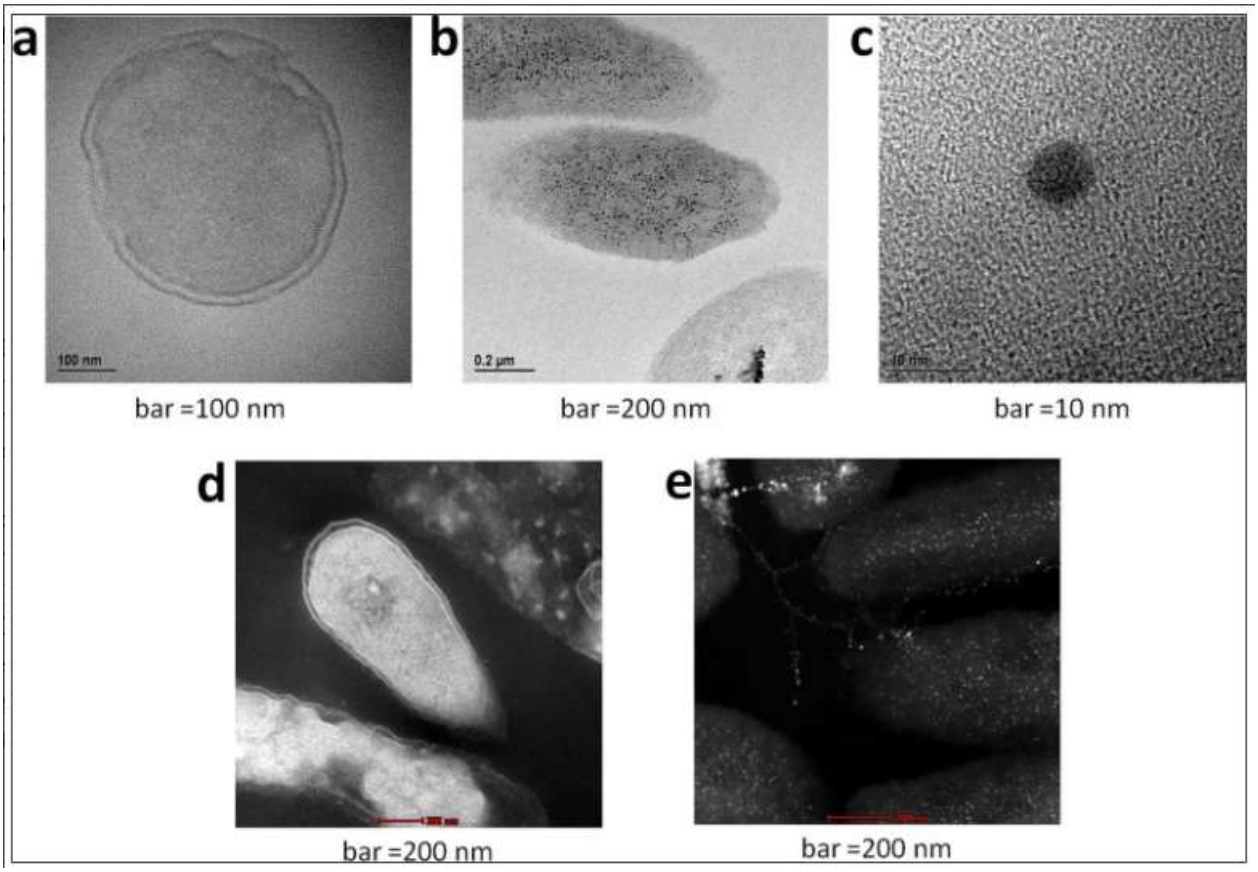

Figure . The zombies effect of PAO1. TEM (bright background) and STEM (dark background) of *P. aeruginosa* before (**a** and **d**) and after (**b**, **c**, and **e**) treatment with silver: the black (**b**) and white (**e**) granules represent silver deposition which account for the "zombies" biocidal action. Courtesy of Wakshlak RB., Pedahzur R., Avnir D., Nature – Scientific Reports, 2015.

It is widely clear that today the two most problematic nosocomial pathogens are *Pseudomonas aeruginosa* and *Staphylococcus aureus* and, both often express multidrug resistance. A number of case-control studies at individual hospitals (it has been measured fluoroquinolone use from 1999 through 2003 in a network of hospitals in the USA) have identified fluoroquinolone use as a risk factor for acquisition of fluoroquinolone-resistant *P. aeruginosa* and methicillin-resistant *S. aureus* (MRSA)[125]. To cope with the problem, a series of samples were prepared for microbiological testing using a similar two-step dipping method as previously described in chapter 2. A simple swell-encapsulation-shrink process was employed to incorporate crystal violet (CV) dye and silver nanoparticles (Ag NPs) into polyurethane using acetone as a swelling solution. In the swell-encapsulation process, the CV molecules and Ag NPs in the acetone penetrate the polyurethane matrix as it swells, and the polyurethane then shrinks when it is removed from the solution. The CV molecules and Ag NPs remain inside of the polyurethane matrix. But this time the silver nanoparticles solution described in chapter 2 (citrate-capped silver) was triple concentrated and,

following the method published by Lambadi P. et al. 2015, a biofunctionalized with polymyxin B silver nanoparticles solution was also prepared. The polymyxin B is an antibacterial peptide[126]. Antimicrobial peptides (AMPs) have been identified in most living organisms (such as bacteria, fungi, plants, invertebrates and vertebrates including humans) as an important component of their natural defences. They form the first line of host defence against pathogenic infections and are an evolutionarily conserved component of the innate immune system. These peptides are potent broad-spectrum antibiotics, they are synthesized constitutively at epithelial surfaces that is the location where the initial contact will all microorganisms takes place[85].

Preparation of chemical stock solutions. The crystal violet solution – solution A was prepared dissolving 60mg of crystal violet powder (CV, Sigma-Aldrich, St. Louis, MO, USA) in 100ml of a solution containing 10ml of DI water and 90ml of acetone. The solution was sonicated in an ultrasound bath for 5 min in order to ensure complete dissolution of CV powder. The solution B was prepared dissolving 45mg (0.26mM) ×3 of $AgNO_3$ (Silver nitrate, Sigma-Aldrich, St. Louis, MO, USA) in 50ml of DI water to produce an approximately 5mM solution. The solution C was prepared dissolving 294.7mg (1mM) ×3 of $Na_3C_6H_5O_7 \cdot 2H_2O$ (tri-sodium citrate dihydrate, Hopkin & Williams Ltd, London, UK) in 50ml of DI water to form a 20mM solution. Synthesis of silver nanoparticles was prepared mixing 10ml of solution B with 180ml of DI water and heated with constant stir. After the mixture was boiled for ~ 2 min, 10ml of solution C was added. With constant stir, the mixture was boiled for a further 30 min and then allowed to cool. The development of a dark-brown colour was observed during the process. The biofunctionalized with polymyxin B silver nanoparticles solution (solution D) was prepared by the addition of freshly prepared silver nitrate (2 mM) and NaBH4 (0.6 mM) to a polymyxin B solution in methanol (Silver nitrate, sodium borohydrate, polymyxin B, methanol, Sigma-Aldrich, St. Louis, MO, USA). The resultant mixture was incubated for 0–30-minute time periods at 30°C under illumination at 40 W yellow light (141.3 lux) as published by Lambadi P. et al. 2015. The development of a yellow colour was observed during the process. The prepared polymyxin B-capped silver nanoparticles (PBSNPs) were dialyzed against milli-Q water for 12 hours using a 10 kDa cut-off membrane to remove unbound polymyxin B and free silver ions. The unbound polymyxin B was removed from PBSNPs by passing the sample through a 10 kDa molecular weight cut-off spin-filter (Vivaspin, Vivaproducts, Inc., Littleton, MA, USA). The morphology and size of silver nanoparticles were observed using TEM (JEM-2100, JEOL Inc., Peabody, MA, USA). The presence of polymyxin B on the surface of silver NPs and the effect of attachment on the secondary structure of peptide were measured with FTIR (Thermo Nicolet NEXUS 670 FTIR; GMI, Ramsey, MN, USA) and CD

spectroscopy (Chirascan™ CD Spectrometer; Applied Photophysics Ltd, Leatherhead, UK), respectively. Free polymyxin B and citrate-capped nanoparticles were used as control as published by Lambadi P. et al. 2015.

Preparation of white light-activated antimicrobial surface. Polyurethane squared samples (1.0×1.0cm) were immersed in 10ml of acetone solution and left to swell in the dark for 24 h and then still wet, were immersed in solution A (CV solution) and left to swell in the dark for 24 h. The samples were recovered from the CV solution and washed using a DI water bath sonicator for 2 times and then air-dried for 24 h in the dark. The samples were prepared as follows: CV only, CV with Ag NPs. Additionally, NPs encapsulated polyurethane samples without CV – polyurethane with Ag NPs, were prepared as follows: polyurethane squared samples (1.0×1.0cm) were immersed in 10ml of acetone solution and left to swell in the dark for 24 h and then still wet, were immersed in the two silver NPs solutions prepared (half in citrate-capped silver NPs solution and half in polymyxin B-capped silver NPs) and, left to swell in the dark for 24 h. Then samples were air-dried for 24 h in the dark.

Material characterization. This part has been performed accordingly with Chapter 2 of this thesis: TEM analysis of silver nanoparticles revealed that both citrate-capped silver NPs and polymyxin B-capped silver NPs were spherical in shape with different diameters; citrate-capped Ag NPs ~43nm and, polymyxin B-capped Ag NPs ~15nm.

The UV-vis absorption spectra against NPs suspensions, control and treated samples were measured using UV-vis Spectrometer (PerkinElmer Inc., Winter St., CT, USA). Absorption was measured from 350 to 900nm. To determine NPs uptake from NPs suspension to polyurethane, the UV-vis spectra of NPs suspension were measured before and after swell-encapsulation-shrink process. The polymer sample was immersed in a mixture of acetone (9ml) and NPs (1ml) for 24 h. The comparison of absorbances *before* and *after* at 409nm (citrate-capped Ag NPs) and at 414nm (polymyxin B-capped Ag NPs) was enable determination of the total amount of NPs absorbed in the polyurethane samples after the treatment.

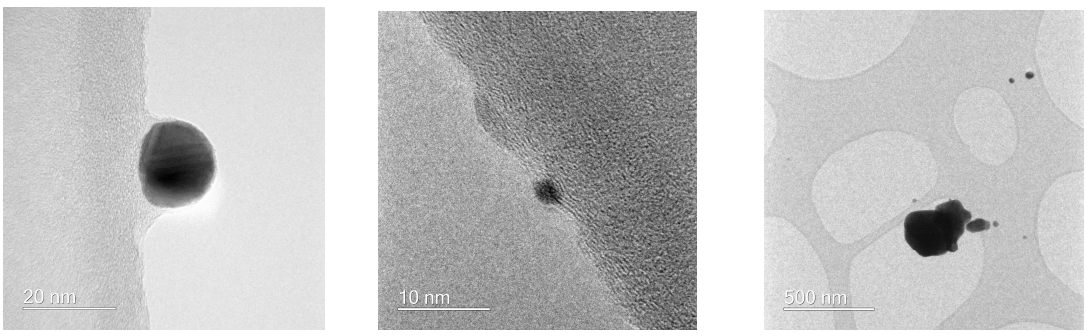

Figure . TEM photos selection of my silver nanoparticles. Courtesy of UCL laboratories.

Antimicrobial tests. To examine the antimicrobial activity, a range of polyurethane samples (1.0×1.0cm) was used to perform the experiments: acetone treated polyurethane (control), crystal violet-coated polyurethane, crystal violet-coated nano-silver encapsulated polyurethane, and nano-silver encapsulated polyurethane. These samples were tested against Epidemic MRSA 4742 representative of a Gram-positive epidemic bacteria (isolated at UCL Hospital) and *Pseudomonas aeruginosa* PAO1 representative of Gram-negative bacteria resistant to the majority of currently used antibiotics (ATCC – LGC Standards, Middlesex, England, UK). These organisms were stored at – 70°C in Brain-Heart Infusion broth (Oxoid Ltd, Hampshire, England, UK) containing 20% (v/v) glycerol and propagated on Mannitol salt agar and Cetrimide agar (Oxoid Ltd, Hampshire, England, UK) respectively, according to the British Pharmacopoeia 2018 (Ed.).

BHI broth (10ml) was inoculated with one bacterial colony and cultured in air at 37°C for an incubation of 18 h with shaking, at 200 rpm. The bacterial pellet was recovered by centrifugation (21°C, 2000×g, 5 min), washed in phosphate buffered saline (PBS) and centrifuged again to recover the bacteria, which were finally re-suspended in PBS (10ml). The 2 times washed suspension was diluted 1000-fold in PBS to obtain the inoculum. The inoculum contained 4.6×10^6 colony forming units per mL (CFU mL^{-1}). The inoculum in each experiment was confirmed by plating ten-fold serial dilutions on agar for viable counts. Duplicates of each polymer sample type were inoculated with 25µL of the inoculum (containing 1.1×10^5 CFU) and covered with a sterile cover slip (22mm×22mm) to ensure good contact between the bacteria and the sample surface. The samples were placed into plastic petri dishes containing moistened filter paper to maintain humidity at room temperature. The samples were then irradiated for up to ~5 hours using a white light source, the white light intensity was measured using a lux meter (LX-101, Lutron Inc., Coopersburg, PA, USA) at a distance of 30cm from the light source. The intensity of the light ranged from 390 to 530 lux. A further set of samples (in duplicate) was maintained in the dark for the duration of the irradiation time. In the dark, the light was completely blocked (0 lux). After light exposure, the inoculated samples and cover slips were placed into 450µl of PBS, and mixed using a vortex mixer for 1 min. The neat suspension and ten-fold serial dilutions were plated on Mannitol salt agar and Cetrimide agar respectively for viable counts. The plates were incubated aerobically at 37°C for 24 h. Finally, the colonies grown on these plates were counted. All experiments, unfortunately, could not be reproduced three times for each bacterial type because the time was not enough.

Results and discussion: In this work it has been used a "facile method" to develop a polymer encapsulated with a phosensitiser dye in addition to silver nanoparticles. In the first step, the polyurethane samples were immersed in an acetone swelling solution. In the subsequent step, the

same samples sill wet, were immersed in a crystal violet solution for 24 h, another amount of samples in a 9:1 crystal violet solution : nano-silver solution for 24 h, and another amount in a nano-silver solution for 24h under dark conditions. Upon exposure to the solvent, the polymer swells enabling the dye molecules to diffuse through the polymer.

The antimicrobial activity of the control, CV dyed polyurethane samples, CV dyed and nano-silver encapsulated polyurethane samples and nano-silver encapsulated polyurethane samples under white light and dark conditions was tested against a representative strain of the Gram-positive bacterium, MRSA and, against a representative strain of the Gram-negative bacterium *Pseudomonas aeruginosa*. The data (of the first experiments performed) show that the antimicrobial activity of the polymers was promoted by exposure of the samples to a white hospital light source; a compact fluorescent lamp which emits light across the visible region of the spectrum and is similar to those commonly found in the UK NHS hospitals. In all experiments, a control sample set was maintained under dark conditions for the same period of time as the samples exposed to light and, in a further experiment, a sample set was incubated under dark conditions for an extended time period (24 h). The antimicrobial activity of crystal violet-coated polyurethane (CV only), crystal violet-coated nano-silver encapsulated polyurethane (CV Ag) and nano-silver encapsulated polyurethane (Ag only) was compared to that of a control, solvent treated polyurethane sample. The lethal photosensitization induced by these samples when exposed to a white light source emitting an average light intensity of ~500 lux at a distance of 30 cm from the samples for ~5 h is shown in Figure.

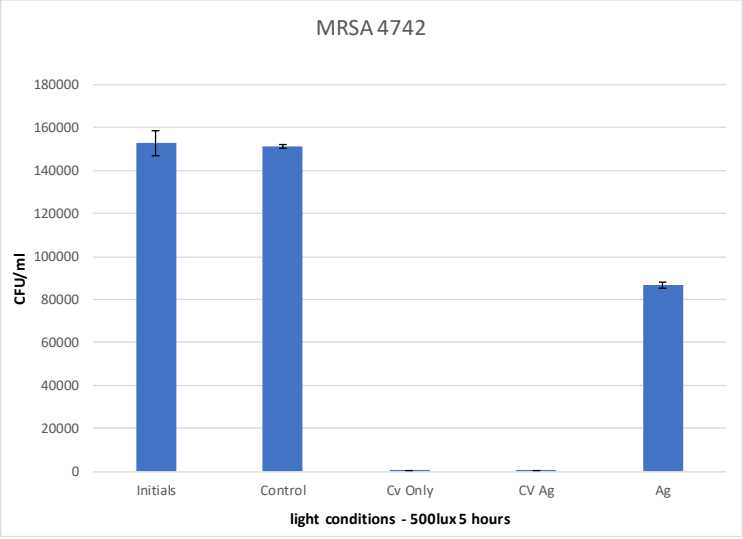

Figure . Antimicrobial activity of control and treated polyurethane (PU) samples on *4742 methicillin-resistant S. aureus* at 500 lux for 5 hours of incubation.

After 5 h at 500 lux, no reduction in the numbers of viable bacteria of MRSA 4742 was observed on the surfaces of the control material (polyurethane alone) and the nano-silver encapsulated polyurethane (Ag only). However, a statistically significant (*P*-value < 0.01) decrease in the number of viable bacteria was observed on the material containing crystal violet alone (2.48 log reduction in bacterial numbers) and crystal violet with Ag NPs (2.48 log reduction). After 5 h in dark conditions no significant reduction has been found in all samples, however after 24 h in the dark polyurethane containing CV alone and CV with Ag NPs showed a significant reduction in the numbers of bacteria below the limit of detection (*P*-value < 0.01, detection limit: below 10^2 CFU mL^{-1}). Additionally, in experiments of polyurethane containing Ag NPs only, no reduction in the number of viable bacteria was confirmed after 5 h incubation in the dark. An additional decrease of viable bacterial colonies has been found by using samples coated with the biofunctionalized silver nanoparticles (PBSNPs) after 5 hours at 500 lux and after 5 hours in dark conditions. However, after 24 h in dark condition, a significant reduction was observed on both polyurethanes coated with Ag NPs (*P*-value < 0.01, detection limit: below 10^2 CFU mL^{-1}).

Concerning the antimicrobial activity of the polyurethane samples against the Gram-negative bacterium *P. aeruginosa*, at the same light and dark conditions used for the MRSA, the following data has been found as shown in Figure .

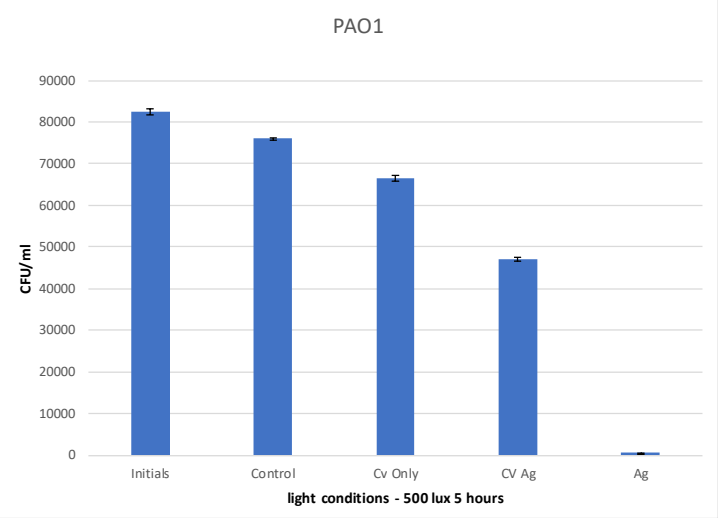

Figure . Antimicrobial activity of control and treated polyurethane (PU) samples on *Pseudomonas aeruginosa PAO1* at 500 lux for 5 hours of incubation.

After 5 h at 500 lux, no reduction in the numbers of viable bacteria of PAO1 was observed on the surfaces of the control material (polyurethane alone), polyurethane with only CV and polyurethane containing CV and Ag NPs. However, a statistically significant (*P*-value < 0.01) decrease in the number of viable bacteria was observed on the material containing Ag NPs alone (2.18 Log

reduction). After 5 h in dark conditions no significant reduction has been found in all samples, however after 24 h in the dark polyurethane containing only Ag NPs showed a significant reduction in the numbers of bacteria below the limit of detection (*P*-value < 0.01, detection limit: below 10^2 CFU mL^{-1}). Additionally, in experiments of polyurethane containing only CV and CV with Ag NPs, no reduction in the number of viable bacteria was confirmed after 5 h and 24 h of incubation in dark conditions. A similar situation has been found performing the same experiments using samples coated with the biofunctionalized silver nanoparticles (PBSNPs) after 5 hours at 500 lux and after 5 hours in dark conditions. Only after 24h all the viable colonies were totally destroyed.

As described in chapter 2, the XPS analysis of all samples confirmed that silver NPs remain inside of the polyurethane matrix and, consequently nothing has been found on the samples surface.

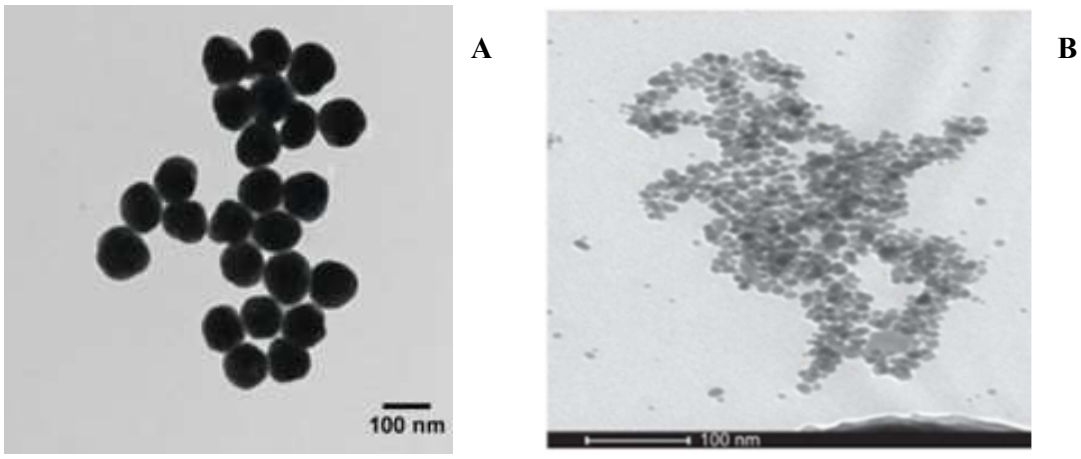

Figure . TEM images of silver nanoparticles; A: citrate-capped Ag NPs (courtesy of UCL laboratories) and B: polymyxin B-capped Ag NPs (courtesy of Prof Navani NK. – Indian Institute of Technology, Roorkee, Uttarakhand, India).

These initial experimental results were expected, although unfortunately there was not enough time to reproduce them three times for each bacterial type. According to Lambadi P. et al. 2015, it has been found that polymyxin B-capped silver nanoparticles had more antibacterial power than citrate-capped silver nanoparticles against planktonic cells of MRSA (gram positive bacterium) and *Pseudomonas aeruginosa* (gram negative bacterium). Apart from the antibacterial activity, it has been investigated the role of polymyxin B on PAO1 biofilm formation. Antimicrobial peptides (AMPs) have recently emerged as excellent antimicrobial agents to address multidrug resistance in bacteria. They act damaging the bacterial cell membrane at low concentrations. AMPs can also stabilize silver NPs by exerting a polyvalent effect, in fact they form layers on the surface of silver NPs and thus they can prevent agglomeration[127-130]. The biofunctionalized silver NPs used in this

study, said Lambadi P. et al. 2015, clearly showed an extensive damage of the bacterial cell membrane in the presence of PBSNPs and, consequently a decrease in MIC as compared with citrate silver NPs for their antibacterial activity against both antibiotic-resistant bacteria. They observed the cellular growth at OD_{600} after 10 hours. Growth above 10% of the OD at 600 nm (OD_{600}) of the positive control (lacking any antimicrobial agent) was considered uninhibited growth. MIC is the lowest concentration of PBSNPs that inhibited the visible growth of microorganisms. CSNPs with the same concentration were taken as a control[126]. The plausible explanation for the damage is that highly cationic polymyxin B peptides first get attached to the bacterial surface and make small and transient ion-permeable holes that disturb the functions of the bacterial membrane. Subsequently, the combined action of SNPs and polymyxin B led to a complete rupture of the bacterial membrane, resulting in leakage of the cell contents and finally cell death[131]. These results indicate that the enhanced antibacterial activity of PBSNPs was due to the presence of polymyxin B molecules on the surface of SNPs. The interaction of these conjugates provided an opportunity for both agents to act on the bacteria simultaneously, thus enhancing its inhibitory effect[132]. Polymyxin B is known to interact with the LPS part of lipid A of Gram-negative bacterial cell walls. LPS is also known as endotoxin, which is shed by Gram-negative bacteria and is notorious for causing sepsis and septic shock[133]. The PBSNPs efficiently removed endotoxin from the test samples (~97%) as compared with control (~16%). The efficient removal of endotoxin could be attributed to the polymyxin molecules present on SNPs owing to their enhanced surface-to-volume ratio as compared with the conventional column matrix[134]. Finally, Lambadi P. et al. 2015, reported that biofunctionalized silver nanoparticles were found to resist PAO1 biofilm formation. The ability of these functionalized nanoparticles for their antibiofilm activity against *P. aeruginosa* was tested: upon the exposure of PAO1 cells to MIC of PBSNPs (4.5µg Ag^0/mL) and CSNPs (12.5µg Ag^0/mL), a complete inhibition of bacterial growth (OD_{600}) occurred, with the disappearance of biofilm formation (OD_{550}) after 6 hours of incubation. These results reveal that PBSNPs display ~3-fold higher antibiofilm activity as compared with CSNPs, suggesting a paramount role being played by the capping agent polymyxin B. Concurrent inhibition of planktonic cell growth and biofilm formation with increasing concentration of PBSNPs suggests that this formulation is refractory to the establishment of bacterial biofilm likely due to inhibition of planktonic cells[126], as showed in the following figure kindly shared by Prof Naveen Kumar Navani research group – Indian Institute of Technology, Roorkee, Uttarakhand, India.

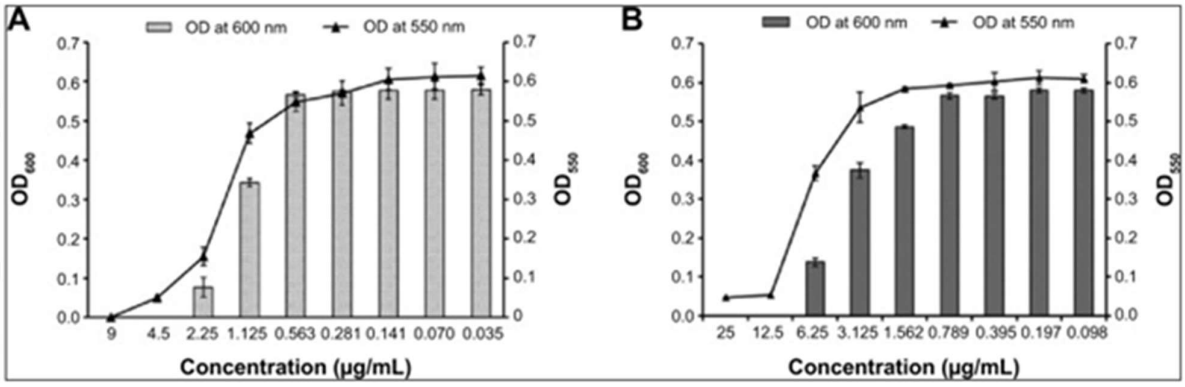

Figure . The PBSNPs inhibition of biofilm formation of PAO1 cells. Courtesy of Prof Navani NK. – Chemical Biology Laboratory, Department of Biotechnology and Centre of Nanotechnology, Indian Institute of Technology, Roorkee, Uttarakhand, India.

The last experiment that has been performed by using silver nanoparticles has been against *Streptococcus mutans* 25175 (ATCC – LGC Standards, Middlesex, England, UK), the Gram-positive bacterium mainly responsible of tooth decay. Unfortunately, there was not enough time left to reproduce the experiment three times, hence only the initial results have been collected. It has been applied the same method and, the same materials used to test the other two bacteria mentioned above. The bacterium has been plated on Columbia blood agar for viable counts (Columbia Agar Base – Lab M Ltd, Lancashire, England, UK + 5% defibrinated horse blood – E&O Laboratories Ltd, Bonnybridge, Scotland, UK).

A set of samples (in duplicate): the acetone treated polyurethane (control), CV dyed polyurethane samples, CV dyed and nano-silver (CSNPs) encapsulated polyurethane samples and nano-silver (CSNPs) encapsulated polyurethane samples have been tested at ~500 lux and under dark conditions (0 lux) for up to 5 hours against a strain of *Streptococcus mutans*. In addition to it, a sample set (in duplicate) was incubated under dark conditions for an extended time period (24 h). The results obtained were pretty much identical with that ones collected for MRSA. After 5 h at 500 lux, no reduction in the numbers of viable bacteria of *Streptococcus mutans* was observed on the surfaces of the control material (polyurethane alone) and the nano-silver encapsulated polyurethane (Ag only). However, a statistically significant (P-value < 0.01) decrease in the number of viable bacteria was observed on the material containing crystal violet alone (2.49 log reduction in bacterial numbers) and crystal violet with Ag NPs (2.49 log reduction). After 5 h in dark conditions no significant reduction has been found in all samples, however after 24 h in the dark polyurethane containing CV alone and CV with Ag NPs showed a significant reduction in the numbers of bacteria below the limit of detection (P-value < 0.01, detection limit: below 10^2 CFU mL^{-1}).

Additionally, in experiments of polyurethane containing Ag NPs only, no reduction in the number of viable bacteria was confirmed after 5 h incubation in the dark. However, after 24 h in dark condition, a significant reduction was observed on polyurethanes coated with Ag NPs (*P*-value < 0.01, detection limit: below 10^2 CFU mL^{-1}). Unfortunately, there was not enough time to test the samples coated with the biofunctionalized silver nanoparticles (PBSNPs) after 5 hours at 500 lux and after 5 and 24 hours in dark conditions (0 lux).

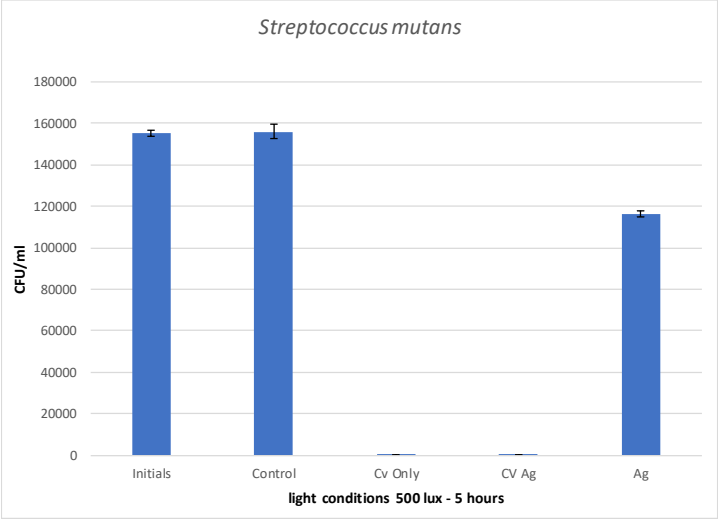

Figure . Antimicrobial activity of control and treated polyurethane (PU) samples on *S. mutans* 25175 at 500 lux for 5 hours of incubation.

These results, although they are not enough at the moment, were expected. According to Prof M. Nisnevitch – Ariel University Israel, an alternative approach to the eradication of bacteria is based on photodynamic treatments with the help of photosensitizers, which are dye compounds capable of transferring the energy of absorbed visible light to surrounding bio-organic molecules (called a Type I photodynamic reaction) or to dissolved oxygen (called a Type II photodynamic reaction). The Type I reaction includes excitation of photosensitizers upon illumination at an appropriate wavelength and energy transition to organic substrates, thus, producing active free radicals and radical ions. The Type II mechanism differs from the Type I in the second stage of action, where energy is transferred from the photosensitizers to oxygen molecules, exciting them and causing the formation of reactive oxygen species. The active products in both cases cause direct and indirect damage to cellular components, such as membrane phospholipids and proteins, leading to membrane leakage, cytolysis, and death of pathogenic cells[135-138]. It has been reported by Strømme M. et al. 2012, that bacteria in biofilms better survive harsh environmental conditions and, consequently these bacteria compared to the planktonic ones have a 10 – 1000 times higher resistance towards antibiotics. This has become a major healthcare concern as antibiotic-resistant bacterial strains like methicillin-resistant *Staphylococcus aureus* (MRSA) are appearing. Multiple

factors contribute to this resistance, including physical and chemical diffusion barriers, reduced sensitivity towards antibiotics due to the slow growth rate of bacteria in biofilms, as well as the structural heterogeneity within biofilms and development of biofilm-specific biocides-resistant bacteria phenotypes. Furthermore, biofilms are often associated with implants (e.g. dental implant) or other biomaterials as such biocompatible materials also provide an ideal substrate for biofilm formation. Understanding biofilms and the antibacterial methods for their removal of inhibition is thus critical in the development of functional biomaterials. The specific growth rate of *Streptococcus mutans* bacteria in biofilm mode of growth has been found by Strømme M. et al. 2012, and it was $0.70h^{-1}$, compared to $1.09h^{-1}$ in planktonic growth. The applied method has been based on the derivation of the specific growth rate of *Streptococcus mutans* bacteria biofilm from a series of metabolic assays using the pH indicator phenol red and, it has been demonstrated that this information could be used to more accurately quantify the relative number of viable bacteria in a biofilm[139]. The Department of oral biology of the Buffalo University – New York (USA) investigated the susceptibility of selected bacteria as well as *Streptococcus mutans* biofilm to MUC7 peptides and compared the activities with those of other known antimicrobial peptides. Among the antimicrobial peptides, histatin and mucins are two families of human salivary proteins that form the innate immunity system, a first-line of the host defence system against pathogens. Histatins and histatin-derived peptides have been shown to possess a significant *in vitro* antimicrobial activity against fungi, bacteria, and bacterial biofilms. The low molecular mass human salivary mucin – MUC7 (357 amino acid residues), protects the oral cavity from microbial infections through more general protective mechanisms (such as binding to and clearance of various microorganisms) rather than the direct killing of microorganisms. Dental caries and periodontitis are common oral diseases: *Streptococcus mutans* is the main pathogenic agent of dental caries and, *Porphyromonas gingivalis* and *Actinobacillus actinomycetemcomitans* are the bacteria associated with periodontitis. The prevention of dental caries and periodontal disease requires the control of these pathogens that exist in an oral biofilm known as dental plaque. The MIC and MBC of peptides for *S. mutans*, *Escherichia coli*, *Streptococcus gordonii*, *Actinobacillus actinomycetemcomitans*, *Porphyromonas gingivalis* and *Pseudomonas aeruginosa* were determined by Wei GX. et al 2006, using the microdilution method. For *S. mutans*, the effects of the peptides on the kinetics of growth inhibition, time-killing and, on biofilm formation and reduction were also examined. The experimental results carried out showed that *S. mutans* was the most susceptible to all peptides tested (MICs of 9.4-25.0 microM), compared with the other species (MICs of 3.1->100 microM). The MUC7 peptides (except MUC7-12-mer-L4) exerted 2-fold higher activity against *S. mutans* than Hsn5-12-mer and magainin-II, and faster killing of *S. mutans* than Hsn5-12-mer. The

MUC7 peptides also had an effect on *S. mutans* biofilm. One day developed biofilm viabilities were inhibited by 49-75%. On hydroxylapatite discs, the formation of biofilm was also considerably reduced. The MUC7 peptides present somewhat preferential antimicrobial activity against *S. mutans* and, they also influence *in vitro* formation and reduction of the preformed *Streptococcus mutans* biofilm[140].

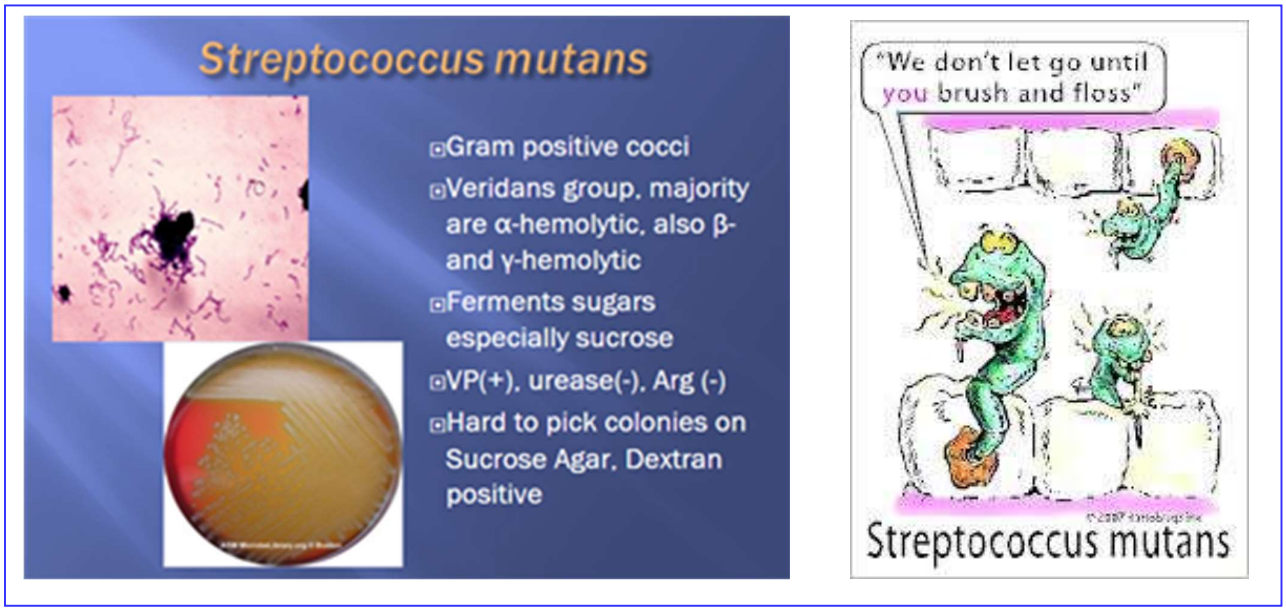

Figure . The bacterium *Streptococcus mutans*. Source: Google Library, PubMed – NCBI. Streptococci and oral streptococci (2011) retrieved from the Oral Environment website: http://www.ncl.ac.uk/dental/oralbiol/oralenv/tutorials/streps.htm and (2012) retrieved from American Dental Association website: www.gsa.ada.org

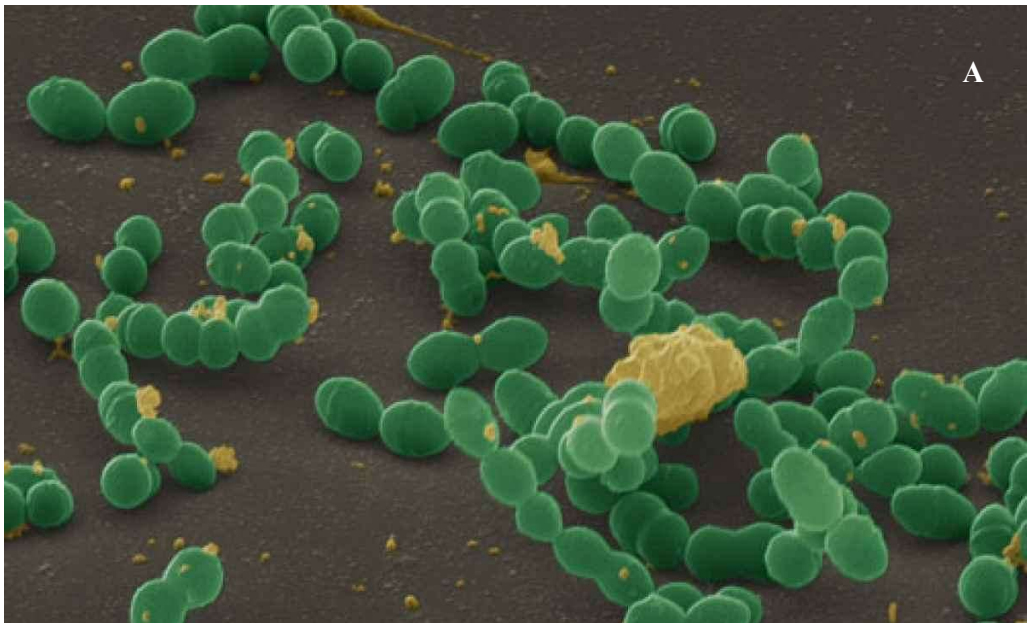

Figure . The bacterium *Streptococcus mutans* (images A, B). Source: Google Library, PubMed – NCBI.

Figure . The mouth microbes. Source: Google Library, PubMed – NCBI.

3.1.3. CONCLUSION

It is widely clear nowadays that infectious diseases cause a huge burden on healthcare systems worldwide and, that pathogenic bacteria establish infections by developing the antibiotic resistance. Unfortunately for us, they can also modulate the host's immune system, whereas opportunistic pathogen bacteria like *Pseudomonas aeruginosa* adapt to adverse conditions owing to their ability to form biofilms. Infections associated with surgical devices and medical implants pose persistent and severe problems that account for high morbidity in hospital settings. The Center for Disease Control and Prevention (CDC) estimated that surgical site infections account for ~22% of hospital-acquired infections[141]. Synthesis of nanomaterials holds infinite possibilities as nanotechnology is revolutionizing the field of medicine by its myriad applications. Silver nanoparticles demonstrated to have the power to overcome this growing problem. It has been shown that combined antibacterial action of silver nanoparticles and polymyxin B in solution exerts a synergistic effect on bacterial pathogens; briefly, the antimicrobial effectiveness of silver nanoparticles is enhanced by the antimicrobial peptide polymyxin B. In other words, the power of silver has been increased by synthesizing biofunctionalized silver NPs. Moreover, the antibacterial property of the polymyxin B-capped silver nanoparticles did not alter significantly over a period of 1 month[142]. It is also clear that photosensitizers, which are dye compounds capable of transferring the energy of absorbed visible light to surrounding bio-organic molecules or to or to dissolved oxygen, can be activated by white light causing the death of bacteria cells. This can be very useful limited to dermatologic and dental problems. The development of efficient antibacterial coating has been recognized as a major challenge in mitigating biofilm formation and controlling the infectious agents in hospital settings.

Future work will be focused on carrying on the missing experiments on antibiotic resistance bacteria to select the best coating material to kill them. Green synthesis of nanoparticles has become the need of the hour because of its eco-friendly, nontoxic, and economic nature. It will be very challenging to produce silver nanoparticles by using the leaf extract of *Rosa damascena* as a bio-reductant to reduce silver nitrate, as detailed by Ahmad N. et al 2015, leading to synthesis of silver nanoparticles (AgNPs) in a single step, without the use of any additional reducing or capping agents[143]. The relatively higher stability of nanoparticles produced by plant sources as compared to microbial ones further tip the scales in favor of synthesis utilizing plant sources. Various plants can be employed for the nanoparticle synthesis such as *Cinnamomum camphora, Medicago sativa, Pelargonium graveolens, Avena sativa, Azadirachta indica, Tamarindus indica, Emblica officinalis, Aloe vera, Coriandrum sativum, Carica papaya, Parthenium hysterophorus, Acanthella elongata, Sesuvium portulacastrum, Chrysanthemum indicum L, Melia azedarach L, Saraca indica,*

Caesalpinia coriaria, Vitex negundo L. Biomolecules like honey can also be used for the synthesis of e.g. gold nanoparticles. Because of their submicroscopic size and unique material characteristics, manufactured nanoparticles may find practical applications not only in engineering, but also in medicine[143] especially in dentistry in fact it will be possible to manufacture antimicrobial aligners or similar (e.g. Invisalign®) to help preventing gingival inflammation and tooth decay.

3.1.4. ACKNOWLEDGEMENTS

I would like to acknowledge my PhD Coordinator and Supervisor Prof Mario Morino and my PhD Vice-Coordinator Prof Alberto Arezzo because they allowed me to go to London for completing my PhD programme. It is a pleasure to acknowledge Dr J.A. Farwell, the librarians and, the kind colleagues working in the Support Team of the Royal Pharmaceutical Society of Great Britain (66-68 East Smithfield, London E1W 1AW) and in the UCL School of Pharmacy (29-39 Brunswick Square, London WC1N 1AX), in particular Ms Nadia Bukhari – Senior Teaching Fellow in Pharmacy Practice, Pre-Registration Coordinator & UCL School of Pharmacy Alumni Coordinator and Prof Ijeoma Uchegbu – Professor of Pharmaceutical Nanoscience. I acknowledge Prof Naveen Kumar Navani and his research group – Indian Institute of Technology, Roorkee, Uttarakhand, India. I am also grateful to Prof Eva Sapi – Chair of the department of biology and environmental science at University of New Haven (USA), Prof Ehmke Pohl – Professor in the Dept. of Biosciences and in the Dept. of Chemistry Durham University, Co-Director in the Biophysical Sciences Institute, Member of the Durham X-ray Centre and Fellow of the Wolfson Research Institute for Health and Wellbeing Durham University (UK), Prof Elspeth Garman – Professor in the Dept. of Biochemistry, University of Oxford, Nicholas Kurti Senior Research Fellow in Macromolecular Crystallography, Brasenose College Director of the Systems Biology Programme at the Doctoral Training Centre, University of Oxford, Professor of Molecular Biophysics, Department of Biochemistry, University of Oxford (UK), Prof Michael Vasil – Emeritus Professor at the Dept. of Microbiology School of Medicine University of Colorado Denver (USA), Prof Nicola A. Carlone – Emeritus Professor at the Dept. of Microbiology School of Medicine University of Turin (Italy) for their experienced and professional suggestions on the bacterium *Pseudomonas aeruginosa*. Finally, I acknowledge the journalists Yasmeen Abutaleb, Ryan McNeill and Deborah J. Nelson who on 18th November 2016 wrote the article entitled *"One life, two donated organs and $5.7 million in bills – a tale of superbugs' deadly costs"* published by Reuters.

3.2 Antibacterial activity in Manuka Honey

3.2.1. INTRODUCTION

Honey has been used as a medicine throughout the history of the human race, its medical use is already reported in the British Pharmacopoeia 2018 (Ed.)[144]. Among monographies, it is reported the European Pharmacopoeia monograph 2051 in which honey is defined as produced by bees (*Apis Mellifera* L.) from the nectar of plants or from secretions of living parts of plants which the bees collect, transform by combining with specific substances of their own, deposit, dehydrate, store and leave in the honey comb to ripen and mature. Production: if the bee has been exposed to treatment to prevent or cure diseases or to any substance intended for preventing, destroying or controlling any pest, unwanted species of plants or animals, appropriate measures are taken to ensure that the levels of residues are as low as possible. Characters – appearance: viscous liquid which may be partly crystalline, almost white to dark brown[144-145]. The British Pharmacopoeia 2018 (Ed.) defines *Apis Mellifera* L. as follows, the body is about 15mm long, black, with a silky sheen, and covered with red hairs with a touch of grey. The broad tibiae are without spines. The posterior margins of the segments and legs are brown, with gradual transition to orange-red. The claws are two-membered, the maxillary palps single-membered. On the hind legs are baskets or scoops invested with bristles. The wings have 3 complete cubital cells, with the radial cell twice as long as it is wide; the 3 cells on the lower margin and the 3 middle cells are closed. A duct connects the barbed sting with the poison sac[144].

Figure . The *Apis Mellifera* L. of Waikato region (NZ). Courtesy of Dr Megan Grainger – University of Waikato, Hamilton, NZ.

As clearly described by Dr Jonathan Stephens in his own manuscript published by the University of Waikato, Hamilton, NZ in 2006, honey has continued to be employed as a traditional therapy in many parts of the world, however it fell from favour in Western society with the development of modern antibiotics (Molan 1999a). One of the most common and persistent therapeutic uses of honey has been as a wound dressing, almost certainly due to its antimicrobial properties. A resurgence of interest in honey has led to an explanation of the reported medical properties. Honey has different actions as a treatment, and whilst the principle agent of healing is antibacterial activity; anti-inflammatory action, stimulation of the immune system, stimulation of cell growth, and antioxidant activity all enhance the therapeutic properties (Molan 1999b, 2001a). The literature describing the effect of honey on a wide range of bacterial species and its effectiveness in healing infected wounds has been recently reviewed (Molan 2001b). The antibacterial activity of honey has been extensively researched and is found to contain four components. The main factor is hydrogen peroxide, termed inhibine until correctly identified (White et al. 1962). Hydrogen peroxide is generated by glucose oxidase, an enzyme added to the nectar during concentration by the honeybee (*Apis mellifera*) from its hypopharyngeal gland (White et al. 1963). The concentration of hydrogen peroxide may be related to the dominant floral source, as ascorbic acid, metal ions and catalase found in varying quantities in nectar all contribute to hydrogen peroxide degradation (Molan 1997). The enzyme is also sensitive to heat and light denaturation, the sensitivity to both dependent to some extent on the floral source (Molan 1997). Two other antibacterial factors are common to honey, the effect of osmolarity and acidity. The water content of honey varies between 15–21% w/v, however due to the interaction between water molecules and the monosaccharide component only a small and insufficient fraction of the water is available for the growth of bacteria (Molan 1992). Likewise, the relatively high acidity of honey is antibacterial: the acidity varies between pH 3.2–4.5 and is beyond the lower limits for growth of most animal pathogens (Molan 1997). The fourth component does not appear to be universal in all honey types. Early work found antibacterial activity remained after the removal of hydrogen peroxide by the addition of catalase (Adcock 1962), and the non-peroxide antibacterial activity was reported to be a minor proportion of total antibacterial activity (Dustman 1979). Antibacterial fractions were recorded in water, alcohol, ether and acetone extracts of honey (Vergé 1951), and Gonnet & Lavie (1960) concluded antibacterial components were derived from phytochemicals present in the nectar source. The origin of the non-peroxide activity has been examined, and the proposals of lysozyme activity (Mohrig & Messner 1968), pinocembrin (Bogdanov 1984), flavonoids and phenolic acids (Russell et al. 1990; Wahdan 1998; Weston et al. 1999) have been dismissed, as the suggested active components are either too

dilute to account for the non-peroxide antibacterial activity or are also found in non-active honeys (Weston 2000)[146].

A number of studies analysing the antibacterial activities of New Zealand honeys have been completed (by Professor Peter Molan – University of Waikato, Hamilton, NZ). Whilst many honey types contained significant levels of hydrogen peroxide antibacterial activity, only mānuka honey often contained a relatively high level of non-peroxide activity (Molan et al. 1988; Allen et al. 1991a; Allen et al. 1991b), a unique property in the world's honey types other than the recently discovered non-peroxide activity in Australian jelly-bush (*Leptospermum spp.*) honey. The non-peroxide antibacterial activity was considered to be linked to the floral source (Molan & Russell 1988). However, mānuka honey samples demonstrated a considerable range of non-peroxide antibacterial activity, with a typical agar diffusion assay study reporting a mean antibacterial activity equivalent to 18.6% w/v phenol for 19 *L. scoparium* honey samples, with a significant standard deviation of 8% w/v phenol (Allen et al. 1991a). The variability was initially attributed to sample misidentification or processing differences (Allen et al. 1991a), and later a regional difference in phytochemical composition or concentration (Molan 1995). For the purpose of indicating the antibacterial activity for the consumer Professor P. Molan named the non-peroxide antibacterial activity of mānuka honey UMF® (Unique Mānuka Factor). The UMF® units of antibacterial activity used commercially are non-peroxide antibacterial activity equivalent to that of w/v% phenol on a standardised antibacterial agar diffusion assay using *Staphlococcus aureus* (NCTC 6571) as the control test organism, established by Allen et al. (1991a). Therefore, mānuka honey with a higher UMF® rating has a greater antibacterial effect and, is consequently more desirable for the production of therapeutic goods. UMF® 12+ mānuka honey is marketed for medical usage, however the UMF® 16+ honeys are obviously increasingly sought-after[146].

Identification of the components of mānuka honey confirmed the constituents are different from those found in the antibacterial *L. scoparium* essential oil (Tan et al.1988). The antibacterial activity of the essential oils is principally ascribed to the triketones, which are not present in the honey. The identified mānuka honey phytochemical components are similar regionally throughout New Zealand (Tan et al. 1989; Wilkins et al. 1993; Weston et al. 2000). There is a difference in the spectrum of antibacterial action of mānuka honey and other honeys in studies that determined the minimum inhibitory concentrations for species of bacteria. Some wound-infecting bacteria were found to be more sensitive to mānuka honey than a honey with activity due to hydrogen peroxide, and other species vice versa (Willix et al. 1992). Methicillin-resistant *Staphylococcus aureus* responded to the same concentrations of mānuka honey and a honey with activity due to hydrogen

peroxide, yet vancomycin-resistant *Enterococcos faecium* required approximately double the concentration of the peroxide honey to be inhibited compared with the mānuka honey (Cooper et al. 2002). Furthermore, hydrogen peroxide antibacterial activity of honey is not effective against all bacterial species; *Heliobacter pylori* was inhibited by an application of mānuka honey but was not inhibited by a peroxide honey (Al Somal et al. 1994)[146].

The recognition of the therapeutic value of mānuka honey has led to the development of an extensive range of medical products. Initially mānuka honey was prepared for the retail therapeutic market; however subsequent development for wound management (Molan 1999c) has established mānuka honey as an accepted topical treatment for wounds (Cooper 2004). Particular effectiveness is displayed by wound dressings impregnated with mānuka honey in treating burns, ulcers, skin-grafts, and skin or muscle infections containing antibiotic-resistant strains of bacteria, and several honey items produced for wound care have been approved by the regulatory health authorities in Australia, Canada, and the European Union member states (Molan & Betts 2004)[146].

Figure . The *Leptospermum scoparium* fruits of both wild and cultivated plants part of the indigenous flora of New Zealand (own pictures taken on 4th Dec 2017 – New Zealand summertime).

Approximately 8000 tonnes of honey is harvested by apiarists annually in New Zealand. The principal monofloral honey types are derived from nine plant families. Five families represent the indigenous flora; and the honey is marketed under the common names of mānuka, kānuka, rātā, pōhutakawa, (*Myrtaceae*); rewarewa (*Proteaceae*); kāmahi (*Cunoniaceae*); tāwari (*Escallioniaceae*); and honeydew (*Nothofagaceae*). Cockayne (1916) recognised at an early date *Leptospermum scoparium* as a major source of honey produced by the introduced honeybee, reflecting both the abundance of the plant and the surplus nectar production. *L. scoparium* is widely distributed throughout New Zealand and, is often described as a dominant member of the indigenous flora (Wardle 1991). Consequently, mānuka honey is harvested throughout the country. Mānuka honey has a very distinct flavour, colour and consistency, and accordingly a unique set of physical characteristics that are clearly different from other honey types harvested in New Zealand. The colour is described as dark cream to dark brown, the aroma an aromatic damp earth, with a slightly bitter mineral flavour. Until recently mānuka honey was used solely for culinary purposes. An increasing percentage of the mānuka honey harvested annually is used for the manufacture of therapeutic goods. This use has emerged within the last five years, after the medical effectiveness of mānuka honey first became apparent and was confirmed by medical trials[146].

Figure . The *Leptospermum scoparium* flower, the white one is typical of wild plants and the red one of cultivated plants both part of the indigenous flora of New Zealand (own pictures).

Figure . The Glasshouse Compound of the Dept. of Biological Sciences of University of Waikato, Hamilton, NZ where *Leptospermum scoparium* plants are cultivated (own pictures).

Figure . The *Leptospermum scoparium* plants blooming in New Zealand spring time (October 2017) at University of Waikato, Hamilton, NZ. Courtesy of Stevie Noe PhD candidate at University of Waikato, Hamilton, NZ.

3.2.2. EXPERIMENTAL

It has been reported by Prof. Dee Carter – School of life and environmental sciences, University of Sydney AUS, that one of the most common and persistent therapeutic uses of mānuka honey has been as a wound dressing due to its antimicrobial properties. Honey is usually derived from the nectar of flowers and produced by bees, most commonly the European honey bee *Apis mellifera* and, it is a complex mix of sugars, amino acids, phenolics and other substances. Phenolics act as antioxidants and may be responsible for anti-inflammatory and wound-healing properties of honey, these phenolic compounds with potential antimicrobial activity are usually present in darker coloured honeys. Honey types derived from different flowering plants vary substantially in their ability to kill bacteria, in fact it can profoundly alter the size and shape of bacterial cells, although the extent of this varies in different bacterial species. Mānuka honey has been tested *in vitro* on a diverse range of pathogens, particularly those that can colonize the skin, wounds, and mucosal membranes, where topical honey treatment is possible. Tests revealed that mānuka honey can effectively inhibit problematic bacterial pathogens like *Pseudomonas aeruginosa*, *Escherichia coli*, *Proteus mirabilis*, *Streptococcus* and *Staphylococcus* species (MRSA included), *Enterococcus faecalis* and many more[Dee A Carter 2016].

It is widely clear that pressure and temperature are important environmental variables influencing bacteria life. It has been examined by Vanlint et al. in 2011 how readily *Escherichia coli* – a nonsporulating and mesophilic bacterium, could build up resistance to extremes of temperature or pressure within a very short evolutionary time scale. This bacterium revealed its own potential to survive under exposure to high temperature or pressure, in fact *Escherichia coli* might adapt to lethal heat or high pressure – extending into the GPa range, two of the most important and general physical constrains on life. While heat resistance could only marginally be increased, experimental data show that piezoresistance could readily and reproducibly be extended into the GPa range, thereby greatly exceeding the currently recognized maximum for growth or survival. Results obtained in this study using the diamond-anvil cell (DAC) and the application of laser heating, revealed that the developed heat resistance was only marginal, shifting the upper survival temperature by approximately 1.03-fold from 58.5 to 60.0°C. However, the developed piezoresistance was extraordinary, and the upper pressure limit for survival readily increased at least 3-fold from 600 MPa to 2 GPa. Consequently, the first irrevocable evidence of microbial survival at ≥2 GPa has been experimentally demonstrated. [ ] It is equally clear that according to Hwang et al. 2016, *Escherichia coli* has been killed by a polyurethane with incorporated Ag NPs only (coming from a citrate-capped silver NPs solution) that exhibited a very strong antimicrobial

activity after 24 h of incubation under dark conditions reducing the number of viable bacteria below the limit of detection (P-value < 0.01, detection limit: below 10^2 CFU mL^{-1})[59].

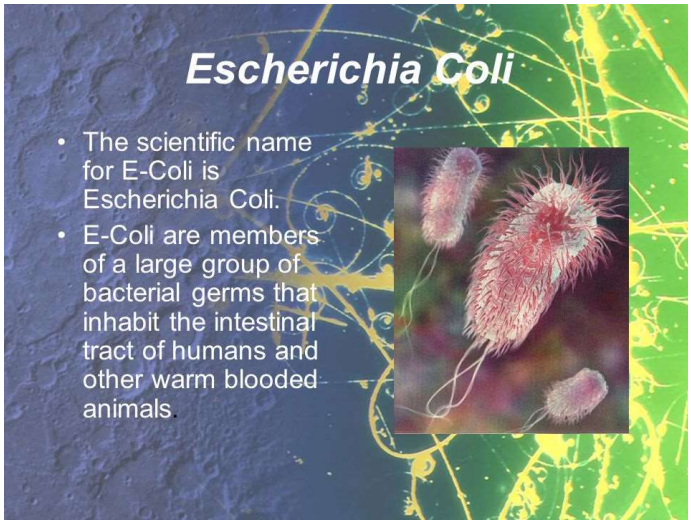

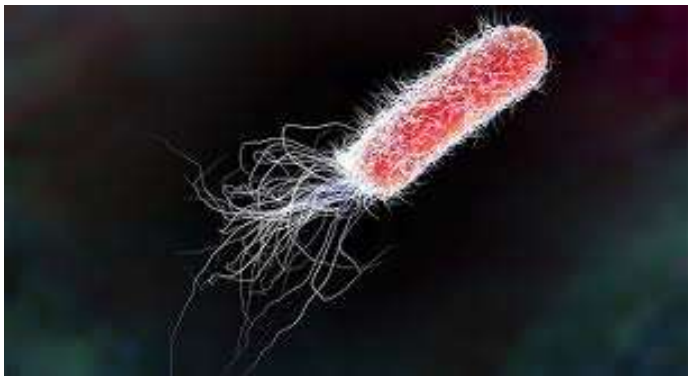

Figure . The bacterium *Escherichia coli* (Enterobacteriaceae family).
It is a Gram-negative, facultatively anaerobic, rod-shaped, coliform bacterium of the genus Escherichia that is commonly found in the lower intestine of warm-blooded organisms. Most *E. coli* strains are harmless, but some serotypes can cause serious food poisoning in their hosts.
Source: Google Library, PubMed – NCBI.

Dr S. Blair – University of Technology of Sydney and Prof R. Cooper – Cardiff Metropolitan University, made respectively some attempts to generate honey-resistant strains in the laboratory that have not been successful and there also have been no reports of clinical isolate with acquired resistance to mānuka honey.[x+y] Furthermore, *in vitro* studies combining therapeutically approved mānuka honey with antibiotic agents conducted by Prof R. Cooper in 2012 revealed a synergistic effect with oxacillin, tetracycline, imipenem, and mupirocin against the growth of an MRSA strain. [ ] The presence of a sub-inhibitory concentration of mānuka honey in combination with oxacillin restored the MRSA strain to oxacillin susceptibility due to the down-regulation of *mecR1* (a protein that encodes an MRSA-specific penicillin-binding protein known as PBP2A) as a result of a mechanism of honey synergy. [ ] Strong synergistic activity between mānuka honey and rifampicin against multiple *S. aureus* strains, including clinical isolates and MRSA strains, has been found by

P. Müller – University of Technology of Sydney in 2013 and the presence of mānuka honey prevented the emergence of rifampicin resistance *in vitro*. This study also revealed that in this case the MGO (methyl glyoxal – it was identified in 2008 as the responsible of the "non-peroxide activity" of mānuka honey. It results from the spontaneous dehydration of its precursor dihydroxyacetone, DHA, a naturally occurring phytochemical found in the nectar of flowers of *Leptospermum scoparium* and some related *Leptospermum* species native to New Zealand and Australia) was not responsible of the powerful synergy. [ ]

The Manuka grading: UMF and MGO are the most commonly used grading systems that convey the medicinal quality of the manuka honey. UMF grades start at 5+ and go as high as 25+ and MGO starts at 30+ and goes above 800+. Grades below UMF 10+ don't have significant levels of antibacterial activity. UMF 10+ is the minimum grade of manuka honey with meaningful levels of antibacterial activity and has been shown to be effective at inhibiting the growth of a variety of bacteria species. Hence, a UMF 10+ manuka honey is recommended for general first aid. The Lund University researchers (Sweden) demonstrated that bacteria from bees can be a possible alternative to antibiotics. They have identified 13 bacteria strains, particularly living lactic acid bacteria, found in fresh honey that have potent antimicrobial properties, these strains found in fresh honey produce a multitude of active antimicrobial compounds. The bacteria healed both severe human infections in the laboratory, and persistent wounds in horses for which other treatments had failed. The living lactic acid bacteria found in fresh raw honey is not found in processed store-bought honey. Manuka honey containing Unique Manuka Factor (UMF) can effectively treat resistant skin infections as well as large wounds that can't be repaired surgically. [ ]

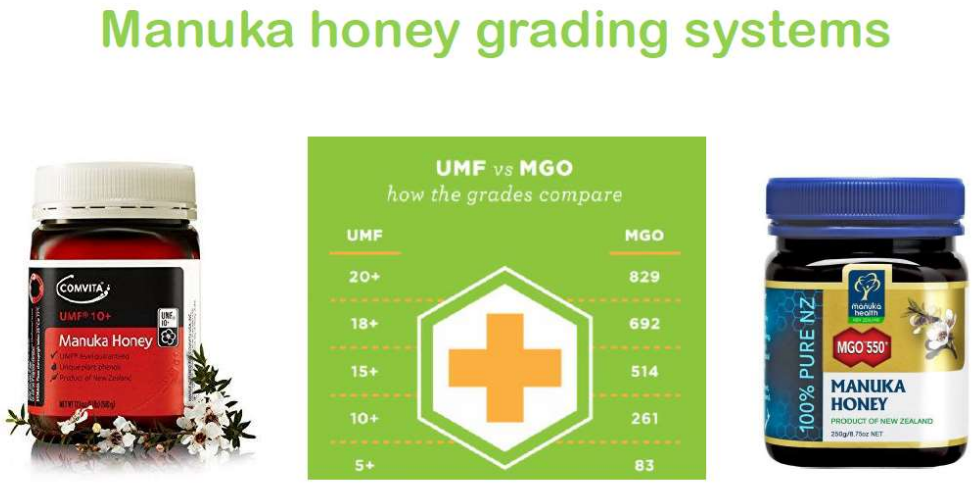

Figure . The Manuka honey grading system, courtesy of Comvita NZ Ltd. – Paengaroa NZ and Manuka Health NZ Ltd. – Te Awamutu NZ 2017.

Figure . The extraordinary healing properties of Manuka Honey, courtesy of Dr Becker – Chicago, USA.

The Manuka bush: Maori used *L. scoparium* for food, medicine, and timber. Pia manuka, the sugary gum found occasionally on young branches, was considered a delicacy and given to infants, or was used to alleviate coughs in adults (Crowe 1981). Brooker et al. (1987) listed a number of traditional medicinal uses. A decoction of leaves was taken, applied as a salve, directly chewed, or the vapours inhaled. The bark was used in a similar way to alleviate bronchial complaints. The tough wood was harvested for implement making, and a review of museum artefacts illustrated seven tools made from the plant's timber (Cooper & Cambie 1991). The first recorded European use was during James Cook's voyages, when *L. scoparium* leaves were initially used as a tea substitute, and later employed as an antiscorbutic in brewing beer (Cooper & Cambie 1991). Whalers continued to rely upon *L. scoparium* as a tea substitute (Brooker et al. 1987), giving rise to tea tree as a common name, and early settlers became so attached to the concoction that the importation of Chinese tea was considered unnecessary by one author (Crowe 1981). *L. scoparium* has continued to be valued for firewood and charcoal and, is often used for smoking fish.

Figure . The Manuka bush, *L. scoparium* in its own environment New Zealand. Courtesy of Manuka Health NZ Ltd. – Te Awamutu NZ 2017.

The hydrogen peroxide that is formed in honey by an enzyme the bees add, and sometimes also particular phytochemicals from the nectar or sap, give honey antibacterial activity that is sufficient to be effective in clearing infection from wounds. The phytochemicals also give honey its antioxidant activity which is also important in wound care, acting to decrease inflammation. With the widespread resistance to antibiotics developing in bacteria, it is now being 'rediscovered', and in many cases is proving to give better results than modern wound-care products. It has the advantage of providing moist healing conditions without the risk of bacterial growth, preventing adhesion of dressings to wound tissues, giving rapid removal of pus, dead tissue, and debris from wounds, decreasing inflammation and thus decreasing swelling, pain and exudation of serum and preventing scarring, and speeding up the growth of tissues to repair wounds. (Molan 2006).

Figure . The wound healing power of Manuka honey, courtesy of Lund University researchers (Sweden).

Dr med. Arne Simon from the Paediatric Haematology and Oncology, Children's Hospital Medical Centre, University of Bonn (Germany) reported the following case: five years ago, a 12-year old patient was submitted to our unit. Doctors at another hospital had removed an abdominal lymphoma, leaving an open drainage site on his abdomen. On admission, his wound was infected with methicillin-resistant Staphylococcus aureus (MRSA). In order to avoid nosocomial spread, the patient was immediately isolated, a difficult situation for the child to comprehend with significant additional costs from the perspective of the hospital. Although the patient was scheduled to receive

chemotherapy, treatment could not commence until the infection cleared. The wound was treated with a local antiseptic (octenidin) for 12 days. Since no improvement occurred, we decided to use an Australian medical honey (Medihoney™), which contains leptospermum honey, a type with excellent in vitro activity against MRSA. The wound was free of bacteria two days later, and the chemotherapy against the underlying illness could be started. (Arne Simon 2008).

Thoracotomy wound of a patient with acute myeloic leukemia after surgical site infection (Medihoney™ was applied on a calcium-alginate dressing and left in the wound for 24 h).

Arne Simon, Kirsten Traynor, Kai Santos, Gisela Blaser, Udo Bode and Peter Molan – Medical Honey for Wound Care—Still the 'Latest Resort'? , Medical Honey for Wound Care, eCAM ***2009;*** *6(2)165–173.*

Figure . The wound healing power of Manuka honey, courtesy of Department of Biological Sciences, University of Waikato, Hamilton, New Zealand.

As well as inhibiting planktonic bacterial cells, mānuka honey – as experimentally demonstrated, can also disperse, and kill bacteria living in biofilms (e.g. MRSA and *P. aeruginosa* in biofilm). Biofilms are communities of cells that are generally enclosed in a self-produced extracellular matrix and found adhering to surfaces, including wounds, teeth, mucosal surfaces, and implanted devices. Microbes resident in a biofilm are protected from antimicrobial agents, antibiotics, and can cause persistent and chronic infections. In 2012 it has been found that mānuka honey disrupts cellular aggregates and prevents the formation of biofilms of pathogen bacteria like *Pseudomonas aeruginosa*, *Staphylococcus aureus*, *Streptococcus mutans* and, shows also an antiviral effect against varicella-zoster virus (the cause of chicken pox and shingles) and influenza. [Maddocks 2012, Roberts 2012]

Foto usi del manuka ……

An important part of my research project has been focused on biofilms and their pathogenicity. The first one I studied, with the kind help of Prof. E. Sapi – University of New Haven USA, has been the *Pseudomonas aeruginosa* biofilm.

3.2.3. CONCLUSION

In ancient history the Egyptians, Assyrians, Chinese, Greeks and Romans all used honey, in combination with herbs and on its own, to treat wounds (Zumla and Lulat, 1989). Aristotle (350 BC) wrote of honey being a salve for wounds (Aristotle, 1910), and Dioscorides (c.50 AD) wrote of honey being "good for all rotten and hollow ulcers" (Gunther, 1934). The usage of honey for wound care has continued throughout all ages, it being displaced from common use in the medical profession when antibiotics came into use in the 1940s. In recent times honey has been `rediscovered' by the medical profession (Zumla and Lulat, 1989), possibly because the 'antibiotic era' is coming to an end as increasing numbers of bacterial strains develop resistance to antibiotics.

KIWI

References

1. Li X., Liu D. C. *Ultrasound speckle reduction based on image segmentation and diffused region growing;* in Proceedings of the 11th Joint Conference on Information Sciences **2008**.

2. Anquez J., Angelini E.D., Grandé G., et al. *Automatic segmentation of antenatal 3-d ultrasound images,* IEEE Trans Biomed Eng., **2013,** *60*, 5, 1388e400.
3. Bonacina L., Froio A., Conti D., Marcolin F., Vezzetti E. *Automatic 3D foetal face model extraction from ultrasonography through histogram processing*, Journal of Medical Ultrasound, **2016,** http://dx.doi.org/10.1016/j.jmu.2016.08.003.
4. Padula F., Vezzetti E., Marcolin D., Conti D., Bonacina L., Froio A., Giorlandino M., Coco C., D'Emidio L., Giorlandino C., Speranza D. *Antenatal automatic diagnosis of cleft lip via unsupervised clustering method relying on 3D facial soft tissue landmarks*, Ultrasound in Obstetrics & Gynecology, **2016,** 48 (Suppl. 1).
5. Savran A., Alyüz N., Dibeklioğlu H., Çeliktutan O., Gökberk B., Sankur B., Akarun L. *Bosphorus Database for 3D Face Analysis*, The First COST 2101 Workshop on Biometrics and Identity Management (BIOID **2008**).
6. EUROCAT Special Report: *Congenital anomalies are a major group of mainly rare diseases*, EUROCAT Central Registry – University of Ulster (EUROCAT **2012**).
7. Todros T., Capuzzo E., Gaglioti P., *Prenatal diagnosis of congenital anomalies,* Images in Paediatric cardiology, **2001,** *3* (2), 3-18.
8. Beth A. Bailey, Ph.D., and Robert J. Sokol, M.D. *Prenatal alcohol exposure and miscarriage, stillbirth, preterm delivery, and sudden infant death syndrome,* Alcohol research and health, **2011,** *34* (1), 86-91.
9. Bertrand J., Floyd RL., Weber MK., O'Connor M., Riley EP., Johnson KA., Cohen DE. *Fetal Alcohol syndrome: guidelines for referral and diagnosis,* Atlanta, GA: Center for disease control and prevention – National Task Force on FAS/FAE **2004**.
10. Zhang X., Sliwowska J.H., Weinberg J. *Prenatal alcohol exposure and fetal programming: Effects on neuroendocrine function and immune function*, Experimental Biology & Medicine, **2005,** *230* (6), 376-388.
11. American Academy of Pediatrics. Committee on Substance Abuse and Committee on Children with Disabilities, *Fetal alcohol syndrome and alcohol-related neurodevelopmental disorders.* Pediatrics, **2000,** *106*, 358-361.
12. American College of Obstetricians & Gynecologists (ACOG: Washington DC) *Substance use: Obstetric and gynecologic implications,* ACOG Special Issues in Women's Health, **2005,** 105-150.
13. Alcohol Research & Health: Highlights from the 10th Special Report to Congress. *Chapter on Prenatal exposure to alcohol*. Alcohol Research & Health, **2000,** *24* (1), 32-41.

14. Bonacina L., Froio A., Conti D., Marcolin F., Vezzetti E. *Automatic 3D foetal face model extraction from ultrasonography through histogram processing,* Journal of Medical Ultrasound, **2016,** *24*, 142-149.
15. Bonacina L., Conti D., Froio A., Vezzetti E., Marcolin F., *Process for processing medical images of a face for recognition of facial dysmorphisms,* WO 2017089953 A1 - Patent **2015** and PCT extension application **2017**.
16. International Conference *"Global Summit on Pharmaceutical Sciences and Clinical Trials"* – Copenhagen, Denmark, 30th Jan – 1st Feb **2017** (Keynote Speaker: Miss Alessandra Piccitto MRPharmS. Presentation title: "SynDiag: the new concept of prenatal diagnosis").
17. International Conference *"World Congress and Expo on Biotechnology and Bioengineering"* – Dubai, UAE, 27th – 29th March **2017** (Moderator and Speaker: Miss Alessandra Piccitto MRPharmS. Presentation title: "SynDiag: the new concept of prenatal diagnosis").
18. International Video Conference *"International Summit on Pharma and Clinical trials"* (Innovate Pharma 2017) – Sydney, AUS, 12th – 13th June **2017** (Speaker: Miss Alessandra Piccitto MRPharmS. Presentation title: "SynDiag: the new concept of prenatal diagnosis").
19. International Conference *"Radiobiological basis of radiation therapy"* – Obninsk, Russian Federation, 20th – 21st June **2017** (Special Guest and Speaker: Miss Alessandra Piccitto MRPharmS. Presentation title: "SynDiag: the new concept of prenatal diagnosis").
20. International Video Conference *"2nd Global Summit on Pharmaceutics and Drug Delivery Systems: Impact of Pharmaceutical Sciences, now and future"* – Singapore, 29th – 30th June **2017** (Speaker: Miss Alessandra Piccitto MRPharmS. Presentation title: "SynDiag: the new concept of prenatal diagnosis").
21. International Conference *"International Conference on Pharmacology and Toxicology studies"* – Philadelphia, USA, 7th – 9th August **2017** (Session Co-Chair and Speaker: Miss Alessandra Piccitto MRPharmS. Presentation title: "SynDiag: the new concept of prenatal diagnosis and therapy").
22. International Video Conference *"Maternal and Foetal Health in Pregnancy"* – London, UK, 18th – 19th September **2017** (Speaker: Miss Alessandra Piccitto MRPharmS. Presentation title: "SynDiag: a new patent developed to improve diagnosis in pregnancy").

23. International Conference *"International Colloquium on Medical, Pharma and Drug Studies"* (Innovate Medicine 2017) – Brisbane, AUS, 29th – 30th November **2017** (Moderator and Speaker: Miss Alessandra Piccitto MRPharmS. Presentation title: "SynDiag: a new patent developed to improve diagnosis in pregnancy").
24. International Conference *"3rd World Congress on Pharmaceutics and Drug Discovery"* – Dubai, UAE, 15th – 16th December **2017** (Session Chair and Speaker: Miss Alessandra Piccitto MRPharmS. Presentation title: "SynDiag: the new concept of prenatal diagnosis and therapy").
25. Levin WP., Kooy H., Loeffler JS., DeLaney TF. *Proton beam therapy,* British Journal of Cancer, **2005,** *93*, 849-854.
26. Liu Q., Ghosh P., Magpayo N., Testa M., Tang S., Gheorghiu L., Biggs P., Paganetti H., Efstathiou JA., Lu HM., Held KD., Willers H. *Lung Cancer Cell Line Screen Links Fanconi Anemia/BRCA Pathway Defects to Increased Relative Biological Effectiveness of Proton Radiation,* International Journal of Radiation Oncology biology physics, **2015,** *91* (5), 1081-1089.
27. Metz J. *Differences Between Protons and X-rays,* The Abramson Cancer Center of the University of Pennsylvania, **2006,** www.oncolink.org**.**
28. Camphausen KA., Lawrence RC. Principles of radiation therapy, in: Pazdur R., Wagman LD., Camphausen KA., Hoskins WJ., Cancer management: a multidisciplinary approach, 11th ed. **2008.**
29. Smith AR. *Vision 20/20: Proton therapy,* Medical Physics, **2009,** *36* (2), 556-568.
30. Degiovanni A., Amaldi U. *History of hadron therapy accelerators,* Physica Medica: European Journal of Medical Physics, **2015,** *31* (4), 322-332.
31. Peach K., Wilson P., Jones B. *Accelerator science in medical physics,* The British Journal of Radiology, **2011,** *84* (spec. n.1), S4-S10.
32. Lui H., Chang JY. *Proton therapy in clinical practice,* Chinese Journal of Cancer, **2011,** *30* (5), 315-326.
33. Richard Wilson, *A Brief History of the Harvard University Cyclotrons*, Harvard University Press, **2004.**
34. Arney K. *Proton therapy is coming to the UK, but what does it mean for patients?* - Cancer Research UK - Science blog, 16-09-**2013** (www.scienceblogcancerresearchuk.org)
35. http://mrrc.nmicr.ru/about/about/ МРНЦ им. А.Ф. Цыба (A. Tsyb MRRC) – филиал ФГБУ «НМИЦ. радиологии» Минздрава России, accessed: June **2017.**

36. Development of Proton Therapy: *Successful cooperating physicists and doctors*. Zao "Protom", Protvino (Moscow Region – Russia) – A. Tsyb MRRC, Obninsk (Russia), **2017** (translated document, original written in Cyrillic alphabet).
37. Innovative Russian development: *The medical proton complex "Prometheus"* – A. Tsyb MRRC, Obninsk (Russia), **2017** (translated document, original written in Cyrillic alphabet).
38. Ion Therapy: *development of the technology of radiotherapy with carbon-12 ions* – A. Tsyb MRRC, Obninsk (Russia), **2017** (translated document, original written in Cyrillic alphabet).
39. Neutron therapy: *The possibilities and prospects for the treatment of cancer patients using the VVR-ts reactor and small-size generators* – A. Tsyb MRRC, Obninsk (Russia), **2017** (translated document, original written in Cyrillic alphabet).
40. MIND project: *Models for the INvestigation of age-related Diseases,* Ministero dell'Istruzione, dell'Università e della Ricerca, **2010,** (www.miur.gov.it).
41. Gaballa MA., Sunkomat JN., Thai H., Morkin E., Ewy G., Goldman S. *Grafting an acellular 3-dimensional collagen scaffold onto a non-transmural infarcted myocardium induces neo-angiogenesis and reduces cardiac remodeling,* The Journal of Heart Lung Transplant, **2006,** *25*, 946-954.
42. Piccitto A. *Advantages of using Magnetic Resonance in Cardiology*, International Journal of Biotechnology and Bioengineering, **2018,** *4* (2), 17-22.
43. Webb AR., Yang J., Ameer GA. *Biodegradable polyester elastomers in tissue engineering,* Expert Opinion on Biological Therapy, **2004,** *4*, 801-812.
44. Ferry JD., *Viscoelastic properties of polymers,* 3rd edition New York, NY: Wiley, **1980.**
45. Christenson EM., Anderson JM., Hiltner A., Baer E. *Relationship between nanoscale deformation processes and elastic behavior of polyurethane elastomers,* Polymer, **2005,** *46*, 11744-11754.
46. Sakar D., Yang JC., Gupta AS., Lopina ST. *Synthesis and characterization of L-tyrosine based polyurethanes for biomedical applications,* Journal of Biomedical Materials Research A, **2009,** *90*, 263-271.
47. Sakar D., Yang JC., Lopina ST. *Structure-property relationship of L-tyrosine-based polyurethanes for biomedical applications,* Journal of Applied Polymer Science, **2008,** *108*, 2345-2355.

48. Ko IK., Lee SJ., Atala A., Yoo JJ. *In situ tissue regeneration through host stem cell recruitment,* Experimental and Molecular Medicine, **2013,** *45*, e57.
49. Shi J., Dong N., Sun Z. *Immobilization of decellularized valve scaffolds with Arg-Gly-Asp-containing peptide to promote myofibroblast adhesion,* Journal of Huazhong University of Science and Technology – Medical Sciences, **2009,** *29* (vol.4), 503-507.
50. Oxford University Conferences Cycle *"Back from the dead"* – Oxford, UK, 9th March – 9th May **2017** (Speaker: Prof E. Garman – Department of Biochemistry, University of Oxford).
51. Rudiño-Piñera E., Ravelli RB., Sheldrick GM., Nanao MH., Korostelev VV., Werner JM., Schwarz-Linek U., Potts JR., Garman EF. *The solution and crystal structures of a module pair from the Staphylococcus aureus-binding site of human fibronectin--a tale with a twist,* Journal of Molecular Biology, **2007,** *368*, 833-844.
52. Levine ME., Suarez JA., Brandhorst S., Balasubramanian P., Cheng CW., Madia F., Fontana L., Mirisola MG., Guevara-Aguirre J., Wan J., Passarino G., Kennedy BK., Wei M., Cohen P., Crimmins EM., Longo VD. *Low Protein Intake Is Associated with a Major Reduction in IGF-1, Cancer, and Overall Mortality in the 65 and Younger but Not Older Population*, Cell Metabolism, **2014,** *19* (3), 407-417.
53. Cheng CW., Adams GB., Perin L., Wei M., Zhou X., Lam BS., Da Sacco S., Mirisola M., Quinn DI., Dorff TB., Kopchick JJ., Longo VD. *Prolonged Fasting reduces IGF-1/PKA to promote hematopoietic-stem-cell-based regeneration and reverse immunosuppression,* Cell Stem Cell, **2014,** *14* (6), 810-823.
54. Lee C., Longo VD. *Fasting vs dietary restriction in cellular protection and cancer treatment: from model organisms to patients*, Oncogene, **2011,** *30*, 3305-3316.
55. Lee C., Raffaghello L., Brandhorst S., Safdie FM., Bianchi G., Martin-Montalvo A., Pistoia V., Wei M., Hwang S., Merlino A., Emionite L., De Cabo R., Longo VD. *Fasting Cycles Retard Growth of Tumors and Sensitize a Range of Cancer Cell Types to Chemotherapy*, Science Translational Medicine, **2012,** *4* (124), 124ra27.
56. Safdie FM., Dorff T., Quinn D., Fontana L., Wei M., Lee C., Cohen P., Longo VD. *Fasting and Cancer Treatment in Humans: A Case series report*, Aging (Albany NY) **2009,** *1* (12), 988-1007.
57. International Conference *"Frontiers in Life and Materials Sciences: Creating life in 3D"* – Brno, Czech Republic, 2nd – 4th September **2015** (Speaker and Award Winner: Miss Alessandra Piccitto MRPharmS. Presentation title: "Materials and Technologies for an in vitro model of the Cardiac tissue").

58. Noimark S., Allan E., Parkin IP. *Light-activated antimicrobial surfaces with enhanced efficacy induced by a dark-activated mechanism*, Chemical Science, **2014,** *5*, 2216-2223.
59. Hwang GB., Noimark S., Page K., Sehmi S., Macrobert AJ., Allan E., Parkin IP. *White light-activated antimicrobial surfaces: effect of nanoparticles type on activity*, Journal of Materials Chemistry B, **2016,** *4*, 2199-2207.
60. Ismail S., Perni S., Pratten J., Parkin I., Wilson M. *Efficacy of a novel light-activated antimicrobial coating for disinfecting hospital surfaces*, Infection control and hospital epidemiology, **2011,** *32* (11), 1130-1132.
61. Office for national statistics, Health Statistics Quarterly **2008,** *39*, 56-66.
62. Office for national statistics, Health Statistics Quarterly **2008,** *39*, 67-76.
63. House of commons, *Reducing healthcare associated infection in hospitals in England*, http://www.publications.parliament.uk/pa/cm200809/cmselect/cmpubacc/812/812.pdf, Fifty-second Report of Session 2008-2009, printed **2009,** accessed: January 2017.
64. Plowman R., *The socioeconomic burden of hospital acquired infections*, Euro Surveillance: bulletin Européen sur les maladies transmissibles = European communicable disease bulletin, **2000,** *5* (4), 49-50.
65. National audit office, *The management and control of hospital acquired infection in acute NHS trusts in England*, http://www.nao.org.uk/wp-content/uploads/2000/02/9900230.pdf, published **2000,** accessed: January 2017.
66. National audit office, *Improving patient care by reducing the risk of hospital acquired infection: a progress report*, Report by the comptroller and auditor general HC 876 Session 2003-2004, http://www.nao.org.uk/wp-content/uploads/2004/07/0304876.pdf, published **2004,** accessed: January 2017.
67. WHO Geneva, 27 February 2017, *WHO publishes list of bacteria for which new antibiotics are urgently needed*, www.who.int/mediacentre/news/releases/2017/bacteria-antibiotics-needed/en/, published **2017,** accessed: February 2017.
68. DeLeon S., Clinton A., Fowler H., Everett J., Horswill AR., Rumbaugh KP. *Synergistic interactions of Pseudomonas aeruginosa and Staphylococcus aureus in an in vitro wound model*, Infection and Immunity, **2014,** *82* (11), 4718-4728.
69. Filkins LM., Graber JA., Olson DG., Dolben EL., Lynd LR., Bhuju S., O'Toole GA. *Coculture of Staphylococcus aureus with Pseudomonas aeruginosa drives S. aureus*

towards fermentative metabolism and reduced viability in a cystic fibrosis model, Journal of Bacteriology, **2015,** *197* (14), 2252-2264.

70. Trizna E., Ryzhikova M., Mukhametzyanova S., Kurbangalieva A., Khabibrakhmanova A., Rozhina E., Fakhrullin R., Kayumov A. *Staphylococcus aureus survives in Pseudomonas aeruginosa biofilm under antimicrobial treatment conditions*, IC2AR Proceedings Book, **2017,** 262.
71. Ayliffe G. AJ., Collins BJ., Lowbury E. JL, Babb JR., Lilly HA. *Ward floors and other surfaces as reservoirs of hospital*, Epidemiology and Infection, **1967,** *65* (4), 515-536; published on-line 2009 (doi:10.1017/S0022172400046052).
72. Page K., Wilson M., Parkin IP. *Antimicrobial surfaces and their potential in reducing the role of the inanimate environment in the incidence of hospital-acquired infections*, Journal of Materials Chemistry, **2009,** *19*, 3819-3831.
73. Boyce JM. *Environmental contamination makes an important contribution to hospital infection*, The Journal of hospital infection, **2007,** *65* (2), 50-54.
74. Singh D., Kaur H., Gardner WG., Treen LB. *Bacterial contamination of hospital pagers*, Infection control and hospital epidemiology, **2002,** *23* (5), 274-276.
75. Hall LB., Hartnett MJ. *Measurement of the bacterial contamination on surfaces in hospitals*, Public Health Reports, **1964,** *79* (11), 1021-1024.
76. Page K., Wilson M., Mordan NJ., Chrzanowski W., Knowles J., Parkin IP. *Study of the adhesion of Staphylococcus aureus to coated glass substrates*, Journal of Materials Science, **2011,** *46* (19), 6355-6363.
77. Ratkowsky DA., Olley J., McMeekin TA., Ball A. *Relationship between temperature and growth rate of bacterial cultures*, Journal of Bacteriology, **1982,** *149* (1), 1-5.
78. Wang EW., Agostini G., Olomu O., Runco D., Jung JY., Chole RA. *Gentian violet and ferric ammonium citrate disrupt Pseudomonas aeruginosa biofilms*, The Laryngoscope, **2008,** *118* (11), 2050-2056.
79. Berrios RL., Arbiser JL. *Effectiveness of gentian violet and similar products commonly used to treat pyodermas*, Dermatologic Clinics, **2011,** *29* (1), 69-73.
80. Saji M. *Effect of gentiana violet against methicillin-resistant Staphylococcus aureus (MRSA)*, Kansenshogaku Zasshi = The journal of the Japanese Association for infectious diseases, **1992,** *66* (7), 914-922 [article in Japanese].
81. Okano M., Noguchi S., Tabata K., Matsumoto Y. *Topical gentian violet for cutaneous infection and nasal carriage with MRSA*, International Journal of Dermatology, **2000,** *39* (12), 942-944.

82. Maley AM., Arbiser JL. *Gentian violet: a 19th century drug re-emerges in the 21st century*, Experimental Dermatology, **2013,** *22* (12), 775-780.
83. Bakker P., Van Doorne H., Gooskens V., Wieringa NF. *Activity of gentian violet and brilliant green against some microorganisms associated with skin infections*, International Journal of Dermatology, **1992,** *31*, 210-213.
84. Fung DYC., Miller RD. *Effect of dyes on bacterial growth*, Applied Microbiology, **1973,** *25*, 793-799.
85. Piccitto A. *New strategies to develop antibiotics for treatment of Pseudomonas aeruginosa and Leishmania spp infections*, Lambert Academics Publishing, **2013.**
86. Jackson R. *Doctors and diseases in the Roman Empire*, British Museum Press, **1988.**
87. Alexander JW. *History of the medical use of silver*, Surgical infections (Larchmt), **2009,** *10* (3), 289-292.
88. Shukla PB., Mishra MK. *Antimicrobial Activity of Supported Silver and Copper against E. coli in Water*, Suresh Gyan Vihar University International Journal of Environment, Science and Technology, **2015,** *1* (1), 11-15.
89. Dunnill CW., Page K., Aiken A., Noimark S., Hyett G., Kafizas A., Pratten J., Wilson M., Parkin IP. *Nanoparticulate silver coated-titania thin films—Photo-oxidative destruction of stearic acid under different light sources and antimicrobial effects under hospital lighting conditions*, Journal of Photochemistry and Photobiology A: Chemistry, **2011,** *220* (2-3), 113-123.
90. Ozkan E., Allan E., Parkin IP. *The antibacterial properties of light-activated polydimethylsiloxane containing crystal violet*, RSC Advances, **2014,** *4*, 51711-51715.
91. Noimark S., Bovis M., MacRobert AJ., Correira A., Allan E., Wilson M., Parkin IP. *Photobactericidal polymers; the incorporation of crystal violet and nanogold into medical grade silicone*, RSC Advances, **2013,** *3* (40), 18383-18394.
92. Page K., Correira A., Wilson M., Allan E., Parkin IP. *Light-activated antibacterial screen protectors for mobile telephones and tablet computers*, Journal of Photochemistry and Photobiology A: Chemistry, **2015,** *296*, 19-24.
93. Vigneshwaran N., Kathe AA., Varadarajan PV., Nachane RP., Balasubramanya RH. *Functional finishing of cotton fabrics using silver nanoparticles*, Journal of Nanoscience and Nanotechnology, **2007,** *7* (6), 1893-1897.
94. Tolaymat TM., El-Badawy AM., Genaidy A., Scheckel KG., Luxton TP., Suidan M. *An evidence-based environmental perspective of manufactured silver nanoparticle in syntheses and applications: a systematic review and critical appraisal of peer-*

reviewed scientific papers, The Science of the total environment, **2010,** *408* (5), 999-1006.

95. Moghimi SM., Hunter AC., Murray JC. *Long-circulating and target-specific nanoparticles: theory to practice*, Pharmacological Reviews, **2001,** *53* (2), 283-318.
96. Panyam J., Labhasetwar V. *Biodegradable nanoparticles for drug and gene delivery to cells and tissue*, Advanced drug delivery reviews, **2003,** *55* (3), 329-347.
97. Ahamed M., Alsalhi MS., Siddiqui MK. *Silver nanoparticle applications and human health*, Clinica Chimica Acta; international journal of clinical chemistry, **2010,** *411* (23-24), 1841-1848.
98. Ji JH., Jung JH., Kim SS., Yoon JU., Park JD., Choi BS., Chung YH., Kwon IH., Jeong J., Han BS., Shin JH., Sung JH., Song KS., Yu IJ. *Twenty-Eight-Day Inhalation Toxicity Study of Silver Nanoparticles in Sprague-Dawley Rats*, Inhalation Toxicology, **2007,** *19* (10), 857-871.
99. Hyun JS., Lee BS., Ryu HY., Sung JH., Chung KH., Yu IJ. *Effects of repeated silver nanoparticles exposure on the histological structure and mucins of nasal respiratory mucosa in rats*, Toxicology letters, **2008,** *182* (1-3), 24-28.
100. Lee HY., Choi YJ., Jung EJ., Yin HQ., Kwon JT., Kim JE. *Genomics-based screening of differentially expressed genes in the brains of mice exposed to silver nanoparticles via inhalation*, Journal of Nanoparticles Research, **2010,** *12* (5), 1567-1578.
101. Kim YS., Kim JS., Cho HS., Rha DS., Kim JM., Park JD., Choi BS., Lim R., Chang HK., Chung YH., Kwon IH., Jeong J., Han BS., Yu IJ. *Twenty-eight-day oral toxicity genotoxicity, and gender-related tissue distribution of silver nanoparticles in Sprague-Dawley rats*, Inhalation Toxicology, **2008,** *20* (6), 575-583.
102. Deshpande A., Cadnum JL., Fertelli D., Sitzlar B., Thota P., Mana TS., Jencson A., Alhmidi H., Koganti S., Donskey CJ. *Are hospital floors an underappreciated reservoir for transmission of health care-associated pathogens?* American Journal of Infection Control, **2017,** *45* (3), 336-338.
103. Exhibition "*The Royal Society SUMMER SCIENCE EXHIBITION 2017*" – London, UK, 4th – 9th July **2017** (Exhibitor: Miss Alessandra Piccitto MRPharmS and Chemistry Dept. UCL colleagues involved in the Smart Surfaces project).
104. International Conference *"World Congress and Expo on Biotechnology and Bioengineering"* – Dubai, UAE, 27th – 29th March **2017** (Moderator and Speaker: Miss

Alessandra Piccitto MRPharmS. Presentation title: "Silver nanoparticles to improve control of nosocomial infections").

105. International Video Conference *"International Summit on Pharma and Clinical trials"* (Innovate Pharma 2017) – Sydney, AUS, 12th – 13th June **2017** (Speaker: Miss Alessandra Piccitto MRPharmS. Presentation title: "A novel bactericidal surface to reduce nosocomial infections").
106. International Conference *"2nd International Caparica Conference in Antibiotic Resistance – IC²AR 2017"* – Lisbon, Portugal, 12th – 15th June **2017** (Speaker: Miss Alessandra Piccitto MRPharmS. Presentation title: "A novel antibacterial material developed to stop hospital infection spreading").
107. Royal Society of Chemistry Conference *"Dalton Division Southern Regional Meeting 2017"* – London, UK, 28th June **2017** (Speaker and Award Winner: Miss Alessandra Piccitto MRPharmS. Presentation title: "A novel bactericidal surface to reduce nosocomial infections improving an Italian Patent").
108. International Video Conference *"2nd Global Summit on Pharmaceutics and Drug Delivery Sistems: Impact of Pharmaceutical Sciences, now and future"* – Singapore, 29th – 30th June **2017** (Speaker: Miss Alessandra Piccitto MRPharmS. Presentation title: "A novel bactericidal surface developed to stop hospital infections spreading").
109. International Conference *"The 2nd International Conference on Sustainable Materials Science and Technology – SMST2"* – Las Palmas GC, Spain, 19th – 21st July **2017** (Speaker of excellence: Miss Alessandra Piccitto MRPharmS. Presentation title: "A novel bactericidal material developed to reduce hospital-acquired infections").
110. International Conference *"International Conference on Pharmacology and Toxicology studies"* – Philadelphia, USA, 7th – 9th August **2017** (Session Co-Chair and Speaker: Miss Alessandra Piccitto MRPharmS. Presentation title: "A novel bactericidal surface to reduce nosocomial infections improving an Italian Patent").
111. Microbiology Society Conference *"Staphylococcus GBI 2017"* – Swansea (Wales), UK, 14th – 15th September **2017** (Speaker: Miss Alessandra Piccitto MRPharmS. Presentation title: "A novel bactericidal surface developed to reduce *Staphylococcus aureus* nosocomial infections").
112. International Conference *"International Colloquium on Medical, Pharma and Drug Studies"* (Innovate Medicine 2017) – Brisbane, AUS, 29th – 30th November **2017** (Moderator and Speaker: Miss Alessandra Piccitto MRPharmS. Presentation title: "A novel bactericidal surface to reduce Superbugs nosocomial infections").

113. International Conference *"3rd World Congress on Pharmaceutics and Drug Discovery"* – Dubai, UAE, 15th – 16th December **2017** (Session Chair and Speaker: Miss Alessandra Piccitto MRPharmS. Presentation title: "A novel bactericidal surface to reduce Superbugs nosocomial infections").

114. Antibiotics: *"WHO names 12 bacteria that pose the greatest threat to human health"*, The Guardian, 27th February **2017** www.theguardian.com, accessed: February 2017.

115. The Uncounted: *"One life, two donated organs and $5.7 million in bills – a tale of superbugs' deadly costs"*, Reuters Investigation, 18th November **2016** www.reuters.com, accessed: November 2016.

116. Conceição T., Diamantino F., Coelho C., de Lencastre H., Aires-de-Sousa M. *Contamination of Public Buses with MRSA in Lisbon, Portugal: A Possible Transmission Route of Major MRSA Clones within the Community*, PLoS One, **2013,** *8* (11), e77812.

117. Das S., Anderson CJ., Grayes A., Mendoza K., Harazin M., Schora DM., Peterson LR. *Nasal Carriage of Epidemic Methicillin-Resistant Staphylococcus aureus 15 (EMRSA-15) Clone Observed in Three Chicago-Area Long-Term Care Facilities*, Antimicrobial Agents and Chemotherapy, **2013,** *57* (9), 4551-4553.

118. Aires-de-Sousa M., Correia B., de Lencastre H. *Changing patterns in frequency of recovery of five methicillin-resistant Staphylococcus aureus clones in Portuguese hospitals: surveillance over a 16-year period*, Journal of Clinical Microbiology, **2008,** *46*, 2912-2917.

119. Albrecht N., Jatzwauk L., Slickers P., Ehricht R., Monecke S. *Clonal replacement of epidemic methicillin-resistant Staphylococcus aureus strains in a German university hospital over a period of eleven years*, PLoS One, **2011,** *6* (11), e28189.

120. Hsu LY., Loomba-Chlebicka N., Koh YL., Tan TY., Krishnan P., Lin RT., Tee NW., Fisher DA., Koh TH. *Evolving EMRSA-15 epidemic in Singapore hospitals*, Journal of Medical Microbiology, **2007,** *56*, 376-379.

121. Bjarnsholt T., Kirketerp-Møller K., Kristiansen S., Phipps R., Nielsen AK., Jensen PØ., Høiby N., Givskov M. *Silver against Pseudomonas aeruginosa biofilms*, APMIS: acta phatologica, microbiologica, et immunologica Scandinava, **2007,** *115* (8), 921-928.

122. Cunningham AB., Lennox JE., Ross RJ. *Biofilms: the Hypertextbook*, Montana State University U.S.A. Eds. 2001-**2010,** www.cs.montana.edu/webworks/projects, accessed: November 2016.

123. Farwell J.A. *Sensitivity of Pseudomonas aeruginosa to silver*, The Bath University of Technology – Royal Pharmaceutical Society Library, **1970.**

124. Wakshlak RB., Pedahzur R., Avnir D. *Antibacterial activity of silver-killed bacteria: the "zombies" effect*, Nature – Scientific Reports, **2015,** *5*, 9555.

125. MacDougall C., Harpe SE., Powell JP., Johnson CK., Edmond MB., Polk RE. *Pseudomonas aeruginosa, Staphylococcus aureus, and fluoroquinolone use*, Emerging Infectious Diseases, **2005,** *11* (8), 1197-1210.

126. Lambadi PR., Sharma TK., Kumar P., Vasnani P., Thalluri SM., Bisht N., Pathania R., Navani NK. *Facile biofunctionalization of silver nanoparticles for enhanced antibacterial properties, endotoxin removal, and biofilm control*, International Journal of Nanomedicine (Dove Medical Press, NZ, Ltd), **2015,** *10*, 2155-2171.

127. Liu LH., Xu KJ., Wang HY., Tan PK., Fan W., Venkatraman SS., Li L., Yang YY. *Self-assembled cationic peptide nano-particles as an efficient antimicrobial agent*, Nature Nanotechnology, **2009,** *4* (7), 457–463.

128. Hancock RE., Sahl HG. *Antimicrobial and host-defense peptides as new anti-infective therapeutic strategies*, Nature Biotechnology, **2006,** *24* (12), 1551-1557.

129. Petty JT., Zheng J., Hud NV., Dickson RM. *DNA-templated Ag nanocluster formation*, Journal of the American Chemical Society, **2004,** *126* (16), 5207-5212.

130. Soonhyang P., Hicham C., Jody W., Nadeau JL., *Antimicrobial activity and cellular toxicity of nanoparticle-polymyxin B conjugates*, Nanotechnology, **2011,** *22* (18), 185101.

131. Daugelavicius R., Bakiene E., Bamford DH. *Stages of polymyxin B interaction with the Escherichia coli cell envelope*, Antimicrobial Agents and Chemotherapy, **2000,** *44* (11), 2969–2978.

132. Bondarenko O., Ivask A., Kakinen A., Kurvet I., Kahru A. *Particle-cell contact enhances antibacterial activity of silver nanoparticles*, PLoS One, **2013,** *8* (5), e64060.

133. Héquet A., Humblot V., Berjeaud JM., Pradier CM. *Optimized grafting of antimicrobial peptides on stainless steel surface and biofilm resistance tests*, Colloids and Surfaces. B, Biointerfaces, **2011,** *84* (2), 301–309.

134. Vincent JL., Laterre PF., Cohen J., Burchardi H., Bruining H., Lerma FA., Wittebole X., De Backer D., Brett S., Marzo D., Nakamura H., John S. *A pilot-controlled study of*

a polymyxin B-immobilized hemoperfusion cartridge in patients with severe sepsis secondary to intra-abdominal infection, Shock (Augusta, Ga.), **2005,** *23* (5), 400–405.

135. Valkov A., Nakonechny F., Nisnevitch M. *Polymer-Immobilized Photosensitizers for continuous eradication of bacteria*, International Journal of Molecular Sciences, **2014,** *15*, 14984-14996.

136. Nakonechny F., Nisnevitch M., Nitzan Y., Firer MA. *New techniques in antimicrobial photodynamic therapy: scope of application and overcoming drug resistance in nosocomial infections*, Science against microbial pathogens: communicating current research and technological advances, A. Méndez-Vilas (Ed.).

137. Nisnevitch M., Lugovskoy S., Pinkus A., Nakonechny F., Nitzan Y. *Antibacterial activity of photosensitizers immobilized onto solid supports via mechanochemical treatment*, Photochemical and Photobiological Sciences, **2014,** *9*, 1-23.

138. Nakonechny F., Nisnevitch M., Nitzan Y., Nisnevitch M. *Sonodynamic excitation of Rose Bengal for eradication of Gram-positive and Gram-negative bacteria*, BioMed Research International, **2013,** *2013*, 684930.

139. Welch K., Cia Y., Strømme M. *A method for quantitative determination of biofilm viability, Journal of Functional Biomaterials*, **2012,** *3*, 418-431.

140. Wei GX., Campagna AN., Bobek LA. *Effect of MUC7 peptides on the growth of bacteria and on Streptococcus mutans biofilm*, Journal of Antimicrobial Chemotherapy (Oxford University Press), **2006,** *57*, 1100-1109.

141. Magill SS., Edwards JR., Bamberg W., Beldavs ZG., Dumyati G., Kainer MA., Lynfield R., Maloney M., McAllister-Hollod L., Nadle J., Ray SM., Thompson DL., Wilson LE., Fridkin SK. *Multistate point-prevalence survey of health care-associated infections*, The New England Journal of Medicine, **2014,** *370*, 1198-1208.

142. Ruden S., Hilpert K., Berditsch M., Wadhwani P., Ulrich AS. *Synergistic interaction between silver nanoparticles and membrane permeabilizing antimicrobial peptides*, Antimicrobial Agents and Chemotherapy, **2009,** *53*, 3538-3540.

143. Ahmad N., Bhatnagar S., Ali SS., Dutta R. *Phytofabrication of bioinduced silver nanoparticles for biomedical applications*, International Journal of Nanomedicine (Dove Medical Press, NZ, Ltd), **2015,** *10* (1), 7019-7030.

144. The British Pharmacopoeia **2018** Edition, published by the Medicines and Healthcare products Regulatory Agency (MHRA) of the United Kingdom.

145. The European Pharmacopoeia (Ph. Eur.) 9th Edition, 2016, published by the European Directorate for the Quality of Medicines & HealthCare (EDQM) of the EU.

146. Stephens J. *The factors responsible for the varying levels of UMF® in mānuka (Leptospermum scoparium) honey*, University of Waikato Publishing, **2006.**

147. Molan PC. *Why honey is effective as a medicine. 1. Its use in modern medicine*, Bee World, **1999a,** *80* (2), 80-92.

148. Molan PC. *Why honey is effective as a medicine. 2. The scientific explanation of its effects*, Bee World, **1999b,** *82* (1), 22-40.

149. Molan PC. *Why honey is effective as a medicine. 2. The scientific explanation of its effects*, Bee World, **2001a,** *80*, 22-40.

150. Molan PC. *Honey as a topical antibacterial agent for treatment of infected wounds*, **2001b,** www.worldwidewounds.com.

151. White JW., Subers MH., Schepartz AI. *The identification of inhibine*, American Bee Journal, **1962,** *102*, 430-431.

152. White JW., Subers MH., Schepartz AI. *The identification of inhibine, the antibacterial factor in honey, as hydrogen peroxide and its origin in the glucose oxidase system*, Biochemica et Biophysica Acta, **1963,** *73*, 57-70.

153. Molan PC. *The antibacterial properties of honey*, Chemistry in New Zealand, **1997,** July 10–14.

154. Molan PC. *The antibacterial activity of honey. 1. The nature of antibacterial activity*, Bee World, **1992,** *73*, 5-28.

155. Adcock D. *The effect of catalase on the inhibine and peroxide values of various honeys*, Journal of Apicultural Research, **1962,** *1*, 38-40.

156. Dustmann JH. *Antibacterial effect of honey*, Apiacta, **1979,** *14*, 7-11.

157. Vergé J. L'activite´é antibactérienne de la propolis du mile et du la gelée royale, Apiculteur, **1951,** *95*, Section scientifique 13-20.

158. Gonnet M., Lavie P. *Influence de chauffage sur le facteur antibiotique présent dans les miels*, Les Annales de l'Abeille, **1960,** *34*, 349-364.

159. Mohrig W., Messner B. *Lysozym als antibakterielles Agnes im Bienenhonig und Bienengift*, Acta Biologica Medica Germanica, **1968,** *21*, 55-95.

160. Bogdanov S. *Characterisation of antibacterial substances in honey*, Lebebsmittel-Wissenschaft und –Tecnologie, **1984,** *17* (2), 74-76.

161. Russell KM., Molan PC., Wilkins AL., Holland PT. *Identification of some antibacterial constituents of New Zealand manuka honey*, Journal of Agricultural and Food Chemistry, **1990,** *38*, 10-13.

162. Wahdan H. A. L. *Causes of the antimicrobial activity in honey*, Infection, **1998,** *36*, 30-35.

163. Weston RJ., Mitchell KR., Allen KL. Antibacterial phenolic compounds of New Zealand manuka honey, Food Chemistry, **1999,** *64*, 295-301.

164. Weston RJ. 2000 *The contribution of catalase and other natural products to the antibacterial activity of honey; a review*, Food Chemistry, **2000,** *71*, 235-239.

165. Molan PC., Smith IM., Reid GM. *A comparison of the antibacterial activities of some New Zealand honeys*, Journal of Apicultural Research, **1988,** *27*, 252-256.

166. Allen KL., Molan PC., Reid GM. *A survey of the antibacterial activity of some New Zealand honeys*, Journal of Pharmacy Pharmacology, **1991a,** *43*, 817-822.

167. Allen KL., Molan PC., Reid GM. *The variability of the antibacterial activity of honey*, Apiacta, **1991b,** *26*, 114-121.

168. Molan PC., Russell KM. *Non-peroxide antibacterial activity in some New Zealand honeys*, Journal of Apicultural Research, **1988,** *27*, 62-67.

169. Molan P. *The antibacterial properties of honey*, Chemistry in New Zealand, **1995,** *59* (4), 10-14.

170. Tan ST., Holland PT., Wilkins AL., Molan PC. *Extractives from New Zealand honeys. 1. White clover, manuka and kanuka unifloral honeys*, Journal of Agricultural and Food Chemistry, **1988,** *36*, 453-460.

171. Tan ST., Wilkins AL., Molan PC., Holland PT., Reid M. *A chemical approach to the determination of floral sources of New Zealand honeys*, Journal of Apicultural Research, **1989,** *28*, 212-222.

172. Wilkins AL., Lu Y., Molan PC. *Extractable organic substances from New Zealand unifloral manuka (Leptospermum scoparium) honeys*, Journal of Apicultural Research, **1993,** *32*, 3-9.

173. Weston 2000et al Weston RJ., Brocklebank LK., Lu Y. Identification and quantitative levels of antibacterial components of some New Zealand honeys, Food Chemistry 70: 427-435.

174. Willix DJ., Molan PC., Harfoot DG. *A comparison of the sensitivity of wound-infecting species of bacteria to the antibacterial activity of manuka honey and other honey*, Journal of Applied Bacteriology, **1992,** *73*, 388-394.

175. Cooper RA., Molan PC., Harding KG. *The sensitivity to honey of Gram-positive cocci of clinical significance isolated from wounds*, Journal of Applied Microbiology, **2002,** *93*, 857-863.

176. Al Somal N., Coley KE., Molan PC., Hancock BM. *Susceptibility of Helicobacter pylori to the antibacterial activity of manuka honey*, Journal of the Royal Society of Medicine, **1994,** *87*, 9-12.

177. Molan PC. *The role of honey in the management of wounds*, Journal of Wound Care, **1999c,** *8*, 415-418.

178. Cooper RA. *A review of the evidence for the use of topical antimicrobial agents in wound care*, **2004,** www.worldwidewounds.com.

179. Molan PC., Betts JA. *Clinical usage of honey as a wound dressing*, Journal of Wound Care, **2004,** *13*, 353-356.

180. Cockayne AH. *The present and future sources of honey in New Zealand*, New Zealand Journal of Agriculture, **1916,** *13*, 14-28.

181. Wardle P. *Vegetation of New Zealand*, Cambridge University Press, **1991.**

182. Carter DA., Blair SE., Cokcetin NN., Bouzo D., Brooks P., Schothauer R., Harry EJ. *Therapeutic manuka honey: no longer so alternative*, Frontiers in Microbiology, **2016,** *7*, 569-579.

183. Vanlint D., Mitchell R., Bailey E., Meersman F., McMillan P., Michiels CW., Aertsen A. *Rapid acquisition of Gigapascal-High-Pressure resistance by Escherichia coli*, mBio, **2011,** *2* (1), e00130-10.

184. Blair SE., Cokcetin NN., Harry EJ., Carter DA. *The unusual antibacterial activity of medical-grade Leptospermum honey: antibacterial spectrum, resistance and transcriptome analysis*, European Journal of Clinical Microbiology and Infectious Diseases, **2009,** *28*, 1199-1208.

185. Cooper RA., Jenkins L., Henriques AF., Duggan RS., Burton NF. *Absence of bacterial resistance to medical-grade manuka honey*, European Journal of Clinical Microbiology and Infectious Diseases, **2010,** *29*, 1237-1241.

186. Jenkins R., Cooper R. *Improving antibiotic activity against wound pathogens with manuka honey in vitro*, PLoS One, **2012,** *7* (9), e45600.

187. Jenkins R., Burton N., Cooper R. *Proteomic and genomic analysis of methicillin-resistant Staphylococcus aureus (MRSA) exposed to manuka honey in vitro demonstrated down-regulation of virulence markers*, Journal of Antimicrobial Chemotherapy, **2014,** *69* (3), 603–615.

188. Müller P., Alber DG., Turnbull L., Schlothauer RC., Carter DA., Whitchurch CB., Harry EJ. *Synergism between Medihoney and Rifampicin against Methicillin-Resistant Staphylococcus aureus (MRSA)*, PLoS One, **2013,** *8* (2), e57679.

189. Olofsson TC., Butler E., Markowicz P., Lindholm C., Larsson L., Vásquez A. *Lactic acid bacterial symbionts in honeybees – an unknown key to honey's antimicrobial and therapeutic activities*, International Wound Journal, **2016,** *13* (5), 668-679.
190. Lund University News and Press Releases, September 8, **2014.**
191. Stephens JMC., Molan PC., Clarkson BD. *A review of Leptospermum scoparium (Myrtaceae) in New Zealand*, New Zealand Journal of Botany, **2005,** *43*, 431-449.
192. Crowe A. *A field guide to the native edible plants of New Zealand*, **1981,** Auckland, Godwit Publishing Limited.
193. Brooker SG., Cambie RC., Cooper RC. *New Zealand medicinal plants*, **1987,** Auckland, Reed.
194. Cooper & Cambie 1991 Cooper RC., Cambie RC. *New Zealand's economic plants*, **1991,** Auckland, Oxford University Press.
195. Molan 2006
196. Dr Arnie Simon
197. Maddocks 2012, Roberts 2012
198. Eva Sapi
199.
200. International Conference *"World Congress and Exhibition on Antibiotics"* – Las Vegas, Nevada, USA, 14th – 16th September **2015** (Speaker: Miss Alessandra Piccitto MRPharmS. Presentation title: "New strategies to develop antibiotics for treatment of *P. aeruginosa* and *Leishmania spp* infections").
201. International Conference *"29th Conference of the international Society for Medical Innovation and Technology"* – Turin, Italy, 9th – 10th November 2017 (Speaker: Miss Alessandra Piccitto MRPharmS. Presentation title: "A novel bactericidal surface to reduce nosocomial infections improving an Italian Patent").
202. Zumla and Lulat, 1989 CONCLUSIONS
203. Aristotle, 1910
204. Gunther, 1934
205.